Available online at www.joac.info

ISSN: 2278-1862

Journal of Applicable Chemistry

2014, 3 (6): 2209-2311

(International Peer Reviewed Journal)

State-of-Art-Review (SAR-Invited)

Mathematical Neural Network (MaNN) Models Part VI: Single-layer perceptron [SLP] and Multi-layer perceptron [MLP] Neural networks in ChEM- Lab

K. RamaKrishna[1], V. Anantha Ramam[2], R. Sambasiva Rao[2*]

1. Department of Chemistry, Gitam Institute of Science, Gitam University,Visakhapatnam 530 017, **INDIA**
2. School of Chemistry, Andhra University, Visakhapatnam 530 003, **INDIA**

Email: karipeddirk@gmail.com, rsr.chem@gmail.com

Accepted on 9th November 2014

(Dedicated with profound respects to V Surya Prakasam, M.Sc. (Hons), A.E.S, former lecturer and Head of Dept. of physics, S R R & C V R Govt. College, Vijayawada during his birth centenary celebrations)

ABSTRACT

Multi-layer perceptron (MLP) NN deals with fully connected feed-forward-supervised NNs in which the flow of data is in the forward direction i.e. from input layer to output layer through hidden ones (IL $\rightarrow$ HL ... $\rightarrow$ OL). Each neuron in a layer is connected to all the other neurons in the succeeding layer. But, the neurons within the layer are not connected. The data comprises of explanatory variables(x) and response (y). In general $LP_NN (with $:0-, 1-, 2- and >2-hidden layers) represents I/O (or 0-LP), S(ingle)LP or 1-LP, 2-LP and M(ulti)LP. Starting with a single neuron, the popular ADALINE and MEDALINE-NNs with illustrative examples like copying, 'AND' 'OR' Boolean gates are described in I/O category. SLP_NN, the life of today's data driven NN paradigm with extensive applications in industry, research and defense has its origin in mid 1980s. It is the start of a new era of NN research, 25 years after the death blow to linear-ANNs for their inability to explain even a simple XOR problem.

*The imbibing character of SLP and its superiority are demonstrated with numerical and literature reports in classification, function approximation, pattern recognition etc. The new NNs emerged (based on input type, TFs, accumulation operators) are complex-, quaternion-, fuzzy-, higher-order SLPs, retaining the basic philosophy of SLP architecture. RBF is also a SLP with Kernel TFs in the hidden layer and recurrent NNs are with partial/complete backward connections. The output of hidden layer of SLP is a transformed form of input into a new space generated through TFs. The applications of SLP and MLP are multifold covering nook and corner of every discipline. Only typical select case studies are briefed engulfing chemistry/chemical engineering, medicine/pharmacy/biosciences, electrical/ mechanical/ computer engineering, robotics, forecast of forex and weather prediction/environment/pollution. Multi-sensor hyphenated instruments generate tensorial data in chemical, environmental, pharmaceutical and clinical laboratory tasks. Mostly, the same sets of algorithms are used in **ch**emometrics, **e**nviromentrics and* **m***edicinometrics (**Chem**) for **tensor** data sets (**Chem_Tensor** abbreviated as **CT**). The computational activity is now accepted as laboratory experiments (**thus CT-Lab**), just the same way of wet and dry labs of last century.*

SLP mimics PCA, non-linear PCA, ARMA and polynomials when suitable object function and architecture are used. The posterior probability and Bayesian estimation are also derived from the output. The evolution in architecture gave birth to dynamic architectures, Ito/Funahashi model, centroid based/adaptive/self-feed-back/cascade correlation MLPs. The selection/sub-sets of patterns, layer-wise learning/pseudo-inverse/mixture-of-experts, dynamic learning, AdaBoost, batch-wise training are a few noteworthy advances in training Ws. The incorporation of a priori-knowledge into MLP is a new dimension. The modifications of basic back propagation (BP) algorithm used to train MLP_NN are extensive. The first-/second- order optimization methods and nature inspired algorithms like SAA, GA, PSO, ABC, ACO and differential evolution increased quality of Ws. Inverse NNs based on SLP/MLP for XOR and function approximation tasks are successfully dealt with. The cognitron, neocognitron, neural gas, spiking nets, complicated NNs mimicking (partial) biological functions, recent intelligent integration of statistics and NNs (NeuralWorks® Predict) and hybrids with nature-inspired algorithms find a niche in the annals of data driven information extraction.

Keywords: Multi-Layer Perceptron (MLP), Neural networks, Function approximation, Interpolation, Pattern recognition, Chemistry, Medicinometrics, Pharmaceutics, Technology, Pollution, multiple-classes.

Contents Multi-Layer Perceptron (MLP)-NN

- Classification of two categories with curved boundary
- Inversion of NNs for real life tasks

- Iris classification
- Character (printed digit) recognition
- Handwritten zip code
- Drug discovery
- Aerospace application using Inversion of MLP_NN
- Output performance of sonar system

8. Applications.Feed_forward_layered NNs

- **Metrics**

- Classification
- Automation of Classification
- Function approximation
- Automatic Speech recognition systems

- Chemometri cs

- Dietetometrics
- Technometrics
- Envirometrics
- Geometrics
- Medicinometrics
- Electric (power) engineering
- Robots
- Communication
- Commerce

9. Architecture Evolution in MLP_NN

- Centroid based MLP_NN

INTRODUCTION

Feed forward supervised neural networks

The neuron popular in connectionist model of the brain is the processing element in artificial neural networks (ANNs). Neural network consists of a bundle of inter connected neurons. Each neuron receives input signals or patters. They are modulated by connection strengths and are accumulated in the confluence operation. A transfer (activation) function operates on it resulting in the output. Neural networks are broadly classified into self-organizing and supervised types based on the data containing only the explanatory (X) factors and X as well as response variables (y). The premise of a supervised NN-model of pattern recognition is the assumption of a (fundamental) relationship between output signals of the phenomenon and the explanatory input factors, although it is not known explicitly many a time. The objective is to extract it, even if the model is approximate or isomorphous. The number of neurons, nowadays called processing elements/units (PEs or PUs), in input and output layers are equal to the number of variables in X and y. Thus, the number of measurements/ observations/ patterns in X and Y space result in matrices of size [NP, dimx] and [NP, dimy]. Each row of the matrix represents a data point or pattern in NN terminology. The mapping or transformation of input to output is in the forward direction and thus referred to as feed forward (FF-) NNs.

Modern NN designers opine the prior reports (ADALINE, MEDALINE, Hopfield, Brain-state-in-a-box (BSB), Willshaw-Vander-Maliburg approach) before the rebirth of NNs can be deemed as classical/historical NNs. Of course, they gave birth to the present form or their modified versions. Professional II, a software package incorporated many of the historical ones for first level user/NN appreciators. In continuation of our reviewing architectural details of NNs and their applications in interdisciplinary research [303-311, 313], the evolution of MLP_NNs and revolutionary progress in learning/ optimization methods for bench mark datasets and real life tasks are described in this review [1-393].

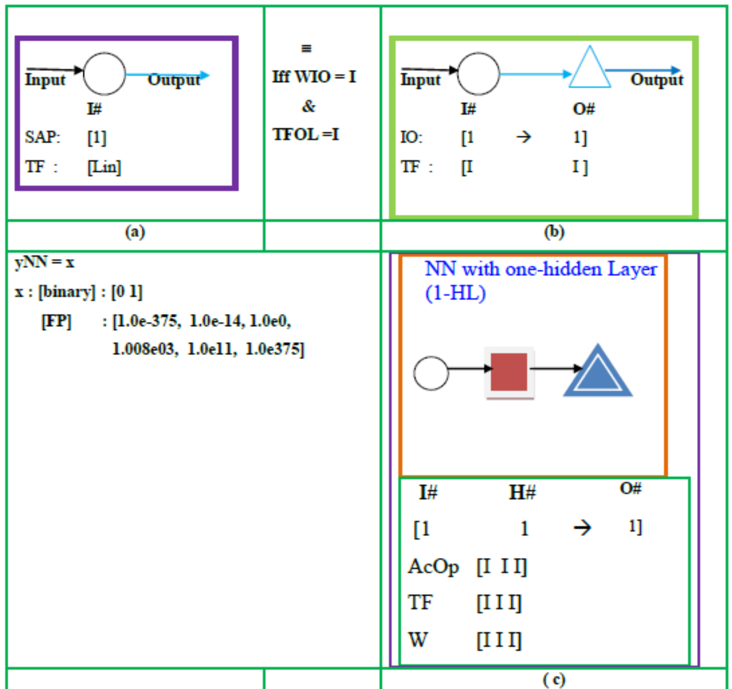

Fig.1: Architecture of ZLP_NN and SLP_NN

2. Z(ero hidden) layer perceptron-ZLP_NN (or I/O NNs)

SAP (simple as possible) is a popular approach in microprocessors and computer technology for pedagogical purposes and finds room in neural networks too. The simplest possible neural network ever dreamt consists of a single neuron (Fig. 1a). It can do copying, negating (Table 1) and inverting operations successfully. It can be represented in the traditional IO_NN using one neuron in each layer (Fig. 1b).

Table 1: Boolean Not operation

Boolean gate	Data			Weight, threshold
	#point	X	y	
Not Gate	1	0	1	w= [-1] th=[0]
	2	1	0	
0 * (-1) = 0 ; 0 = threshold (0), hence fires i.e. y = 1				
1 * (-1) = -1 ; -1 < threshold, hence does not fire i.e. y = 0				

McCulloch and Pitts NN

McCulloch-Pitts-neural network with fixed connection weight (i.e. no learning) models/ simulates/explains/mimics/emulates Boolean (and, or) gates (Table 2, Fig. 2, chart 1). Here, X is the input, W is weight and yNN is output vectors of NN. The response surface for three dimensional input is 4D- and thus, only numerical values are given. The simple copying operation of MC neuron is illustrated in (Table A1-9a).

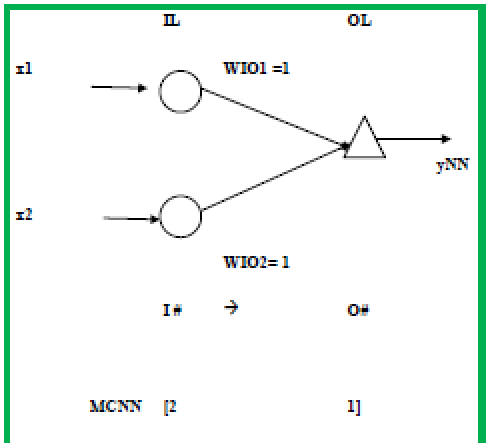

Fig.2: Archit.McCulloch and Pitts NN

Chart 1: McCulloch and Pitts NN

- Boolean 'AND' 'OR' gates
- Fixed weight

- Dead end

- Cannot produce XOR
  - **Remedy :** SLP
- No learning i. e. No provision for Ws refinement
  - **Remedy :** Training algorithms

Table 2: Boolean 'AND', 'OR' operations with McCulloch and Pitts NN

Gate: AND

#point	Data: Supervised / Unsupervised x1	x2	y	Results: yNN	Model acceptability	Intermediate results: X^T*W	Sign $(X^T*W - th)$
1	0	0	0	F	yes	0	-2
2	1	0	0	F	yes	1	-1
3	0	1	0	F	yes	1	-1
4	1	1	1	T	yes	2	0

w=[1 1]';
th=[2]

Ynn= [X^T *W >= th]

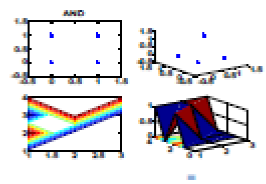

Gate: OR

#point	Supervised / Unsupervised x1	x2	y	yNN= [X^T *W >= th]	Adequacy of Model	X^T*W	Sign $(X^T*W - th)$
1	0	0	0	f	yes	0	-1
2	1	0	1	t	yes	1	0
3	0	1	1	t	yes	1	0
4	1	1	1	t	yes	2	1

w=[1 1]';
th=[1]

OR Input x1	x2	x3	y1
0	0	0	0
1	0	0	1
0	1	0	1
0	0	1	1
1	1	0	1
0	1	1	1
1	0	1	1
1	1	1	1

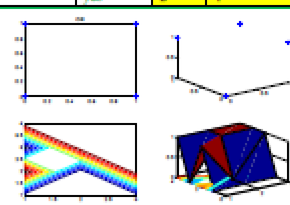

AND Trajan output				
x1	**x2**	**y**	**yNN E. E_000**	**Error E. E_000**
1	0	0	9.393e-09	9.393e-09
0	0	0	-1.876e-08	-1.876e-08
0	1	0	9.367e-09	9.367e-09
1	1	1	1	0

Threshold	36.27571	1.876e-08
E_000	17.79275	
E_000	17.79186	
h1#01		2.99592

Architecture
2-1-1
SLP_NN(Trajan)

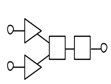

If IO_NN & I# = O#

Then Eigen values & PCs

Rosenblatt, in 1962 proposed input-output layer neural network (IO_NN) with linear learning rules as an excellent model for human brain. It is also a simple architecture with parallel computation and efficient learning of Boolean gates like ‘and’, ‘or’ etc. The advances in IO_NNs paved way to calculate eigen values, linear-PCs and dimension reduction of input space. The results of function approximation of tanh (y = tanh(x)) and linear (y =x) I/O mappings with TRAJAN software are given in table 3. Minsky and Papert showed that this NN failed to classify XOR patterns.

Table 3a: Function approximation of tanh(x) with SLP_NN (1-1-1)

	Y	yNN	Error
E_000	E_001→ a2	T. a2	E. a2
-1.8	-0.946806	-0.946806	-2.889e-05
-1.6	-0.9217	-0.9217	4.906e-06
-1.4	-0.8854	-0.8854	2.485e-05
-1.2	-0.8337	-0.8337	2.569e-05
-1	-0.7616	-0.7616	-1.518e-05
-0.8	-0.664	-0.664	-1.022e-05
-0.6	-0.537	-0.537	-5.29e-06
-0.4	-0.379949	-0.379949	-1.114e-06
-0.2	-0.1974	-0.1974	1.652e-06
0	0	0	2.689e-06
0.2	0.1973753	0.1973753	2.262e-06
0.4	0.379949	0.379949	1.065e-06
0.6	0.5370496	0.5370496	-1.744e-07
0.8	0.6640368	0.6640368	-9.787e-07
1	0.7615942	0.7615942	-1.243e-06
1.2	0.8336546	0.8336546	-1.054e-06
1.4	0.8853517	0.8853517	-5.927e-07
1.6	0.9216686	0.9216686	-1.302e-08
1.8	0.946806	0.946806	5.639e-07
2.0	0.9640276	0.9640276	1.1e-06

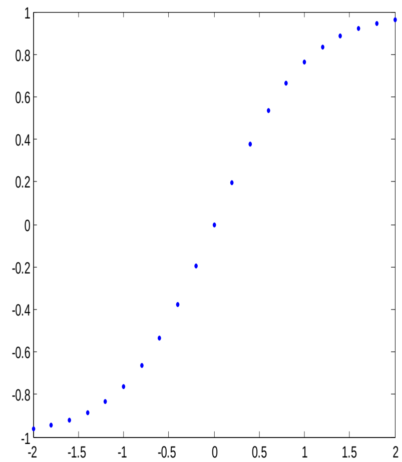


```
%
% tanhsim.m   7/8/07
inc = 0.2;
[x]= [-1.8:inc:2]';
  y = tanh(x) ;
figure,plot(x,y,'b.'),hold on
z = [x,y];save tanhsim.dat z -ascii
type tanhsim.dat
```

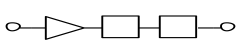

Table 3b: Function approximation with IO_NN using TRAJAN

(a) y=x ; x = [0 :0.1:1]’;

Chart 2: ADALINE

- It functions as an adaptive FIR filter with tapped input. The higher order transfer function can be obtained through z-transform
- Cannot solve XOR, since the separating hyperplane is non-linear

☏ **Remedy :** SLP

	0	0	IO : [1-1]
	0.1	0.1	
	0.2	0.2	Threshold 1.287e-17
	0.4	0.4	VAR1 1
	0.6	0.6	
	0.8	0.8	y=x
	1	1	

	Convert Scale	Missing	Min/Mean		Max/SD	Shift
VAR1	Minimax	Mean	0	1	0	1
VAR3	Minimax	Mean	0	1	0	1

	VAR3	T. VAR3	E. VAR3	Error
01	2.393e-17	0	2.393e-17	0.01213
02	0.1	0.1	1.388e-17	0
03	0.2	0.2	0	0
04	0.4	0.4	-5.551e-17	0.004469
05	0.6	0.6	-1.11e-16	0
06	0.8	0.8	-1.11e-16	0.003196
07	1	1	0	0.007028

If $y_i * (\langle w_i * x_i \rangle, threshold\ ) > small$

Then Data set is linearly separable

Alg. 1: Training of ADALINE with Widrow-Hoff rules

Do until convergence

$$\begin{aligned} &\Delta w \ = yi - ynni \\ &wcur = wap + \Delta w \\ &if\ |wcur - wap| < tol \\ &\quad converged \\ &endif \end{aligned}$$

endDO

ADALINE

Bernard Widrow, at Stanford, proposed adoptive linear neuron (Alg. 1) in the year 1959. Under his direction, there was a proliferation of real life applications of neural computing for the first time in major real world tasks viz. speech/character recognition, weather prediction, vector-cardiogram diagnosis, adaptive filters to eliminate echoes on telephone lines etc. ADALINE uses linear perceptron updating learning rule. Novikoff proved the convergence theorem for ADALINE and it can be considered as a threshold logic device. It is applicable to linearly separable classification tasks. The binary logic gates are implemented with binary weights. The transfer function here can be deemed as identity. It accepts and generates bistable values (-1 and +1) also. The architecture consists of an input and output layer corresponding to number of input and output variables. It maps a n-dimensional input pattern (X_i) into a scalar output (y_i). It also failed to find solution to non-linearly separable XOR classification (chart 2).

MADALINE (Multiple ADALINE)

A set of ADALINEs combined together into a single feed forward network. They are fully connected to each of the ADALINEs in parallel. The MADALINE output unit receives the outputs of ADALINE layer. The weight matrix connecting ADALINE layer to output neuron is identity. It implements even non-linear separable mapping viz. XOR.

The function of the output unit is based on majority vote concept. If 50% of the weights are +1, the output is +1, else it is -1. Professional II implements it. The weather forecasting (precipitation) at several locations around San Francisco bay area was reported by Widrow et al in 1963 using barometric pressure and the difference from the previous and earlier two days data with MADALINE-NN. The prediction of precipitation in the day and night were better compared to other procedures available at that time. Further applications include stock-market prediction, horse racing and flack Jack.

$$y\_IO = \left[\left\{ x^T * WIO \right\} \right]$$

$$If\ scaling\ is\ needed,\ y\_IO = \left[Unscal \left\{ \left(\left\{ scal\left(x^T \right) \right\} * WIO \right) \right\} \right]$$

3. S(ingle hidden) layer perceptron (SLP)-NN

In 1986, Rumelhardt proposed a single hidden layer perceptron (SLP)-neural network (NN) affecting the data flow from input, hidden to output layers. The layers are successively connected and there are no feedback or far off direct connections. Each unit in any layer has fan-in connections from all units in the preceding (immediately below) and fan-out connections to all units in succeeding (immediately above) layer. The word hidden is used as an end user is not interested in the details of operations in it. The strengths of connections are termed as weights (W) in analogy with synaptic strength in neurobiology. A simple nonlinear (sigmoid) function is used as TF in the hidden layer. Further, it is neither a rule nor exception of restricting a single transfer function in a PE and/or in each layer.

The weights (WIH, weight matrix of connections from input to hidden layer, WHO, weight matrix of connections from hidden to output layer) are learnt (refined) by back-propagation algorithm, which is steepest gradient procedure tailor made for on-line learning. A transformation of input with a non-linear (sigmoid) TF and back-propagation learning algorithm not only successfully implemented XOR gate, but has became a laudable architecture for a reborn NN paradigm. It has only a little more intelligence in solving pattern recognition task. But, SLP imbibes a galaxy of hither to available matured mathematical/statistical procedures. This paradigm opened new vistas in non-collapsing learning of even odd data structures with unknown complex functional relationships. The input to output (I/O) mapping in NNs is affected by choosing architecture (i.e. number of hidden layers, type of connections between neurons), TFs and training sets [19]. The advantages of sigmoid TF in hidden layer are faster convergence, lower recognition error, and less sensitivity to learning parameters

$$y\_SLP = \left[Unscal\left[\left\{ TFHL\left[\left(\left\{ scal\left(x^T \right) \right\} * WIH \right) \right]^T \right\} * WHO \right] \right]$$

Why a linear TF is preferable compared to nonlinear-TF in output layer?

When the output layer of FF-MLP_NN uses a non-linear TF (like sigmoid), there arise more local minima compared when a linear TF is employed. It was reported that re-constructive error surface for a sigmoidal auto association consists of multiple local values compared to the linear one. When the weight vector of a neuron reaches saturation area of a sigmoidal PEs, the derivative is zero. The error function for the final layer activation is nearly a flat region around this point. It is well known that the gradient techniques fail to find the optima of such surfaces. In binary classification [18], the output values are in the range of zero to one.

Copying operation with SLP

Obviously, copying operation is successful with an SLP of configuration 1-1-1 and hard limiter TF for hidden and output layers (table 4).

Table 4: Mapping of input to output in copying a binary bit by SLP

Input	output	Network parameters	Network
$X = \begin{bmatrix} 0 \\ 1 \end{bmatrix}$	$y = \begin{bmatrix} 0 \\ 1 \end{bmatrix}$	$wih = [-8]$ $biasi = [4]$ $who = [-8]$ $biash = [4]$	I#-H#-O# 1 -1 -1; lin-hardlimitor-lin

pattern 1: x = 0
IH1 = x1*wih +biasi = 0*(-8) + 4 = 4;
OH1 = TF(IH1) = hardlimitor(4) = 1

wih	who	biasi	biash	

IO1 = OH1* who+ biash =1* (-8) +4 = -4;
OO = TFO(IO1) = hardlimitor(-4) =0
y = 0 ; yNN= OO; y-yNN = 0;

pattern 2: x = 1
IH1 = x1*wih +biasi = 1*(-8) + 4 = -4;
OH1 = TF(IH1) = hardlimitor(-4) = 0
IO1 = OH1* who+ biash =0* (-8) +4 = 4;
OO = TFO(IO1) = hardlimitor(4) =1
y = 1 ; yNN= OO; y-yNN = 0;

-8	-8	4	4	Global
8	8	-4	-4	Global
-8	-8	0	0	Global
0.8	0.73	0	0	Local

Function approximation_SLP

SLP_NN and in general NNs approximate functions, but the practical issue is the number of hidden neurons needed for a viable approximation. The simulated results for approximation of a quadratic function ($y = x^2$) are detailed in application of NNs for modeling ozone [308]. The heuristics for function approximation by NNs are in KB. 1 and function approximation of y = x is given in table 5.

Table 5: function approximation (y = x) by SLP

		VAR3	T. VAR3	E. VAR3	Error
01	0.0	-0.031	0	-0.031	0.031
02	0.1	0.09627	0.1	-0.003729	0.003729
03	0.2	0.2225399	0.2	0.02254	0.02254
04	0.4	0.4608925	0.4	0.06089	0.06089
05	0.6	0.6662254	0.6	0.06623	0.06623
06	0.8	0.8302175	0.8	0.03022	0.03022
07	1.0	0.9534527	1	-0.04655	0.04655

Threshold 0.1445435 1.118388
VAR1 2.174794
h1#01 2.343879
lin-logistic-linear
1-1-1 SLP

	Convert	Missing	Min/Mean	Max/SD	Shift	Scale
VAR1	Minimax	Mean	0	1	0	1
VAR3	Minimax	Mean	0	1	0	1

SLP

+ Polynomials approximated by SLP
- FF_NNs cannot model dynamic systems

Remedy: Recurrent-NNs

KB. 1: Heuristics for function approximation with NNs

If	SLP		&
	TF is ridge function		&
	Continuous almost everywhere		&
	Locally essentially bounded		&
Then	SLP approximates any continuous function with uniform norm		
If	SLP	A1	&
	TF : NonLinear	A2	&
	High number of neurons	A3	&
Then	Approximates any function	C1	
If	fn(x) is continuous in a closed interval [a,b]		&
	fn(x) has M extrema		&
Then	SLP with M+1 sigmoid neurons approximates function		
If	polynomial with odd degree terms		
Then	TF : logistic sigmoid with null threshold		
If	polynomial with even degree terms		
Then	TF : Gaussian		
If	TF is analytical		&
	TF is non-polynomial		
Then	fn approximation with W as small as possible		
If	P(x) is a polynomial of degree p		&
	TF has continuous derivatives upto p+1 order		
	TF(x) ≠ 0 for 0<=I<=r		
Then	SLP approximates the polynomial		&
	number of hidden neurons = norm(p(x)-yNN) <= ε		&

Table 5b: Architectures of XLP_NNs in Matlab neural network toolbox

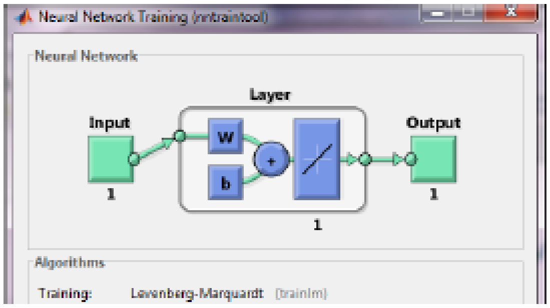

1-[0]-1 ZLP

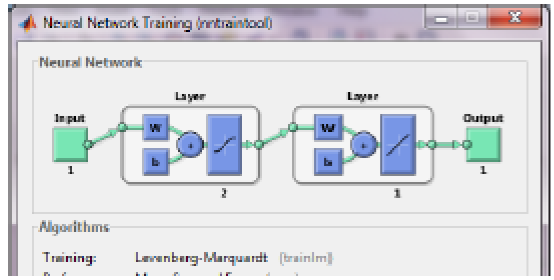

1-[2]-1 SLP

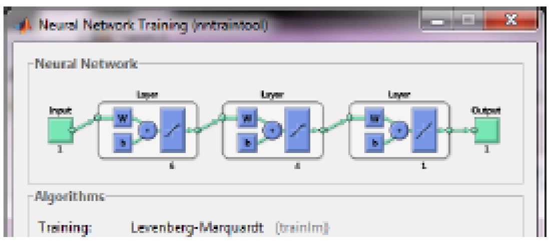

1-[6-4]-1SLP

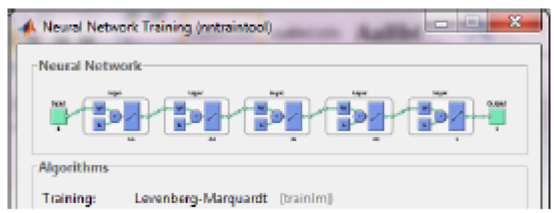

1-[56-44-26-19]-1 M (4)LP

4. M(ultiple hidden) LP-NN

MLP_NN contains one input layer, one output layer and many (two to four or more) hidden layers. The role of hidden layers is multiple non-linear transformations of weighted input values.

$$\left(Unscal\left[TFO\left(\left\{\left(TFH2\left[\left\{TFH1\left[\left(\left\{scal\left(x^{T}\right)\right\}*WIH1\right)\right]^{T}\right\}*WH1H2\right]\right)*\ WH2O\right\}\right)\right]\right)$$

These are versatile for supervised classification and function approximation (chart 3). The details of MLP_NNs are described earlier in modeling ozone in environment [308]. A column of neurons is imagined as a layer when the data flow is represented from left to right (SLP) and row of neurons if the data transfer is from bottom to top (ART, ARTMAP). In the case of neocognitron NN, a layer consists of matrix of neurons. Thus, a vector or first order tensor is apt for earlier NNs. In SOM NN 1D-, 2D-, 3D- structure of neurons is used in self organization. The general notation for XHL_NN obviously explains IO-, SLP-, MLP-, SOM-, neocognitron- NNs.

Chart 3: Highlights and limitations of MLP_NN

- \+ MLPs are global models and use all patterns
- \+ Exploits the plasticity of hidden layer weight
- \+ Information is distributed globally in the network

❄ Neural gardening tools

Using minimum error and/or maximum of performance criteria, an optimum network is arrived. Yet, automatic selection of architecture of NN is still in a state of infancy. Pruning methods, sensitivity analysis, information content and data/goal accuracy/precision are instruments in the hands of NN modeler. Recently, they are referred as neural gardening tools [14]. Karkkainen [18] performed sensitivity analysis of FF-MLP_NN layer wise, comparing different weight decay (linear, quadratic and convex) techniques. The object function is sum of Least Mean Squares (LMS) and squares of Ws connecting.

- Weights (even in SLP) have no physical meaning
- Static i.e. time or space variation cannot modelled
- Greedy BP training settles in local minimum of error surface
- Lack of localizability of Sigmoid TF → converges slowly
- Long training time
- Does not guarantee convergence of learning to desired function
  - ☎ **Remedy :** RBF-NN
- Cannot account for higher order correlation
  - ☎ **Remedy :** Higher-order-NNs
- Learns noisy patterns also with increasing number of hidden neurons
- Cannot handle discontinuities in input data

X		$$_NN
Z(ero)	0	IO
S(ingle)	1	SLP
T(wo)	2	M(2)LP
M(ulti)	6	MLP

5 Quantum NN

A quantum NN basically works on quantum neuron [304] and qubits. A Quant_NN exponentially gains speed over classic neural networks through superposition of values entering and exiting a neuron (chart 4). Georgia Tech and Oxford University also focus on futuristic systems. The valid input to Qubit-NN is within the range 0 to 1. The input neurons convert the numerical value into quantum states in the range 0 to $\pi/2$. It is passed through the hidden layer and output layer. The final output gives the probability of the basic state of neuron. The training is with quantum modified BP.

6. Inverse SLP (Output → Input (O/I) mapping)

The word inverse is obvious as it is upside down of the original. The inversion of a matrix or trigonometric function is well known. The product of a number/variable and its reciprocal is unity. Thus, the simplest reciprocal operator can also be considered as an inverse operator. The inverse of a non-singular square matrix is easily calculable. The product of it and its inverse is an identity matrix of same dimension ($A * A^{-1} = I$). The near singularity arises as a result of physical or numerical correlation. Pseudo-inverse circumvents singularity problem by chopping off the dependent rows or columns. It is like removing cancerous cells from healthy ones in an organ. The natural logarithm ($\log_e$) of an exponential (exp) of a number (x) is the number of itself [$\log_e(\exp(x)) \rightarrow x$]. Similar instances are sin and $\sin^{-1}$, and differentiation and integration and so on.

Chart 4: Advantages of Quantum NN

- NN with a small number of neurons is adequate
- Reduction in the number of layers
- Greater efficiency

It appears to be trivial even for simple processes like first order kinetics and some of the systems at equilibrium. The transformation of A to B and back is a popular process in physical sciences. The latter one B to A is an inverse of the forward process (A → B). In biochemistry, physics and molecular biology, simple mono-phasic to multi-phasic (more steps) processes involving multiple components are investigated with mathematical and experimental rigor. The mapping from output space to input space is called inverse mapping. It is a locally ill posed problem as there is no unique solution. Further, it is globally ill posed since there are multiple solution branches. Thus there is no closed form expression for the inverse mapping. Added to it, ill- conditioning increases as the complexity of the system grows. The realizations for expected results in drug discovery are still a rosy dream of beauty and fragrance but also with (inseparable) thorns.

The prime objectives of inversion of neural networks are to detect generalization error and obtain different network inversions for a given output data set. It enables one to explicitly express functional and constraints on the network inversion. It paves way to probe into similar constrained optimization problems. Further, the relationship between network inversion and parameters also can be thoroughly examined for a successfully inverted NN (MLP or RBF).

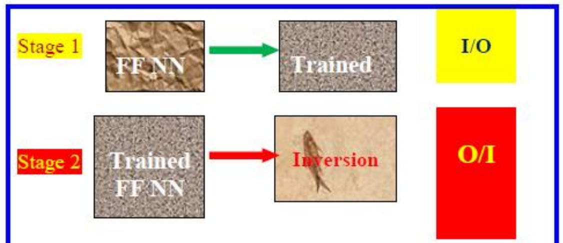

Fig. 3: Training and inversion of FF_NNs

☎ Methods for inversion

Several algorithms are proposed for output to input mapping within the framework of FF-NN, especially for SLP, RBF and MLP (Fig. 3) datasets. The output to input (generally many to one) mapping is conceived here, as inverting FF-NNs. The solution proposed earlier in the literature was by iterative inversion algorithms. Later, adapted linear, non-linear and separable programming are employed. Modified simplex is used in separable programming procedure. It does not require gradient and also explicit form of the functional relationship. The necessary condition for application of simplex is the existence of functional relationship which may be simple or complicated. The ill-posed output to input mapping is translated as a constrained optimization problem. Natural algorithms (PSO) found a niche in this activity. The network architecture and types of inversions are crucial in selecting the method. The solution of inverse problems with the available jargon revolutionized, parameter estimation in remote sensing and training of NNs. Results of inversion of large feed forward NNs opened new understanding in generalization, sufficiency of training/test data space. A bird's eye view of typical inversion procedures follow.

Direct method: The inverse kinematics problem is typical in robotics. It is solved by direct mapping of FF_ NN.

Jorden and Rumulhant procedure: This approach to invert FF NN involves two stages. It starts with training NN to approximate the forward mapping. In the next phase, another network is connected to the already trained one. The learning of identity mapping across the composite net is continued.

LEE and Kil method: This method involves a local update employing Lyapaunov function and relocation rule using the predefined or no information. The knowledge may be that involved in the forward mapping or the probabilistic description of the possible location of the solution for the inverse problem. With this approach, the inverse mapping of a continuous function is calculated.

Conditional density estimation: It is a conditional density estimation based method. The deficiency of using ESS to arrive at one-to-many inverse mappings are analyzed.

Lu method: The concept used here is that an inverse problem can be deemed as an NLP problem. Based on the architecture and a type of inversion, NLP is a separable programming problem or a linear programming task.

Alg. 2: Inversion of simple as possible (SAP) NN
- ⇨ Input : A desired output (ydesired)
- ⇨ Forward training
  - Trn data: [X,y]

- Model : y = Fn(X; Ws,TF, AccOp)
- Trn: (batch wise or point wise)
- ⇨ Estimate Reverse activity (input vector) corresponding to desired output
- ⇨ Output : X_InvNN

Modified Simplex: Inversion of NLP or RBF is performed and applied to a separable programming problem.
Inversion of MLP: A set of input patterns which produce a target output pattern are to be found (Alg. 2). The steepest descent algorithm affects the minimization of the cost function. Inversion of MLP or RBF is possible with separable programming method. It is possible to invert NNs including prob_NN with differentiable activation functions.

7. Applications.Inverse_FF_layered (XHL_NNs)

ॐ Inverse-XOR using inverse_SLP

A 2D-binary XOR problem consists of two inputs x1 and x2 each with either one or zero. The output is 1 for heterogeneous input (x1+x2 = 1), while it is zero for homogeneous data (x1+x2 = 0 or x1+x2 = 2). The inverse problem is to find out x1 and x2 for a known value of ytest. It is solved by two approaches viz. inversion of MLP_NN and inversion of RBF-NN.

Inversion of SLP_NN: A SLP_NN with architecture 2-2-1 was trained with BP. The inversion of MLP for the output 0.9 (ytest) was performed with Imin and Imax procedures by converting I to O mapping of MLP as a constrained NLP. The x1_invMLP, x2_invMLP (input) obtained are well within the acceptable limits. The sigmoid function was approximated over the range -16 to +16 and the approximate LP was solved by simplex procedure with restricted basis entry rule. By increasing the number of grid points, errors will further be reduced.

The inversion of NN is performed with gradient descent algorithm. The distribution of points on hyperplane depends upon the basin of attraction. Thus, a break appears. In a separate experiment, SLP with bipolar inputs and tanh TF is trained. The inversion with evolutionary algorithm results in a even distribution of points. Hypinv is a pedagogical algorithm extracting rules from a trained NN in the form of hyperplane for continuous or binary inputs. Table 6 depicts the rules for XOR obtained by the inversion of NN.

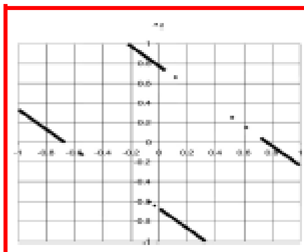

Inversion with Gradient descent

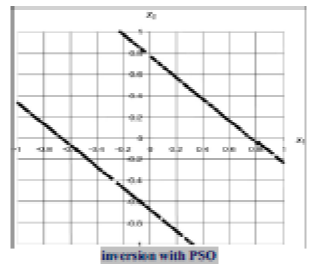

inversion with PSO

Extraction of rules from trained NNs

The weight matrices for 2-2-1 (lin-sig-lin) SLP trained are
WIH1 = (−3.179332, −4.820779, 4.715858) [theta, w1,w2]
WIH2 = (−1.665238, 3.051616,−3.410621)
WHO = (−2.145716, 4.830636, 4.300482).

Rules extracted for the XOR problem and the corresponding points x1 and x0

x1	x0	Rule antecedent
(0.983, 0.758) (0.0118, 0.997)	(1.16 , 0.56) (0.197, 0.819)	$A1 : -0.174x1 + 0.198x2 + 0.09 < 0$ $A2 : -0.185x1 + 0.178x2 - 0.11 > 0$
Rule Base: If A1 _ A2 then x 2 C+		

Table 6 : Inverse XOR by SLP NN

ॐ Classification of two categories with curved boundary by inversion of SLP

Rule Base:
If A1 ^ A2 ^ A3 ^ A4 ^ A5 ^ A6 ^ A7 then x2
where
$A1 : -0.233x1 - 0.095x2 - 0.178 < 0$
$A2 : -0.336x1 + 0.276x2 - 0.305 < 0$
$A3 : +0.255x1 + 0.183x2 - 0.221 < 0$
$A4 : +0.038x1 - 0.121x2 - 0.091 < 0$
$A5 : -0.057x1 - 0.173x2 - 0.128 < 0$

Training and testing of 1000 samples each for a two class problem with points inside circle belonging to one class and then outside to another class are modeled with 2-8-1 SLP_NN. HYPINV extracts the most influential and important variables first followed by less important ones. It approximates the discriminatory function with network decision boundaries using conjunction of 7 rules (chart 5)

A6 : $0.268x1 - 0.108x2 - 0.199 < 0$
A7 : $0.031x1 + 0.266x2 - 0.191 < 0$.
Simplification of extracted rules leads to

If $x2 > 0.83206$ then negative class
Else calculate rules

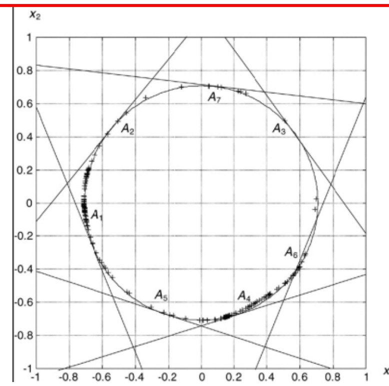

Chart 5: Extracted rules for two class task with curved boundary by inverse_SLP
(Courtesy of E.W. Saad, D.C. Wunsch II, *Neuralnetw.*, *20*, **2007**,78-93)

ॐ Inversion of NNs for real life tasks

Inverse problems occur in electromagnetic surface design, flight control, vulnerability of large power stations, snow parameters from passive microwave remote sensing measurements, kinematics, vibration analysis etc. For that matter of fact, inversion is needed in each and every activity in animate and inanimate life cycle of the universe in both space and time. Drug discovery and synthesis of materials of desired characteristics are vital inverse tasks. The available data and model are guidelines of retaining influential variables in I → O mapping. The difficulties in inverting each operation of the forward process are not well explored area. With all these difficulties, still there are encouraging and noteworthy results in this decade.

⇅ Iris classification task - Inversion of SLP

A SLP_NN of 4-3-2 architecture was trained with BP resulting in correct recognition rates of 100%, 93.3% and 96.7% for setosa, versicolor and virginica. In this study the training set and test set comprise of 60 and 30 points for each class. The performance of the test data is acceptable as it is an interpolation task. The study of inversion of MLP_NN reported that extrapolation behavior of the system cannot be inferred based only on test data within the interpolation region.

⇅ Character (printed digit) recognition_ inverse_SLP

The printed digits (i.e. integers 0 to 9) together with 540 noised patters are trained with SLP_NN (35-12-4). The input values obtained by NN-inversion for the digit '0', were fed to SLP_NN and the digit was recognized as zero. But the naked eye could not decipher some of the patterns.

⇅ Handwritten zip code – inverse_SLP

From a database of 7291 training and 2007 test hand written zip code characters (fig. 4), 500 patterns are used to train SLP (256-30-4) with BP. Each input for NN consists of 16 x 16 pixels for a character. The correct recognition rates for 2007 and 6791 test samples are 78.1% and 82.9% respectively. It appears that the performance of NN is commendable. But, a peer inspection whether the test data set covers the entire input space or confined to a narrow range (like a small patch) in a rectangular grid is important to understand generalizability of NN model.

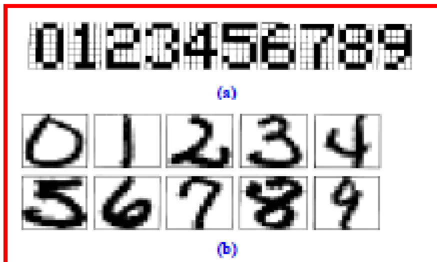

Fig. 4. Digits zero to nine (a) images of printed digit (b) handwritten ZIP codes

Drug discovery

The experimental and simulated data available in pharmacy and mutagenicity is the start of invoking inverse models. In drug discovery for a best pharmaceutical product, the range of physical, chemical, toxicological and biological variables are computable with today's available state of the art of inversion of NNs. It iteratively improves the quality of the drug. Although inclusion of a priori knowledge is essential, traditional wisdom further complicates the situation. Inversion of this part is much more difficult at the moment.

Aerospace application using Inversion of MLP_NN

The safe escape envelope of the ejection of a seat in military airplane depends upon velocity, altitude etc (Fig. 5) of the flight. The simulation of high fidelity ejection of a seat by EASYS software is very slow for real time advice to the pilot. In fact, simulation of 302,330,880 (approximately 0.3 trillion) points designed requires 35years of time. Instead the data from modest simulations are trained with NN (8-5-O#) using node decoupled extended Kalman filter (KF) and query based learning. Fidelity is the ratio of number of points in the test set where both rules and neural network agree to the total number of points. The accuracy of rules corresponds to the ratio of number of points where the rules give correct classification to the total number of points. Fidelity of 80-85% is observed in several runs with different random seeds and three rules (KB. 2, table 7) resulted.

KB. 2: Rule base in safe escape

If A1 _ A2 ^ A3 then x 2 C+

Simplified rule base

If alt > 162.3995 then safe
If alt < 94.84994 then saf.
Else calculate rules.

A1 : 6.493 * pitch − 2.1422 * roll + 94.551 *FPA − 2.0456 * p +1.1002 * q − 1.8886 r + 318.29 * alt + 20.43 1vel −1.133 × 105 > 0

A2 : −3.2914pitch + 11.603roll + 58.099FPA + 9.9544p −8.5739q + 5.1669r + 293.43alt − 40.824vel +4572.2 > 0

A3 : −0.90337pitch − 10.133roll − 48.159FPA − 5.5235p −1.2003q − 5.4438r − 135.53alt − 4.6534vel +27927 < 0

Table 7: Fidelity, rule accuracy and information measures for the rule extracted in the aerospace problem

#Rules	(%)		*I(R,N)*	*I(R,D)*	*H(R)*
	Fidelity	Rule accuracy			
1	80.57	81.66	0.0968	0.115	0.765
2	82.6	82.41	0.0044	0.0043	0.0771
3	83.35	84.74	0.0759	0.1005	0.5635

Output performance of sonar system with inversion of MLP_NN for optimization

The inverse task is to estimate a set or subset of input parameters which maximize SIR in the chosen target area. A surface ship dips a sonar unit into the water body. The environmental parameters viz. wind speed, roughness of surface, shape of the sea floor and bottom type contribute to the effectiveness of the sonar. The output performance of the sonar system in varying environmental conditions is a complex inverse problem.

The forward problem i.e. measurement of SIR (signal to interference ratio) with acoustic emulator itself is a computationally intensive. Hence the data collected for a long time from the emulator was trained by NN. Data outside the region of interest are assigned "Don't care status" and are not included in the evolution of fitness function. MLP_NN of architecture 27-40-50-70-1200 was trained and sigmoid TF was used with three hidden layers. The inverse problem of achieving maximum SIR in an ocean floor region of interest was solved by keeping SIR at higher unachievable values. Particle swarm optimization (PSO) was used for inverting NN and CORDIC algorithm was employed to invert sigmoid TF. The real time implementation of inversion of NN was affected on SRC-6e reconfigurable computer. Two identical virtex 2 FPGA (field programmable gate arrays) are used. The inversion time decreased from 1.8 to 0.36 second. It is contemplated that with a little modification, twenty network inversions are possible in a second. The input (special characteristics) computed by NN inversion for the pixel areas for maximum SIR are found to be excellent and effect of environmental variables will take the study the higher heights.

8. Applications.Feed_forward_layered NNs

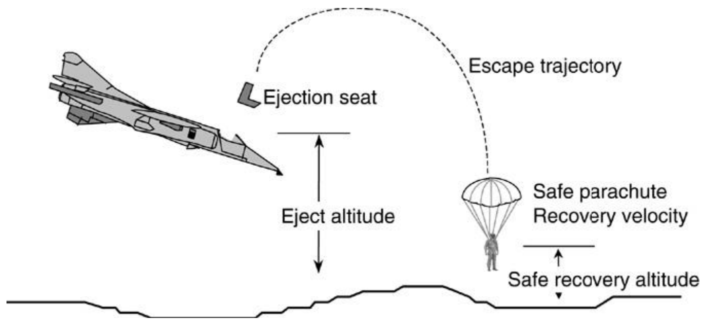

Fig. 5:Safe escape
(Courtesy of E.W. Saad, D.C. Wunsch II, *Neuralnetw.*, *20*, **2007**,78-93)

Applications of NNs in pharmaceutical chemistry, environment and fisheries had steadfast growth since 1990s. We reviewed earlier the prospects of NNs in piscimetrics [316], envirometrics specifically concerned with ozone [308] and Chemometrics [322, 319]. The unignorable benefits of state-of-the-art-NN-architectures in tasks pertaining to pharmaceutical science, drinking water, disposal/treatment of waste water/solid sludge/nuclear wastes, nano-science to product cycle, clinical/instrumental diagnosis of diseases, surgery, ICU-patient care/life expectancy, optimum operating conditions by response surface methodology (RSM) in laboratory/industry, SXR will follow. Till now, common NNs are dealt in algebraic/matrix notation except those of geometric NNs. In the software front, object oriented (OOP) approach is available in MATLAB-neural network toolbox.

Recent advances emphasize tensorial format right from scalar to multi-way data structures as well as for solution methods and computations. The perceivable advantage is brevity/continuity of zeroth to mth order tensors/generalizability/operational ease both for paper-pencil exercise and software code development. Further, 3D-surfaces/2D-contours of I/O transformations, intermediate results and even every step of computation enables one to have mental mapping of one-to-one correspondence of abbreviated mathematical formulae/solution algorithms and geometric representation. This is what missed (save elite groups) during stepwise progressive transition of geometry, algebra, matrix/ extended matrix/ tensor algebras. The emphasis here is notational ease, computational efficiency at the cost of comprehension through visualization of procedures/equations and stepwise solutions. The focused tutorials 'computational tensor (CT) laboratory (lab)' imbibes matrix/vector/scalar manipulations make the swing from one end to the other an enjoyable mental exercise. Expert systems had good beginning in chemistry (Dendral) and medical diagnosis (Mycin, Meta Mycin) in 1960s. Their impact in clinical diagnosis, medical imaging techniques, (robotic) surgery, ICU care, and prediction of mortality/morbidity/post-operative periods in health care is significant.

Physico-chemical properties, biological activity/toxicity data, extreme-phenomena-responses (earth quakes, solar flares, deep-ocean bio-geo-physical-chemical variations) monitoring to control, hind-, now-, fore-cast are very complicated issues. The application of FF_NNs in physico-chemical properties (viz., melting point, solubility, boiling point, density, viscosity, refractive index), pharmaco-chemical relevant values (log P, toxicity, eye/skin irritation, mutagenicity etc.) are extensively studied during the last two decades using hundreds to thousands of compounds and explanatory factors from single digit to two digits from a pool of a few thousands of molecular descriptors. In this decade, multiple- experimental techniques, instruments, experts all direct towards Pareto-optimality in multiple-conflicting objectives. This realistic trend will bring realization of possibility against single-best/best-set of paths to achievable with the state-of-art in time/space with cost-to-benefit-ratio in terms of man/brain/computer time and materials (quantity, purity, nano to mega structures).

Metrics

Classification

A singleton cluster analysis is the simplest of the tasks with one class containing a single pattern. Binary classes comprising two clusters of different number of points/data structures/ distributions/ boundary profile is a well-researched arena for over a century starting with simple Fisher linear discrimination analysis to today's NNs through SVMs. Multiple classes in multiple-dimensions with correlated features/ missing data/ complicated decision boundaries drew special attention. Added to it, if clusters exist in a hierarchical frame, the task becomes still complicated. Further, when a pattern belongs to more than one class at each hierarchical level of the tree, the consequence is that the task is NP hard.

The sweet flavored and eye catching adjectives are sometimes just used to uplift the results like the word 'state-of-the-art-$$$' with relatively simple data sets or comparing with already known inferior methods over decades. The trust worthy paradigms viz. computational intelligence, knowledge based systems emerge only after several evolutions. But, combating with ill-effects, finding solutions for hurdles, incorporating best from the other domains, enhancing synergistic positive features, eliminating negative aspects and/or limitations and at the same time retaining the best characteristics is a long journey. In this attempt the basic philosophy of domain is safe guarded respectably.

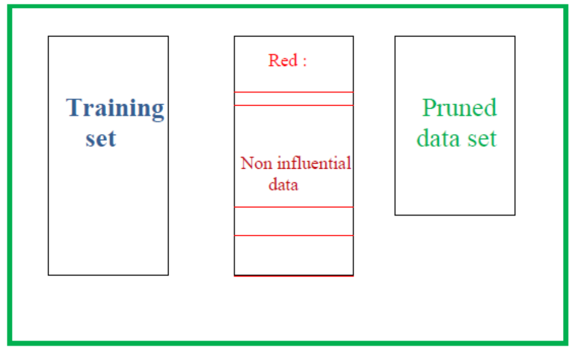

Fig. 6: Pruning data set

Alg. 3: dynamic smote hybrid_MLP_NN

Stage I

- Apply over-sampling procedure to minority class to partially balance classes size

Stage II

- Hybrid algorithm applied
- dataset is over-sampled in different generations of the evolution
  → generates new patterns in the minimum sensitivity class
- → Class with worst accuracy for best MLP_NN
- + Handles class imbalance

Imputation

García-Laencina et al. [179] proposed mlulti-mask earning (MTL) based procedure to train MLP_NN for data sets with missing values. MTL achieves a credible balance between classification and imputation. The experimental results establish that MLP_NN is never worse compared to traditional algorithms. The uninfluential data points are removed for better modeling (Fig. 6)

Imbalanced datasets (Dynamic Smote Hybrid MLP_NN)

Fernández-Navarro et al. [187] reported dynamic smote hybrid_MLP_NN for multi_class classification of imbalance datasets (Alg.3). The accuracy of method is 72.63%.

Feature selection

Hu [258] proposed novel similarity-based perceptron using non-additive indifference indices to estimate an overall rating. It has greater generalization ability than many multi-criteria collaborative filtering approaches. Souza et al. [240] analyzed Box–Jenkins gas furnace and gas mileage data and also fluoride concentration in the effluent of a real urban water treatment plant with MLP_NN using a new variable selection method (chart 6).

chart 6 : Advantages of feature selection procedure

+ Selects lowest number of

Chart 7: Execution time for different Procedures and data sets

Alg.	Time	dataset

variables and variable delays
+ Trained in one epoch
+ Low computational cost
+ Prospects in soft sensor application

BP	Back propagation
EANNE	Embedded ANN evolver
OBD	Optimal Brain Damage
OBDG	OBD-based ANN generation alg
ReliefF	Filter alg
WANNE	Wapper ANN evolver

BPT ReliefF OBD OBDG	few sec 45 min.	Iris Madelon
WANNE	41 min 70–80 h	Iris

Hardware
Intel Core Duo
2.50 GHz
processor
3 GB RAM

Feature selection with rough sets

Earlier, a non-empty core is generated for a discrete dataset by core-generating approximate minimum entropy discretization (C-GAME) procedure. It outputs maximum number of minimum entropy cuts. Tian et al. [209] improved C-GAME (Alg. 4) for feature selection algorithm when rough sets are used and compared its efficiencywith NNs/statistical classifiers (chart 7, 8) on ten UCI machine learning datasets (chart 9). The working of GA and Johnson's algorithms for rough set feature selection (RSFS) is also studied

Chart 8: Feature selection with rough sets

+ Improves classifier performance
+ Removes redundant attributes
+ Retains influential factors
+ Preserve classification power of original dataset

– Processes only discrete attributes
Remedy : Continuous attributes discretized

Alg. 4: Modified C-GAME_Tian

- A constraint added
  + Eliminates possibility of single reduct in C-GAME- dataset
- Upper bound on total number of reducts within a dataset

Discretization

+ Determines core size of a discrete dataset

Discretization methods

— Do not consider the core size during discretization

Chart 9: clustering algorithms compared with C-GAME_Tian

C4.5 k-nearest neighbors	MLP_NN RBF_NN	Recursive Minimum Entropy Partition Chimerge Boolean Reasoning and Equal Frequency discretization

$$$	Def of $$$
Reducts	Feature subsets selected by RSFS
Core	Intersection of all the reducts of a dataset

Comparison of 12 classification algorithms

Fernández-Delgado,et al. [255] compared the functioning of 12 classification algorithms on 42 benchmark datasets including linear Direct Kernel Perceptron (DKP). This procedure coded in C- and Matlab is extremely efficient and has higher accuracy compared to more than 50% classifiers (chart 10). The noteworthy feature is analytical closed form expression is solved and requires only training patterns. The Ws in the feature space minimize a combination of training error and hyperplane margin.

Chart 10: Classifier algs.

MLP	LDA	Random Forest	**k-NN**
RBF	SVM	Bagging of RPART decision trees	
Generalised ART	ELM		
Adaboost			

Bench mark data sets **(MLP_NN + Biogeography-Based Optimization)**

Mirjalili et al. [205] trained MLP_NN with Biogeography-Based Optimization (BioGeo Based.Opt.) algorithm for classification (five datasets) as well as function approximation (six data sets) tasks. A comparison with BP, extreme learning machine (Extr.Lrn.Mach) and heuristic algorithms showed that BioGeo Based.Opt. is competitive with Extr.Lrn.Mach.

Chart 11a: Chaos-based digital modulation

- Chaos Shift Keying (CSK)
- Chaotic On–Off Keying (COOK)
- Differential Chaos Shift Keying (DCSK)
- Correlation Delay Shift Keying (CDSK)
- Symmetric Chaos Shift Keying (SCSK)
- Frequency-Modulated Differential Chaos Shift Keying (FM-DCSK).

Wavelets

- Daubechies,
- Biorthogonal,
- Coiflets,
- Symlets wavelet

Chart 11b: Input and models

Input database

- In vitro research settings
- Drug chemical structure
- Physico-chemical parameters

Models

- MLP_NN (BP)
- Neuro_fuzzy_ Mamdani MISO
- Tfs : sigma, tanh
- Tr : 447 records
- Compounds:175

MLP_NN:
I#-3-2-O#
TF: sigma

Chaos-based signals (MLP_NN + wavelet entropy)

Türk and Ogras [190] analysed 1806 CBDM (chaos-based digital modulation) signals by MLP_NN and wavelet entropy method with a classification rate of 98.76% (chart 11).

Classification of macro-invertebrates

Joutsijoki et al. [162] tested 13 algorithms to train MLP_NN for automatic identification of eight different macroinvertebrates from1350 images (table 8). The scaled conjugate gradient BP is the best training method for this task.

Table 8: Comparision of NNs in identification of macroinvertebrates

NN	%Accuracy
RBF	95.7
Prob	92.8
MLP	95.3

Hierarchical multi-label classification

In hierarchical multi-label classification, the classes are hierarchically arranged. Each sample belongs to more than one class simultaneously in the same level as well as in hierarchy. Cerri et al. [220] proposed a new algorithm (Alg.5) and tested with several hierarchical multi-label classification datasets. The results are better than those for two decision-tree induction methods. For many real life tasks of this decade, modelling/prediction become a challenge even to arrive at Pareto optimality, leave alone an unique analytical global optimal solution.

Alg. 5: Hierarchical multi-label classification

Input
For level =1: #levels_of_hierarchy
- Trains MLP_NN
- Input ← compute predicted values

End
output

Automation of Classification

Although evolutionary methods have been in use for feature selection, structure design and training weights of NNs, there are only a few reports on simultaneous evolution of whole classification/ function approximation task. Mostly, exploiting/ taking advantage at the same time respecting divide-and-conquer strategy has benefited in enhancing accuracy of solutions. Castellani [262] reported embedded approach is better than wrapper method (chart 12, KB.3) for 15 bench mark data sets from UCI.

Function approximation

Guo [11] introduced an adaptive FF-MLP_NN with no user defined parameters for function approximation and pattern recognition. The number of neurons in each hidden layer is equal to NP in the training set. It is like strict interpolation popular in RBF (SI-RBF) from the point of view of number of neurons of the hidden layer. But, Ws are estimated by matrix inner product and pseudo-inverse, which give exact solution. The transmission of learning errors only in the forward direction and layer wise training are the unique features. The procedure is automatic and requires only the desired accuracy. The results show that it is faster than BP and other gradient algorithms

KB. 3: Number of feature vs methods

If	Feature spaces are of small &medium size
Then	Evolutionary algorithms perform best & reject redundant features effectively
If	Feature correlations are preferable on under sampled data
Then	Classical filter-based algorithms
If	Large number of irrelevant features present
Then	Correlation- & saliency-based selection method

Automatic Speech recognition systems

Automatic speech attribute transcription (ASAT) is a lattice-based speech recognition system. Siniscalchi et al. [261] studied deep_NN with five to seven hidden layers and each hidden layer containing up to 2048 neurons in classification accuracy task of phonetic attributes (phonological features) and phonemes. The speaker-independent dataset of Wall Street Journal corpus resulted in 90% accuracy. In automatic speech recognition systems, MLP_NN derived acoustic features along with standard short-term spectral-based ones have excelled in consistent performance. Park et al. [152] introduced discriminative training approach on large training corpora. If the database is very large, multiple individual MLPs are trained, each requiring shorter amount of time, followed by combining the results of the ensemble system. The test bed for this mega system is Arabic large vocabulary speech recognition. It includes both conversation test data and news broadcasted. Mirhassani and Ting [160] studied speech recognition task from utterances of six Malay vowels by 360 children of age between 7 and 12 years. The features are extracted by fuzzy based discrimination method. It is better than Mel-frequency cepstral coefficient. MLP_NN and HMM are applied for speech recognition with success. The weights of MLP_NN are trained by GA.

Chart 12: Evolutionary approach for whole classification task

Wrapper approach NN_structure Input feature vector training Ws	Embedded approach Simultaneous Evolution of whole classifier
Datasets- Bench marks Thirteen PR	Performance comparison Methods ▪ Two manual ▪ two automatic
Inference Embedded >> Wrapper	+ Compactness of solution + Classification Accuracy − Computational costs

Chemometrics

CO_2 absorption data in a packed absorption column: Shahsavand et al. [236] found RBF_NN performs better than MLP_NN in filtering measurement noise in modeling CO_2 absorption data in a packed absorption column. The pilot plant experiment was to separate CO_2 from air at different concentrations and rates of flow of methyl di-ethanolamine and di-ethanol amine (DEA).

Structure X relationships (SXR)

A number of studies have been carried out for many protein ligands and/or drugs targeted to large number of target proteins or receptors of varying affinity. González-Díaz et al. [244] selected ligands or drug-

ALg. 6: Multi-target QSAR (mt-QSAR) classifier	
Input	
MARCH-INSIDE	Calculate structural parameters of drug and target
SLP	20-15-1

Chart 13: QSAR

- + Reduction in time resources
- + Not available compounds
- + Unsynthesized compounds
- - Predict activity against only one protein target
- - Not in online format accessible on public web server

Table 9. QSAR				
		Training		
		NP	**Correct classification**	**%sensitivity**
DTPs		678	611	90.12
nDTPs		3408	3083	90.46
		Prediction		
		NP	**Correct classification**	**%sensitivity**
DTPs		338	310	91.72
nDTPs		1674	1527	91.22

Chart 14: applications of NL MIND-BEST			
Compounds	**Prediction**		
antiplasmodial a cytotoxic activities of oxoisoaporphine alkaloids derivatives	Quantum QSAR study	2-DE, ▶ MALDI-TOF, TOF/TOF MS, ▶ MASCOT search ▶ MM/MD ▶ 3D structure modeling ▶ NL MIND-BEST	NL MIND-BEST prediction of potential target proteins

target pairs (DTPs/nDTPs) either with high affinity or non-affinity. The SLP_NN model (Alg.6) favorably compares with other models. The two unique applications are described in Table 9 (chart 13, Chart 14). NL (Non-Linear) MIND-BEST (MARCH-INSIDE Nested Drug-Bank Exploration & Screening Tool) found a new protein in the proteome of the human parasite Giardia lamblia. It is a promising anti-parasite drug-targets discovery.

XPropRel:

Vaferi et al. [297] modeled solubilities of solid aromatic compounds in supercritical carbon dioxide with SLP using 19 neurons in the hidden layer. Chart 15 shows the prediction with SLP is better than SAFT and PRSV EOS.

Solubility in supercritical carbon dioxide

Lashkarbolooki et al. [199] developed predictive MLP_NN models for the solid solubilities of aromatic hydrocarbons, aliphatic carboxylic acids, aromatic acids, heavy aliphatic and aromatic alcohols in the supercritical carbon dioxide (table 10,11). The NN model is more accurate than Peng–Robinson (PR) and Soave–Redlich–Kwong (SRK) EOSs for the same compound set (chart 16).

Chart 15: solubilities in super critical CO_2 by SLP

Experimental data
published research reports

Input for each solute

- Temperature
- Pressure
- Critical properties
- Acentric factor

Opt #HL neurons
Minimum(.)
- Absolute average relative deviation (AARD%)
- Mean square error (MSE)

Suitable regression coefficient (R2)

Archi-tecture	I#-19-O#
TrnAlg:	BP

Prediction of experimental data	
AARD%	4.99
MSE	7.08 × 10−7
R2	0.99699

Method	Prediction	
	Parameters	AARD%
SAFT	1	16.15
	2	12.32%
	3	7.65%
PRSV EOS		21.10

Table 10: Solubilities by MLP_NN in super critical CO_2

AARD%	0.98
MSE	2.8 × 10−5
R2	0.9981

Table 11: Dataset

Tr	627
val	343
test	970

Prediction of percentage of oil, water and air: Roshani et al. [251] applied NN to predict precisely the water, air and oil (chart 17) from measurements with a nuclear technique in annular multiphase regime. Here, only one detector and a dual energy gamma-ray source are employed.

Material science

Chemical absorbents: Bastani et al. [196] employed MLP_NN for predicting CO_2 loading capacity of chemical absorbents in a broad range of temperature, pressure and concentrations.

Smart materials: In the advanced technical applications, size, weight and performance of smart structures is crucial. It poses a challenge for positioning actuators and sensors on smart gadgets in vibration controlled devices. The piezoelectric ceramics/ polymers based actuators excite only elastic modes of the structures without disturbing rigid-body modes.

Piezoelectric actuators: Mehrabian et al. [243] reported an accurate way of arriving at location of piezoelectric actuators for vibration suppression of flexible structures (chart 18). MLP_NNs along with surface modeling and a stochastic invasive weed optimization algorithm adequately guided for a solution this complicated goal.

➪ Dietetometrics

Loutfi et al. [223] reviewed electronic noses in quality monitoring of foods (meat, fish), milk/milk products and beverages (tea, coffee, wines). The ways and means of bridging gap between research output and industrial practices are focused. Gill et al. [143] applied wavelet and MLP_NN to classify grades of black tea with 82.33% accuracy. The textural features are calculated from tea images followed by wavelet decomposition into sub-bands. ANOVA assisted as a check tool in assessing accuracy. Mateo et al. [200] successfully predicted deoxynivalenol (DON) accumulation in barley seeds by F. culmorum with MLP_NN and RBF_NN (chart 19).

Chart 16: Cubic Peng–Robinson (PR) and Soave–Redlich–Kwong (SRK) equations of state with mixing rules	
1.	Wong–Sandler rule
2.	Orbey–Sandler rule
3.	Van der Waals one fluid rule with one (VDW1)
4.	Van der Waals one fluid rule with two (VDW2) adjustable parameters
5.	Covolume dependent rule
6.	Esmaeilzadeh–As'adi–Lashkarbolooki mixing rule

Chart 17: I/O in nuclear technique	
Input	**Output**
Detector output ☞ First and second full energy peaks	Percentage of ☞ Oil ☞ Water ☞ Air
Error criteria MAE < 1	

Chart 18: Location of piezoelectric actuators on smart materials

- **Goal :** Optimal placement of piezoelectric actuators on smart fin
- **objFN :** Max(FRF peaks)
- **Discrete data:** simulation with finite element method
- Model :Surface fitting
- **Method:** Three MLPs

Error criteria

- Max(weighted summation of FRF peaks)
  - Invasive weed optimization

Chart 19: forecast accumulation of deoxynivalenol in barley seeds

Input

- Temperature (20–28 °C),
- Water activity (0.94–0.98)
- Inoculum size (7–15 mm diameter)
- time

output

- DON concentration

Models

- MLP_NN
- RBF_NN

Error criteria

- MSE

Performance

- SLP>> MLP
- R BF_NN >>MLP
  - – RBF_NN has large number of neurons

➪ Technometrics

(Technology + metrics)

Shape optimization: Jahangirian and Shahrokhi [154] reported MLP_NN trained with real-coded population dispersion (PD) GA for shape optimization of transonic airfoils (Alg. 7). The computational time of this algorithm is 60% less than that for GA.

Rolling stainless steel: Park et al. [231] reported echo state NNs is better than MLP_NNs in rolling stainless steel and silicon sheets with Sendzimir mills (ZRMs). A small diameter of ZRM is bent easily; it is desirable to have high rigidity with complex shapes. MLP has a limitation of loss of shape recognition data.

Alg. 7 GA trained MLP_NN

Step 1: Cal objective function value with MLP_NN
Step 2: Real-coded GA with population dispersion
+ Increases robustness and convergence rate
Step 3: New airfoil shape parameterization method
+ Optimal efficient shapes at viscous flow conditions.
Step 4: Dynamic retraining and normal distribution of the training data
+ Well-trained parts of the design space of NN are determined

Fretting wear: Anand Kumar et al. [247] predicted fretting wear behavior with SLP_NN trained with gradient descent algorithm (chart 20). The untreated Ti–6Al–4V fretted against alumina and steel counter bodies and treated surface mechanical attrition are used as samples in the study.

Chart 20: Prediction of fretting wear with SLP_NN

- Input
  - Normal load
  - Hardness of counterbody material
  - Surface hardness of test material
- OutPut
  - Tangential force coefficient (TFC)
  - Fretting wear volume
  - Wear rate

	%Accuracy
TFC	96.6
wear volume	96.1
wear rate	92.2

Alg. 8: MLP-NN + PSO for liquefaction potential

- Mesh_free-local RBF- differential quadrature procedure
  Equations of seismic accumulative excess pore pressure are solved
- PSO
  best location of the trench layer found
- MLP_NN (BP)
  data training
- Output of NN
  liquefaction potential prediction

Liquefaction potential: Choobbasti et al. [298] reported MLP_NN and PSO models to find minimum liquefaction potential through calculating optimum positions of trench layer around a pipeline (Alg. 8).

Alg. 9: Pareto optimal solution

Phase I: MLP_NN
Prediction of break power
Phase II: modified NSGA-II
Multiple-objective-optimization
ε-elimination algorithm
+ preserves diversity of MOO solutions.
Phase III: TOPSIS
Best compromise solution.

- Output
  Max(brake power)
- Multiple objFn
- Min (.)
  - BSFC
  - PM
  - NOx
  - CO
  - CO2

Alg. 10 : MLP_NN model for chemical flooding

- Trained initial structure of the network
- Optimize architecture of the trained network
  - Architec: I#-8-O#
  - TrAlg: Bayesian regularization
- Optimum structure compared with RBF_NN neural network, quadratic and multi-objective regressions

Error is always less than 5%

- Neuro-simulation of chemical flooding reliable
- Inexpensive
- Fast
- Accurate prediction of both RF and NPV in one model

Optimal operation of biodiesel engine (MLP_NN + NSGA-II Pareto): Etghani et al. [135] reported a Pareto optimal solution for the multi-objective performance and emissions of a diesel engine using biodiesel (Alg. 9).

Oil recovery of reservoirs: Karambeigi et al. [238] reported modeling of chemical flooding (which enhanced oil recovery of reservoirs) using surfactant and polymer via prediction of both recovery factor (RF) and net present value (NPV) with MLP_NN (Alg.10). Vaferi et al. [239] proposed MLP_NN to develop data driven automatic recognition of oil reservoir model. The training and testing data is simulated by analytical solutions of popular physical concepts (chart 21).

Fault detection in distillation plant: The abnormal operations in a plant develop anomalies with a consequence of crossing the safety limits. An early detection prevents catastrophic events in chemical process industry as well. Chetouani [279, 296] reported MLP_NN for fault detection using Wald's sequential probability ratio test (SPRT). The detection of faults before breakdown avoids quality of product, major damage to the machinery and accidents to humans. The data for training and testing were generated at different operating conditions. The other data set is realistic fault developments in a laboratory scale distillation plant. The statistics viz. mean, SD of residuals are from NARMAX.

Chart 21 MLP_NN for oil reservoir detection

ॐ HL_neurons :12 ॐ TrAlg.: Scaled CG Minimization ▶ MeanRelErr ▶ MeanSquareErr	ॐ Homogenous and dual porosity reservoir models ▶ Outer boundaries ⇨ No flow ⇨ constant pressure ⇨ infinite acting ⇨ Single sealing fault boundaries

Fault detection in fan engine of aircraft: Tayarani-Bathaie et al. [256] reported a method to detect and isolate faults in dual spool turbo fan engine of aircraft using MLP_NN with IIR filter in neurons (Alg. 11). It is validated with a large number of simulation datasets.

Alg. 11: Fault detection with MLP_NN using IIR filter

Phase I : Model development

- ॐ Infinite impulse response (IIR) filter is used in HL neurons of SLP→ Dynamic NN
- ॐ Train multiple Dynamic_nns using different operating modes of healthy and faulty engine conditions
- ॐ Fault detection and isolation scheme developed

Phase II : Test with real life task

- ॐ Cal NN_output
- ॐ Cal residual between NN_output and measured engine output
- ॐ Isolate and detect fault in engine operation

Gasoline engines fault detection: In the case of gasoline engines in automotive vehicles, malfunctioning/faulty components are detected based on analysis of ignition patterns of engine. The learnt/work experience of mechanic and code books to probe into wave form of ignition pattern is a sought after and many a time successful exercise. But, the dead end of manual approach is many faulty ignition patterns are very similar to the naked human senses, necessitating machine learning approach. Vong and Wong [192] picked up features in ignition profiles from multi-procedural protocol. The multi-class_LS_SVM has higher diagnostic accuracy compared to MLP_NN (Alg. 13)

Alg. 12: MOO with MLP_NN + ABC

Phase 1: Engineering Equation Solver software Estimation of parameters for second and third pump for different values of the outlet pressures Phase 2: Three MLP_NNs trained with data of phase 1. Phase 3: For each ojective of multi_object_Fn, one MLP_NN trained	**MulObjfns for estimation of parameters** ❆ Thermal efficiency ❆ Exergy efficiency ❆ Specific work

Process Engineering: Saghatoleslami et al. [235] –predicted overall efficiency of sieve tray with 1.21% error using MLP_NN for hydrocarbon system with different compositions (chart 22). Balcilar et al. [208] made a comparative study of NNs for estimation of drop in pressure and convective heat transfer of R134a. Rashidi et al. [170] reported a hybrid algorithm (Alg. 12) of MLP_NN with ABC for multi-objective optimization (MOO) of water for regenerative Clausius Rankine cycles (CRC) and R717 for organic Rankine cycles (ORC) with two feedwater heaters (Chart 23). The results throw light on optimal objective functions and decision variables of the task.

⇨ Envirometrics (Environ-metrics)

Chart 22a: Components of binary mixture	
1	2
Ethanol	Water
Acetone	Water
Methanol	Water
Acetic-acid	Water
Toluene	Water
Mibk	Water
Aniline	Nitrobenzene
Cyclo-hexane	n-heptane

Alg. 13 : Comparision of MLP_NNand multi-class_LS_SVM in Fault diagnosis of gasoline engines

- wavelet packet transform
  Features of the ignition pattern extracted
- Cal statistics of occurrence of features over the frequency sub bands of the pattern
- Classification of engine faults using
  - + Reduction in number of diagnostic trials

Chart 22b: Prediction of sieve efficiency

Model	% of abs(error)
MLP_NN	1.21
Corr_Garcia -Fair	18.22

Chart 23: Modeling of heat transfer

Set	Test	Trn	Val
I	33	120	30
II	68	300	---

Err : ±5% ; CV : 5 fold

- SLP (5-13-1)
- RBF_NN
- GenReg_NN
- ANFIS

Conventional energy, Pollution and alternate energy sources: The quantum of energy (electrical/nuclear/fossil fuel/petrol (gas)) consumption per capita is a sign of advancement and level of civic life. But, during last century, increasing energy consumption led to release of pollutants (including greenhouse gases, solid wastes) with a consequence of perturbation of eco-system beyond bringing it back to normalcy. Also, ill effects on human health, agriculture, natural ecosystems, and earth temperature are now a menace and threat for earthly world. To combat with this monster, alternate sources of energy (solar, hydrogen, wind, methane nodules etc.) are researched and technology is now available. But cost, time tested-proofs, policies, tech/knowledge transfer and mind set (most subtle factor) are yet hurdles in implementation all over the globe to at least partially relieve from exceeding local pollution levels. Thus, accurate estimation and forecasting of renewable (conventional, alternate) energy is vital for policy and decision-making process in energy sector.

Wind power: Wind power and solar panels are alternate sources of energy and the best part is they are pollution free. Yeh et al. [211] reported a hybrid forecast NN model for wind power at Mai Liao Wind Farm, Taiwan. PCA and partial autocorrelation function select the features in the experimental data for a five year period (September 2002 to August 2007). MLP_NN trained with improved PSO excels many other algorithms in vogue.

Chart 24: Transient HCCI modeling with MLP_NN and RBF_NN

⇨ Input
- ❄ Net mean effective pressure
- ❄ Combustion phasing
- ❄ Maximum in-cylinder pressure rise rate
- ❄ Equivalent air–fuel ratio

⇨Preprocessing
- PCA

⇨Models
- MLP_NN, RBF_NN
  - + Highefficiency
  - + Reduced emissions

Homogeneous charge compression ignition (HCCI): Janakiraman et al. [127] developed MLP_NN model for Homogeneous charge compression ignition (HCCI) (chart 24). It is a futuristic combustion technology. The combustion behavior during transient operation involves complicated nonlinear dynamics difficult to develop physics based models.

Renewable energy: Azadeh et al. [282] developed MLP_NN to forecast renewable energy consumption using monthly data between 1996 and 2006 in Iran with environmental and economical explanatory factors. The results are 99.9% accurate and better than fuzzy regression approaches. This study is vital guide for policy makers and also useful for regions with no base line data.

Atmospheric general circulation model (ECHAM-X): Max Planck Institute for Meteorology developed Global Climate Model named ECHAM (EC: abbreviation of ECMWF; HAM(burg) place where its parameterization package was developed). Echam5 [280] corresponds to fifth-generation atmospheric general circulation model (ECHAM5) and is in FORTRAN 95. ECHAM6 is atmospheric general circulation model, and couples the two processes.

Acronym	Meaning
MPI	Max Planck Institute
MPI-M	MPI for Meteorology
MPI-OM	MPI ocean model
ECHAM-X	X : 4, 5, 6

Solar radiation: Voyant et al. [169] studied effect of exogenous meteorological parameters and endogenous inputs on MLP_NN to predict daily solar radiation on surfaces. For two sampling stations (for years 2006 and 2007) in Corsica Island, France, inclusion of exogenous variables decreased RMSE by 0.5 and 1% compared to those of endogenous parameters alone. Voyant et al. [121] reported single (MLPNN, ARMA and persistent) and hybrid models with Bayesian rules for prediction of solar radiation with high accuracy (table 12). This Information of hourly global radiation is a novel tool for grid managers of electrical distribution. It throws light on how to plan for fluctuations in clouds and optimize injection of alternate energy. Dong et al. [167] found MLP_NN hybridized with exponential smoothing state space (ExpSmoothStateSpace) excelled traditional TS models for hourly forecast of solar irradiance using cloud cover index and category of clouds in Singapore. Geostationary satellite images provide information of cloud and SOM outputted cloud cover index. Caner et al. [195] modelled thermal performances from the experimental data obtained through solar air collectors during five days (between 10.00 and 17.00 h) at Karabuk (chart 25). Matlab nftool module is used for MLP_NN trained with Levenberg–Marquardt (LM) algorithm.

Alg. 14: Forecast model for outdoor temperature	**Chart 26: Factors affecting forecast accuracy of MLP_NN+ wavelet Transform**
▪ Input: time series - High variability ▪ Apply discrete wavelet transform ○ Divides TS into sub-sequences (named coefficients) frequency wise + sequences of past data decomposition + Preserves temporal characteristics ▪ Prediction with MLP_NN → future subsequences of 4 h and 30 min. ▪ Outdoor temperature and thermal power consumption ← sum(coefficients)	○ # past sequences ○ Time interval **Discrete wavelet transform** ♈ Wavelet order ♈ Decomposition level **NN** ⇨ Topology ⇨ Trn. alg.

Chart 25: Models for prediction of daily solar radiation
ॐ Persistence ॐ ARIMA ॐ MLP_NN with preprocessing of inputs ॐ Endogenous (Summer) ॐ Endogenous + exogenous (Cloudy period)

Table 12: Prediction of solar radiation by different paradigms

Model	% RMSE
Single	
Persistent	51
MLP	40.5
ARMA	40.5
Hybrid	
MLP_NN+ Bayesian	**37**
ARMA + Bayesian	**37**

Forecast of outdoor temperature with MLP_NN+ Discrete wavelet transform

Eynard, et al. [173] made a short term (four hour) forecast of outdoor temperature and thermal power consumption to optimize and control a multi-energy district boiler in La Rochelle, west coast of France. The modeling paradigm is a hybrid environment of NNs and multiple-curve resolution (Alg. 14, chart 26).

Environment monitoring: In the second half of last century, environment monitoring was mostly manual and point estimates were used to summarize or derive information for managers. Availability of hyphenated instruments, remote/automatic monitoring centers and satellites outpour multidimensional data (in shorter intervals) of longer time series called Big-data. It is out-of-question to rely on classical data structure and statistical procedures. Interval estimates, multidimensional control charts derived from nature inspired algorithms are indispensable. But, the transfer of whole scenario in all environmental labs and quality control centers is not pragmatic overnight. Thus, a slow pace of smooth transition is implemented in a phased manner depending upon intensity of pollution.

Pollutant (NO_x, SO_x) monitoring: Balsama et al. [137] reported the results of MLP_NN and GenReg_NN models for ten chemical species during 1970 to 2008 from Emissions Database for Global Atmospheric Research (EDGAR) over the globe. It is considered as a first ever type of modeling and forecast study and non-linear trends have been found in 3000 subsectors. GenReg_NN excelled for imputation of missing data in EDGAR_time_series . PCA resulted in two clusters, one corresponding to emission trends of CO_2, SO_2 and NO_x and the other to CH_4. MLP_NN is better in multi-step-ahead forecast compared to the GRNN, although it has slightly higher absolute mean error. A deep level study revealed eleven years period is optimum for predicting three consecutive years ahead and accuracy is 98%.

Table 13: Performance indices of MLP for forecast of PM10 and PM2.5

Index	Thessaloniki	Helsinki
% Kappa	60	60
Agreement	0.80	0.85

PM10: Voukantsis et al. [286] applied MLP in the one-day-ahead-forecast of concentration levels of PM10 and PM2.5 for urban areas of Thessaloniki and Helsinki in Greece and Finland (Table 13), An inter comparison of patterns of air pollution in the two cities was made with PCA.

Pollen: Csépe et al. [285] predicted ragweed pollen daily concentrations and also 1–7 days ahead alarm levels (chart 27) in Szeged (Hungary) and Lyon (France) making use of time series data during the years 1997–2006.

Chart 27: Predictive models and factors in daily Pollen (ragweed)

Input	#
Meteorological	8
Pollen/ alarm level	1
Serial number of given day of the year within pollen season	1
Models	
MLP	
M5P	
REPTree	
DecisionStump	
MLPRegressor	
Factor analysis	

Chlorophyll trends: Millie et al. [176] studied chlorophyll trends with MLP_NN and polynomial regression (table 14). The meteorological and hydrological data were measured in 2009 using autonomous instruments in Sarasota Bay, Florida (USA).

Pollutants degradation: Vaferi et al. [221] applied SLP_NN for prediction of extent of degradation of pollutants (MTBE, BTEX) in contaminated synthetic waste water (chart 28). The absolute average relative deviation AARD and MSE are 10.26 and 5e-4 for SLP with 15 hidden neurons. Brandão et al. [201] predicted for the phenol concentration as a function of time with MLP_NN using experimental degradation results of the organic pollutant from direct contact thermal treatment (DiCTT) process

Table 14: comparision of MLP_NN and polynomial regression for chlorophyll data

	CC (measured, Modeled conc.)	Method
Chlorophyll (CHL) a	>0.90	NN
CHL classes	83% :Accuracy 0.79 to 0.91 : Precision	Categorical ANNs
CHL concentrations= f(temperature,salinity)	Adj. r2 = 0.99, p < 0.001	A 10th-order Chebyshev bivariate polynomial
	0.80 to 0.90 : Model efficiencies	

⇨ Water resources forecast

The long term forecast of water resources in large perineal rivers is of global importance for sustenance of life on the planet earth. In spite of multi-facet advances, predictive modeling of hydrological phenomena from micro-processes is not yet fool-proof. Su et al. [280] modeled hydrological variables using climate factors as explanatory variables. The case study is prediction of precipitation and stream flow in Songhuajiang River basin, China during 2011–2050. Here, climate conditions of the ECHAM5/MPI-OM under three SRES (Special Report on Emissions Scenarios) and the ensemble mean of the CMIP5 models under three RCP scenarios are considered.

Chart 28: MLP_NN model for degradation of organic pollutant degradation

Operational parameters	**Value-units**
Molar stoichiometric ratio of phenol /hydrogen peroxide	170 L h−1;
Burner dissipated power	38.6 kW at 10% excess air
Initial $[phenol]_0$	500 mg L−1
Combustion gas recycling rate	50%.

Response	**Instrument**
Concentrations: phenol, catechol, hydroquinone, para-benzoquinone	HPLC
TOC	TOC analyser
pH	pH meter

	% R
optimal condition for complete phenol degradation	75
TOC conversion	60

Model :	SLP (2-7-3)
R^2 :	0.99
Software:	Statistic 8.0" "Neural Networks"

Storm water runoff: He et al. [225] reported a predictive MLP_NN model for quality (chart 29) and quantity of storm water runoff. The data of previous 3-week total rainfall improved forecast of turbidity and conductance. This model is better than multiple linear/ non-linear regression (MLR, MNLR) models. The mechanistic details of discharge of pollutants induced by rainfall are still incomplete and thus data driven NNs are appropriate.

Chart .29: **Storm water runoff quality**

- Quality
  - Turbidity
  - Specific conductance
  - Water temperature
  - pH
  - Dissolved oxygen
- Input variable selection
  - Partial mutual information

Forecast of river runoff: Piotrowski and Napiorkowski [118] reported for the first time the application of MLP_NN with higher order neurons for prediction of runoff in hydrology. In this higher order_ FFNN, inputs are raised to exponential of weights for neurons in hidden layer. As training of unbounded weights is difficult, the bounded interval of [-1, 1] is chosen. The hybrid algorithm of Levenberg–Marquardt and differential evolution with global and local neighborhood method excelled MLP_NN and conceptual hydrology model for the dataset at Annapolis River, Nova Scotia, Canada. These authors [226] applied the hybrid algorithm to forecast of daily rainfall–runoff in Annapolis catchment area (chart 30). This location is selected forecast of rain based on complicated factors and climatic conditions. LM and diff.evol. with global and local neighbors are superior. A multi-start approach surmounted trapping of LM in local minima.

Cold-water reservoir: Siahoui et al. [168] compared MLP_NN with analytical solution for thermal characteristics of an underground cold-water reservoir (chart 31). The inference is that a stable thermal stratification is preserved in the reservoir all through the withdrawal cycle.

Chart 30: Complex factors in runoff and training algorithms for MLP_NN

Levenberg–Marquardt Alg. Versus

- Differential Evolution (Diff.Evol.) (version 1)
- Distributed Diff.Evol. with Explorative–Exploitative Population Self-Adaptive DE
- Diff.Evol. with global and local neighbors
- Grouping Diff.Evol.
- JADE
- PSO
  - Comprehensive learning
  - Efficient population utilization strategy PSO

River flow characteristics

- Seasonal changes in runoff
- Rapid floods
- Dry summers
- Severe winters with snowfall
- Snow melting
- Frequent freeze and thaw
- Presence of river ice

Chart 32: Input for evapotranspiration model

Input

- Sodium chloride
- Concentration in feed solution, C
- Feed temperature, T
- Feed flow-rate, Q
- Operating hydrostatic pressure, P

Response

RO performance index

Optimum operating conditions

- Four input variables
- Brackish water
  - 6 g/L
  - 30 g/L

Chart 32b: Comparative modeling of evapotranspiration

Input (daily climaticdata)

- Solar radiation,
- Air temperature,
- Relative humidity
- Wind speed

Sampling site

- Santa Monica, LA, USA

Models

NN

- **MLP**

Empirical

- CIMIS Penman,
- Hargreaves
- Ritchie

Perforance statistics

- Root mean square error
- Mean absolute error
- Determination coefficient

Inference: S-ANFIS >> [G-ANFIS and MLP]

G-:	Grid
S-:	Subtractive clustering

Chart 31: Underground cold-water reservoir thermal stratification

Boundary condition of temperature distribution in reservoir

Linearized	Analytical soln
Non-linear	MLP_NN

⇨ Prediction of water resources

Rampone [128] applied MLP_NN to predict 3- and 6- months ahead of water resources at karstic aquifers in the Terminio massif (Southern Italy), especially in high stress months of July and August. The rainfall–discharge relationships are modeled with tenfold CV for the aquifer which supplies water in the Naples area, Southern Italy. The three-month and six-month-ahead discharge forecast errors are 5 and 10%.

Evapotranspiration: Cobaner [227] compared the performance of grid partition and subtractive clustering based ANFIS and MLP NNs for evapotranspiration (ET0) data in Los Angeles. FAO-56 Penman–Monteith equation is used to calculate ET0. A comparative study showed S-ANFIS excels MLP (chart 32) and CIMIS Penman, Hargreaves_Ritchie methods based on RMSE, R^2 and MAD.

Waste water treatment: Bagheri et al. [278] applied MLP_NN and RBF_NN to model data of municipal wastewater treatment (chart 33) in a sequential batch reactor.

Wastewater treatment plant: Ay and Kisi [228] integrated MLP with k-means and applied in modeling of COD in the upstream of the municipal wastewater treatment plant at Adapazari province of Turkey. The input variables are daily measured pH, discharge, temperature and TDS. The hybridization of MLP_NN and k-means is superior in terms of RMS, mean absolute error and R in prediction. The results of MLR, MLP_NN, RBF_NN, subtractive clustering /grid-partition FIS_NN models are compared.

Chart 33: Wastewater treatment with MLP_NN and RBF_NN

Input	Output
Influent concentration (IC) Filling time (FT) Reaction time (RT) Aeration intensity (AI) SRT MLVSS concentration	Effluent concentrations TSS TP COD NH4+-N

	Optimum conditions
FT	1 h
RT	6 h
Aeration intensity	0.88 m^3/min
SRT	30 days

Removal efficiencies	
TSS	86
TP	79
COD	94
$NH4^+$-nitrogen	93

Inference : MLP_NN > RBF_NN

Automatic detection of bin level and amount of solid waste: Earlier, many approaches viz. GIS, Radio-frequency Identification (RFID), or sensor intelligent bins have been proposed for Solid Waste Management (SWM) system. The key point is to fix the position of camera to obtain bin image. Islam, et al. [300] put forward dynamic time warping (DTW) procedure to detect and crop the bin area. The features of image of bin are calculated with Gabor wavelet (GW) and inputted to MLP_NN. The output consists of level of bin and amount of waste inside it. The statistical analysis of classification is performed with ROC and the achieved accuracy in this study is 98.50%. Hannan et al. [301] proposed MLP_NN to detect automatically the waste bin level of filling ((table 15).). The bin image texture is analyzed with gray level aura matrix (GLAM) approach.

Table 15: solid waste bin level detection with gray level aura matrix

Model	%Classification	
	Class	Grade
MLP	98.98	90.19
k-NN	96.91	89.14

Crack propagation in pavement ([MLP or RBF] + FiniteEleMeth): Gajewski et al. [150] made sensitivity analysis of non- destructive testing of crack propagation in pavement bituminous layered structures with hybridization of FF_NNs (MLP, RBF) with finite element method (chart 34). The outcome is cracking increases with lowering the bituminous layer (B2) thickness. The cracking of the subgrade layer is less influenced by asphalt layer (B1) thickness.

Desalination: Khayet et al. [233] compared predictive models for desalination by reverse osmosis (RO) process with RSM and NN models. NN far excelled the sought after quadratic RSM model.

The maximum RO performance indexes are experimentally attained with optimum operating conditions from Monte Carlo simulations.

Chart 34: Input to [MLP or RBF] + FiniteEleMeth

Inputs

For each layer of creating pavement
- ⇨ Thickness of layers
- ⇨ Load value
- ⇨ Young's moduli

end

Ocean floor: Kajiyama et al. [276] predicted execution time of MC simulations with MLP_NN. The input data are execution times recorded for different cases of simulation under a variety of environments. The ultimate goal this pursuit is prediction of execution times for simulations of parallel Monte Carlo (MC) radiative transfer with applications in ocean color.

⇨ Geometrics (Geology + metrics)

MLP_NN + PSO for rock fractal parameters: The determination of fractal dimension of roughness profiles (D) is still a complicated task due to both stochastic and systematic errors which cannot be

Alg. 15: Hybrid MLP_NN and PSO for fractal parameters of rocks

Step 0	☞ Simulate large number of fractional Brownian profiles at varying numerical

modeled by an explicit function. Babanouri et al. [215] applied a hybrid of MLP_NN with PSO procedures to estimate roughness profiles D of Barton's standard roughness profiles and digitized surfaces of natural rock fractures (Alg. 15). In each iteration information is exchanged with MLP_NN and PSO to optimize values of fractal parameters.

	values of D and standard deviation ☞ Extract relevant statistical features were
Step1	▶ Inputs ☞ Features of profile ☞ RMS of profile ☞ First derivatives
Step2	Iterate until fractal parameters values optimized exchange information between PSO and MLP _NN end iterate
Step3	Output Best set of fractal parameters for a rock fracture profile

Thermal conductivity of rocks: Gitifar et al. [216] reported MLP_NN and ANFIS models for effective thermal conductivity (ETC) of porous reservoir rocks with temperature, pressure, porosity and bulk density as inputs (table 16).

Rock permeability: Bagheripour [217]) found committee of NNs (Comm_NN) is an adequate model (Alg. 16) for reduction of rock permeability from well log data from Kangan and Dalan Formations of South Pars Gas Field-Iran.

Earth quake: Akhoondzadeh [117] reported the adequacy of MLP_NN (over ARMA) with total electron content (TEC) time series of 20 days duration with two hour resolution in detecting seismo-ionospheric anomaly to estimate earthquake parameters. The results are similar for wavelet and Kalman filter models.

Table 16: Modeling of conductivity of rocks

Model	AARD (%)
MLP_NN	2.91
ANFIS	3.80
NP :872	
AARD:	average absolute relative deviation

Alg. 16: Committee of NNs for rock permeability

- ▶ Phase I : PCA eliminates overlapping conventional well log data
- ▶ Phase II: Prediction of rock permeability by MLP_NN, RBF_NN, and generalized regression NN with PCs as input
- ▶ Phase III: prediction of rock permeability output of NNs is inputted to CNN. A weight factor represents the relative influence of each NN in overall output. Weight is assigned to each NN by GA.

Paleoclimatology: Carro-Calvo et al. [263] reconstructed paleoclimatic variables of winter precipitation in the Mediterranean back to year 1700 using MLP_NN.

Mining: Kapageridis and Triantafyllou [155] developed LavaNet which employs RBF_NN, MLP_NN and SOM_NN implemented in Stuttgart Neural Network Simulator. This integrated package is in a format familiar to geologists and mining engineers. VULCAN (Fig. 7) is full-fledged software with advanced graphics, database and a set of physical models. LavaNet is executed within VULCAN and training data can be pulled either from the available drill hole database or simulated datasets from block models from model_base. The results of NN model for mining task (chart 35) are also viewed in 3D-graphics.

Data mining: Nisanci et al. [189] compared efficiency of MLP_NN with data mining procedures for prediction of electric field level in the reverberation chamber. The design and optimum values of extrema (mode and null) of electric field which depends upon the stirrer position are studied.

⇨ Medicinometrics

Physical as well as mental health is a cumulative consequence of genetic factors, life style and environment quality. The science of medicine, intervention procedures and surgery are to put in right direction of wayward micro to macro processes during the life time of a human being. The near perfection diagnostics with gold standard approaches, drugs with minimum side effects, robotic surgical theatres and personal concern of individuals diminished mortality rate in U.S. due cardiac disease, carcinoma, chronic lower respiratory disorders, stroke in brain/kidney, Alzheimer's disease, diabetes, influenza and kidney problems during 2011-2012. The ensured life span of new born now is 76 years for a male child and 81 years for a female baby. The state-of-art of medicinometrics with MLP_NNs follows.

Chart 35: Typical data mining procedures

- Regression
  - Linear
  - Pace
  - Discretization (RD)
- **NN**
  - **MLP**
- Random SubSpace
- M5P
- RepTree
- Decision Table models
- KStar

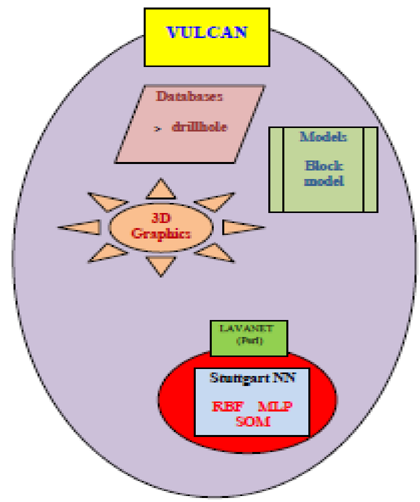

Fig. 7: LavaNet inside VULCAN for mining

☞ Cardiac diseases

Cardio-toxicity risk: Polak et al. [132] proposed estimation of structure- cardiotoxicity risk potential of particular drug_

Chart 36: Multi-Filtration Feature Selection strategy

- Data sets : 22 (Medical)

Four stage strategy
- Feature extraction
- Feature subset selection
- Feature ranking
- Classification

Models
- Naïve Bayes
- SVM
- MLP
- J48 decision tree

Chart 37: MLP_NN hybrid alg for ECG classification

Diagnosis of arrhythmias

For each QRS region
Detect major events
image ← Discrete wavelet transform

image divided into eight polar sectors

Feature ← Cal curve length of each excerpted segment
End
Hybrid alg.

Hybrid alg
- Two MLPs of different architecture
- Prob NN
- SVM

Input
- ECG signal
- Heart beat data

Data source	%,Accuracy of model
MIT-BIH	98.18
8 arrhythmias case	97.37

relationship (SCardToxR) with lipophilic (log P) parameter value from MLP_NN and FIS models. The focus of this study is on developing at least an empirical model for the hERG channel–drug interaction triggered by drugs from publicly available databases.

Gharehbaghi et al. [252] introduced a time growing neural network (TimeGrow_NN) for classification of short-duration heart sounds and to detect heart systolic ejection click in children. A dataset of 614 samples with normal and abnormal cardiac cycles are analysed using different types of NNs (table 17).

Sasikala et al. [120] employed four-stage feature extraction method in feature selection and classification (chart 36) of increased accuracy for medical data mining. Variance coverage parameter is fine-tuned to arrive at a model through optimal influencing features.

Table 17: systolic ejection click in children

Input :	Spectral power in adjacent frequency bands	
$$$_NN	**% Correct Classification**	**Sensitivity**
Time Grow	**97.0**	**98.1**
Time delay	85.1	76.4
MLP	92.7	85.7
⇨ TimeGrow_NN		
✚ Better immunity to noise		

Arrhythmias

Homaeinezhad et al. [289] proposed a hybrid NN (chart 37) for arrhythmias and analysed with MIT-BIH arrhythmia database.

☞ Cancer

Classification of benign and malignant masses

Tahmasbi et al. [157] used Zernike moments as descriptors of shape and margin characteristics in minimizing false negatives in breast cancer detection by mammography (Alg. 17)

Alg. 17 : Performance of MLP_NN for classification of benign and malignant masses in breast

- Input regions of interest (ROIs) are segmented manually
- Preprocessing → two processed images of translated masses
- Image-1: represents shape characteristics of mass
- Image-2: describes margin characteristics
- Two groups of Zernike moments are extracted
- Feature selection stage
- MLP_NN

ॐ MLP_NN Training	Sensitivity:	0.976
BP	Specificity:	0.975
Opposition-based Learning	FNR:	0.0
	FPR:	5.5

☞ Lower Respiratory diseases

Bhuvaneswari et al. [163] classified (chart 38) bronchitis, emphysema, pleural effusion and normal lung with more than 90% accuracy with MLP_NN.

Chart 38: Discrimination of lung (lower respiratory) diseases

Input::	▶ CT images
Pre-processing	Gabor filter transform ✚ Walsh ✚ Hadamard
Feature extraction	▶ MAD technique
Selection of top ranked features	GA
Classification	decision tree

	KNN MLP-NN
CT: Computed tomography	
MAD: Mean absolute deviation	

Liver transplantation

Child–Pugh–Turcotte score: The subjective and objective clinical parameters (chart 39) determine the score and are used for liver transplantation (LT) based on 'sicker patient first'. Here subjective parameters are influenced by treatment with diuretics or paracentesns for ascites and lactulose for encephalopathy. Mayo model was later named as MELD and predicts three months mortality of 227 in queue for LT (chart 40). This is taken as priority level to overcome normal waiting pattern 'sicker patient first'. It was found MLP_NN with 18 different liver transplant recipient and donor variables predicted more accurately outcomes post-LT compared to MELD and SOFA scores. Singal et al. [219] reviewed the state-of-the-art-MLED and opines that it continues to be an acceptable score till a new one comes into prominence with authority and approval.

Chart 39: Liver allocation score
Objective
Severity
1. Serum albumin
2. Serum bilirubin
3. Prothrombin time
Subjective
4. Ascites
5. Encephalopathy

	Liver disease
CTP	Child–Pugh–Turcotte
HRS	Hepatorenal syndrome
LT	Liver transplantation
MELD	Model for end-stage liver disease
SOFA	Sequential organ failure assessment

Chart 40: MELD score

Best predictor of

- Survival period after transjugular intrahepatic portosystemic shunt
- Mortality of patents with end-stage liver disease
- Survival of patients with alcoholic hepatitis, following variceal hemorrhage, infections in cirrhosis
- Post-surgical life span of patients with cirrhosis including liver resection, trauma, and hepato-renal syndrome

Brain and CNS disorders

Resting state network (RSN) from fMRI: Hacker et al. [267] modeled blood oxygen level dependent (BOLD) correlation maps with specific resting state network (RSN) identities with MLP_NN. The network outputs more spatially specific RSN maps compared to dual regression and LDA. Further, RSN topography values in individuals are correct even in the brain regions not represented in the training dataset.

Detection of Alzheimer's disease: Park et al. [148] detected Alzheimer's disease with 95.8% classification accuracy from analysis of 272 Raman spectra of platelets in rat blood with MLP_NN (chart 41). The features chosen are intensity at 1658 cm^{-1} and ratio of intensity of 757 to that at 743 cm^{-1} correponding to amide I mode and cytochrome c.

EEG

Basic emotions and facial expression: The facial/verbal expressions of a human being for a visual/ psychological stimulus (chart 42) are common across the cultures. In fact, they are selected by nature and are due to their high survival factors. Rahnuma et al. [273] classified EEG signals corresponding to four emotions (happy, calm, sad and fear) with MLP_NN using inputs of features obtained from kernel density estimation. EEG of eight healthy subjects from different states in Malasia is recorded and the study is with an objective of probing into effects of depression and stress on mental health. Shams et al. [272] proposed emotion recognition system (Emot.Recog.) from Electroencephalographic (EEG) signals. The subjects of this study are ten healthy kids of 5 to 6 years and are shown photographs from Radbound faces database (RaFD) followed by EEG analysis for basic emotions (Chart 43). Majumder et al. [269] used extended Kohonen_SOM for recognition of six basic emotions in facial expression with data from MMI facial expression database. The analytical face model with 26 features is integrated within the algorithm. The comparison of results show superiority of SOM_NN over MLP_NN, RBF_NN etc. (chart 44). Danisman et al. [291] used MLP in recognition of facial expression. The best and worst feature window position for a set of face images from GENKI, JAFFE and FERET databases are obtained from exhaustive searches. It leads to a non-rectangular emotion mask and eliminates irrelevant data. The backward elimination of features further enhances the performance.

Chart 41: Raman spectra for Alzheimer's detection

- 278 Raman spectra

Preprocessing

- Separate all significants peaks
- Find most discriminat peak as a reference feature
- Cal cc(most significant peak vs all peaks)
- Discard highly correlated peaks
- Preliminary classification
- Peak value and their ratio of the remaining features
- 10% cases with most frequently appearing features are picked up
- Classification

Chart 44: Facial expression

Database

- MMI facial expression database

- Analytical face model
  - Eye, lip and eyebrow feature points
  - 26-Dimensional geometric feature vector

- MLP_NN
- RBF_NN
- Kohonen_SOM

Ext.SOM > [mcSVM, MLP, RBF]

Chart 42: Emotions of humans

Basic emotions

- Neutral
- Happy
- Fear
- Anger
- Sad
- Surprise
- Disgust

Complex (Combination of basic) emotions

- Shame
- Disappointment

Chart 43: Analysis of emotions in kids with EEG

Feature extraction	Time Difference of Arrival
Classification	Regul.LS MLP
Wavelet coefficients	% Correct Classification
User independent	96
User dependent	100

☞ Dermatology

Özçift et al. [161] compared MLP, Bayesian network wrapped with GA to diagnose six dermatological diseases. The most influential features out of 34 in the erythemato-squamous dataset are selected by GA in the hybrid approach and the accuracy of classification is 99.2% (Table 18). GA was found to be far superior to sequential floating methods.

(Human) Skin color classification

Detection and quantitative measure of skin color is vital in tracking of human body parts, face/ naked people detection/ recognition, retrieval of a person in multimedia databases and human computer interaction. Razmjooy et al. [249] proposed hybrid MLP_NN and Imperialist competitive algorithm

(Imp.Compet.Alg) in solving human skin color classification. The socio-political processes of imperialistic competition of mankind in the real world are the inspiration and it makes searches for high quality solutions with minimum classification error, while MLP_NN take care of constraints of task.

☞ Clinical analysis (Chemometrics + soft_sensors + Clinical procedures)

Sharma and Tambe [139] compared efficiency of soft sensor (SS) based MLP_NN, SVR, genetic programming (GP) to predict time-dependent lipase activity and amount of accumulated polyhydroxyalkanoates. Soft-sensors are software based process monitoring systems which searches and optimizes both the form (structure) and parameters of NNs. GP_SS are superior to MLP_NN based on RMS and R (Table 19).

Table 18: Comparison of Methods for dermatological diseases

Method	%Accuracy
SVM	98.36
MLP	97.00
Simple Logistics	98.36
Functional Decision Tree	97.81

GA wrapped + Bayesian Network	
Accuracy %	99.20
Misclassification number	3 out of 366

Diagnosis of Collagenous Colitis: Malekian et al. [253] reported screening of Collagenous Colitis (CC) with MLP_NN using colon tissue images. Chronic watery diarrhea is a symptom of microscopic colitis, but endoscopic and radiographic tests show normal. The gold standard for a confirmative diagnosis of CC is measurement of thickness of the sub-epithelial collagen (SEC) from colon tissue biopsy samples.

☞ Biochemical studies (Biometrics + Chemometrics + soft sensors)

Microarray technology -- DNA-Genes: DNA is one of the most complicated codes in nature and its tracking is now a sought after venture. Thousands of spots in a micro-array image correspond to different genes. The segmentation of image is to match gene with pixels. The noise and variation of pixels makes the task harder. Wang et al. [151] found MLP_NN and Kohonen_NN resulted in superior peak signal-to-noise ratio (PSNR) for cDNA images compared to GenePix®.

Table 19: Comparison of efficiency of soft sensor based models

Process	Prediction	Soft sensor based on		
		GP	SVR	MLP_NN
Extracellular production of lipase enzyme	Time-dependent lipase activity (U/ml)	0.96	<<0.96	<<0.96
Bacterial production of poly(3-hydroxybutyrate-co-3-hydroxyvalerate) copolymer	Amount of accumulated polyhydroxyalkanoates (% dcw)	0.98	0.98	0.94

⇨ Electric (power) engineering

Transient stability assessment: Sharifian and Sharifian [210] reported hybridization of MLP_NN with type-2_fuzzy_NN for transient stability assessment (TSA) in power systems (chart 45). For every disturbance causing a fault in TSA, many non-linear equations need to be solved requiringhigh cpu time. It leads to delayed actions for signal control rendering the situation alarming. With the hybrid data-driven AI approach, the accurate estimation of critical clearing time, an index of TSA is done and the system is scaled up to a large power system.

Household consumption: Azadeh and Faiz [134] made a critical study of annual household electricity consumption (chart 46) in Iran during the period 1974 to 2003 and found MLP_NN along with experimental design has superior performance.

⇨ Robots

Inverse kinematics: Aggarwal et al. [274] reported an inverse kinematic solution for a PUMA 560 robot with MLP_NN trained with robot's end-effector Cartesian co-ordinates along with corresponding configurations at joints. The trained NN predicts the behavior more confidently

➪ Communication

Many communication algorithms identify only few kinds of digital signals, that too at very high S/N ratio. Shrme [191] reported a hybrid MLP_NN-ABC (Alg. 18) in automatic recognition of communication signal with high accuracy even for low signal-to-noise ratios. Fuzzy sets [393] and neural networks are used in mobile commnunications

Chart 45: Transient stability assessment by MLP + Type-2 fuzzy_NN	
Data:	IEEE standard New England 10-machine 39-bus test system
▶ Type-2 fuzzy_NN	Deals with uncertainty in Power system measurement
▶ MLP_NN	Non-linear mapping of input to output
Performance measures: 🕮 Accuracy 🕮 Computational cost	**Training** ▶ Fast resilient BP **Selection of Inputs** ▶ Sensitivity analysis
Inference Hybrid Type-2 fuzzy_NN + MLP >.> MLP_NN	

➪ Commerce

Exchange rates: Guresen et al. [186] compared MLP_NN, dynamic_NN and the hybrid GARCH_NN in extracting input variables for real exchange daily rates (NASDAQ Stock Exchange index values) in terms of mean square error (MSE) and mean absolute deviation (MAD). Sermpinis et al. [230] compared MLP_NN, Rec_NN, Psi-sigma_NN to forecast EUR/USD, EUR/GBP and EUR/CHF exchange rates. The hybridization with KF, GP and SVR showed that hybrid SVR outperformed for bench mark data sets. A specialized loss function for NNs and hybrid leverage factor based on volatility forecasts and market stocks are introduced. The ensemble of MLPs and hybrid algorithms resulted in good prediction of credit score of Australian, German, and Japanese data sets.

9. Architecture Evolution in MLP_NN

The number of hidden layers is mostly restricted to two and the research is focused around addition/pruning of hidden neurons. Multiple optimization criteria are not yet in rampant use. For many tasks, development of ensemble and combination of results from different NNs to arrive at a hypothesis is not in wide spread use, although gaining momentum in this decade. RBF-NN, Fuzzy-NN (Fuzzy.SLP), Recurrent-NN (Rec.SLP), Jordon_NN, Elman_NN, SLP_NNs with tapped delay are the NNs with a single hidden layer but with many novel characteristics [303-308].

Chart 46: Forecast of electricity consumption for household

- ॐ Experimental design (Expt. Des)
  - ANOVA
  - Duncan Multiple Range Test

Models

- ॐ MLP_NN
- ॐ Regression
  - Error criteria
    - Average of (.)
      - ▶ Minimum Absolute Percentage Error
      - ▶ Mean Square Error
      - ▶ Mean Absolute Error

Optimum number of hidden neurons in the hidden layer: Apart from the heuristics to choose the number of neurons in the hidden layer, the three approaches for adequate NN with high generalizability and low over training are pruning, construction and regularization methods.

Pruning method: A larger network than required is trained until an acceptable solution is obtained. Hidden neurons or weights are pruned based on their contribution. In classification, the noise in data arises from wrong measurement of one or more input values or wrong assignment of class labels. It results in either assigning a correct input to an incorrect class, or incorrect input to a correct class. The trained NN for a classification task was pruned employing a discriminant component analysis (DCA) which involves pruning matrices of summed contribution between layers of NN. When least significant component is removed reliability and generalizability are increased with smallest possible rank. The explained variance is lower compared to that of full rank but it has little effect.

Constructive method: A NN of minimum architecture (I#-1-O#) i.e. with a single hidden neuron is trained. Then the neurons are added followed by layers until an adequate model is arrived or convergence criteria are met.

Combination of methods: Recently constructive and pruning algorithms are implemented together to automatic selection of FF-NN architecture. An interesting attempt is in combining pruning, optimal brain surgeon algorithm, quadratic regression (Quad.Reg.) in subset based training.

Alg. 18: MLP_NN +ABC in communications	
Input : Communication signal **Phase I** ⇨ Cal higher (up to eighth) order moments ⇨ Features ← cumulants of higher (up to eighth) order moments ⇨ MLP_NN as a classifier **Phase II** ⇨ Selection of the best features with Bees Algorithm (BA) Output: Discriminated signals	Tr.Alg : ॐ Quick prop (QP) ॐ Extended delta-bar-delta (EDBD) ॐ Super self adaptive back propagation (supersab) ॐ Conjugate gradient (CG)]

MLP with splitting H1 layer into sub units: The hidden layer of the assembly NN is split into sub-units equal to the number of output classes. Further, the sub-units are interconnected in a feed forward manner in addition to direct connections [73].

ॐ Centroid based MLP_NN (MLP.centroid.)

Lehatokangas [15] proposed centroid based MLP_NN with two hidden layers (HLs). Here, in the first hidden (called centroid) layer, inverse principal component analysis (inverse_PCA) is performed. Adaptive centroid vectors, which correspond to kernel centers, are used and the output of each centroid unit becomes the Euclidean distance between input and centroid vectors. Here, a special transformation of input data is performed which is akin to radial basis layer of RBF. A sigmoid TF is used in the second HL. Then number of centroids, their co-ordinates and weight vectors (WH1H2 and WH2O) are refined with BP. The advantage is PCA of X-matrix reduces the number of centroids to a remarkable level. The first step of algorithm calculates approximate lower bound used as starting point by PCA. In the next phase, the adequate minimum number of centroids is estimated at a user specified level of accuracy. It results in a compact (less complicated) architecture even for difficult classification tasks. The number of centroid units was determined empirically.

ॐ Dynamic architecture-2 (DA2-)-MLP_NN

The closed form of set equations are solved [6], partially alleviating black box dilemma of NNs. The number of neurons is fixed to four. The initial architecture consists of a single layer with connections I --> G1 --> F1, I --> F0 --> F1, I --> H1 --> F1 and bias to F1. Sine, cosine and linear transfer functions are used in G1, H1 and F0 respectively. The number of layers is limited by the desired accuracy. The linear component is calculated in the neuron F0 and sine and cosine of input are estimated with H and G neurons. F1 collects the weighted outputs of F0, G1 and H1. If the residual is greater than the convergence limit, an additional layer is added and the process is repeated. At each stage the four neurons viz. G, H, F and bias constituting a new layer is added and the five parameters are calculated.

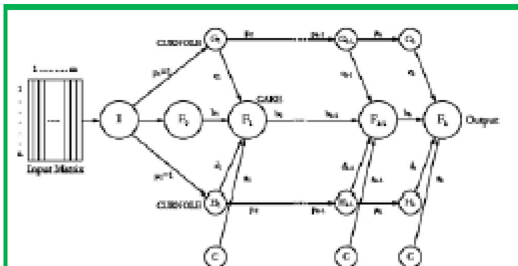

DA2--MLP_NN architecture of [courtesy of Ref 6]

+ Entire data set is analyzed in one stroke instead of presenting pattern by pattern

In this NN, The parameters are estimated with both non-gradient (bisection, golden search, Brent) and first order gradient (DSC-Powell, Fletcher-Reeves) non-linear least squares procedures. Ghiassi and Saidane [6] opined a thorough research of other optimization (GA, ant colony and Evolutionary) techniques would result in utilizing the full strength of DA2-NN model. DA2-NN captures non-linear process and is good in forecasting.

ॐ Combination of MLP_NNs

Multiple ordinate NN (MO-NN) is made up of several small MLPs. It is better compared to a big MLP for classification problems with a large number of classes.

ॐ Deep neural networks (Deep_NN)

These are MLP_NNs having many hidden layers. In speech recognition tasks, like phoneme recognition, vocabulary word detection, and these nets are widely successful [261].

ॐ Hybrid methods [10]

If the performance of the two methods based on different philosophies is comparable, equations are checked for similarity. If there are subtle differences in the approach (mathematical model, algorithm, basic postulates, necessary and sufficient conditions), then a combination (fusion etc.) results in a new method with synergistic benefits. SVM and FF-NN (BP) function similarly for a linearly separable classification task and their combination has multifold benefits.

Granular-oriented self-organizing Hybrid Fuzzy polynomial neural networks (Gran. SO. Fuzzy. Poly. NN): Oh et al. [264] proposed complete fuzzfication of SLP_NN with hidden layer containing Context.Poly.Neuron. The hybridized NN is applied to standard machine learning data sets (chart 47).

Chart 47: MLP_NN with context-based polynomial hidden neurons

IL	Clusters from information granules
HL	Context based polynomial neurons
OL	Clusters based on predefined fuzzy sets

+ Tunability
  - Number of contexts
  - Number of clusters
  - Collection of the specific subset of input variables
  - Order of the polynomial
+ Model
  - Flexibility
  - Simplicity
  - Compactness

10. Activation (Trasfer) functions Evolution in MLP_NN

A single non-linear basis function in real domain is common in MLPs. But, recently a set of combinations are in practice. Complex transfer functions entered the field in complex multilayer perceptron (CMLP)-NNs. The weights, activation functions and outputs are all complex in a few reports. The nonanalytic bounded function can be represented as quaternions in quaternion multiplayer perceptron (QMLP)-NN. Guo and Lyu [11] generate support multivector machines (SMVMs) in the form of two-layer networks.

Higher order neurons (Appendix-A1b)

Many researchers in late eighties proposed higher order (HO-) NNs of sigma-pi type. They recognize translation/ rotation invariances and also account for higher order correlations. Thus, a variety of functions are exactly modelled. It is applicable to interpolation of data at corners of the hypercube. The associative memories with higher order neurons have much larger storage capacity compared to traditional Hopfield model. A comparison of results of modeling of IRIS data with NNs using classical and higher order neurons show the unique advantages of higher order neurons in SLP architecture (Table 20, chart 48).

Chart 48: Higher order-SLP

+ Fewer number of neurons (compared to linear- or non-linear ones) are adequate in hidden layer even for complex tasks
+ Higher order neurons with (binary/ternary) cross product terms ensure interaction between variables

- Difficult to train Ws
- Small variation in Ws may cause large change in output
- Inherent instability of system

Quaternionic-SLP_NN (Appendix-A1b)

Quaternion SLP is employed for time series prediction, image compression and night (color) vision with better performance compared to real-valued NNs. A single quaternion is sufficient to solve a 4-bit parity check problem. However, they are less employed in application fields. It is an extension of the CMLP. The weights, activation functions, and outputs of this net are represented in terms of quaternions.

Table 20: IRIS data with higher order neurons

NN	Epochs	Number of misclassifications	
		Average of 250 trials	Best
3-hidden layer NN	1000	2.2	1
Fuzzy hyperbox	--	--	2
Fuzzy ellipsoids	1000	--	1
Higher order neuron –supervised NNs			
Order of neuron			
2	1	3.08	1
3	1	2.27	1
4	1	1.60	0
5	1	1.07	0
6	1	1.20	0
7	1	1.30	0
Unsupervised			
Super paramagnetic		25	
LVQ or GLVQ	200	17	
k-means		16	
Hyper ellipsoidal		5	
Higher order neuron NN			
Order of neuron			
2	20	4	
3	30	3	

11. Learning Evolution in MLP_NN

Knowledge and or/ skill acquisition process in any discipline in the universe (material/sub-particles/ radiation/ gravity/ charge) is learning. The storage of this knowledge requires memory. The printed books represent the passive form, while the active forms now prevalent are magnetic/optical storage devices in computers. Above all, the biological counterpart is the great-human-brain. It is a carbon based miraculous lifeless molecular assemblage, but indispensably supported by life. The size is much smaller and requires very low amount of energy for unit time. The first teacher of a child is the mother and later surroundings as well as formal/ informal learning/training. However, emphasis is to be laid for pre-natal learning nowadays, to understand the strange performances of child prodigies and to probe into hardware/ pre-loaded information, knowledge and even base line-intelligence/ ignorance/ never perceived targets/ learnt skills. Post-natal parental care and social/ethical factors have profound influence on the software of growing child. It is not yet prevalent to think of firmware in the context of brain on one-to-one correspondence with artificial systems.

Learning (Alg. 19) is through experience, training and more pertinently with integration of acquired data/ information/ knowledge and intelligence at that point of time. Training requires a formal/informal teacher and most of the tools are within a rigid frame of yesteryear's science and technology since latest findings have a time lag for every one's routine practice. Science comprises of sets of tools to perceive nature, reperform manmade experiments/materials and theoretical/utopian formulations. Technology on the other hand is a translation of scientific observations into commercial finished products of desired/dictated characteristics for an end user who may be an expert, technocrat, bureaucrat or layman. The end results are targeted for the benefit of mankind. But the rare catastrophic accidents/incidents are not the sin of hither to consolidated concreted efforts of hundreds of thousands of man-years of scientists/technologists but are arte-facts of misuse, ill-use and/or carelessness/over-confidence/callous attitude. This prompted the software industry to promote the slogan 'the xxx company does not hold responsibility for the mishap with the use of zzz package'.

Alg. 19: Learning algorithm

```
Iterate until satisfied learning

      cal   residuals
  If not satisfied
      Modify/correct/rectify/repair
      Go to perform
   Else
      Stop
   Endif
End iterate
```

Data conforming to the necessary and sufficient conditions of basis of frame ensure end results but fail for many real life tasks of 21st century. However, the methods with open-ended philosophies yield always a result and never crash. Yet the solution may be inferior to hard/rigid/restricted solving techniques. Which method for a task within the limits of time/cost/need of the solution and its utility/ returns is the best remains as a black hole. Self-efforts and self-styled/mimicked ways of doing things open a new world of realizing the truth for the benefit to himself/environment why to the galaxy.

It reminds the efforts of classical artificial intelligence practitioners of nineteen sixties in developing a generalized problem solver, shaky robots and natural language processor. Many advances occurred over these four decades and the modules of AI-2 now are computational intelligence and nature-mimicking computational tools with classical/hard mathematical/statistical algorithms for sub-goal attainment without creeping of their ill effects. Learning specially related to RBF, SOM, ARTx, ARTMAPx, RecurNNs etc. are detailed earlier [303-308] and Hebb learning is described now in appendix-A2a.

Emergent movements: Long duration memories as well as both positive and negative affections cooperate with each other. The increasing indefiniteness of environment is compensated in animals where the reflux nerves cannot work efficiently. The experiences are contracted and used. It is suggested that local reinforcement is responsible for simultaneous pursuit of stability and plasticity

State-of-the-art-of (SA) learning/**Training (Salt)**
Salt is essential for sustenance of life. Similarly learning and/or training of NNs to the desired accuracy is the heart of I/O mapping. Just like excess salt is detrimental to health, overtraining/overlearning also models errors in data as information. Thus, an apparently better model for the naked eye of amateur, in fact, functionally misleads compared to an inadequate model. The latter, of course, can be improved. The ideal goal is landing on a good model for good_ data. The meta heuristics guide to cross over pits (bad_model for good_ data, good_model for bad_ data, and the worst possible bad_model for bad_ data) on the way.

12. Training algorithms Evolution in MLP_NNs

Rumelhart proposed backward propagation (BP) as a means of self-learning of feed forward layered neural networks (FF-MLP_NNs) [111]. In fact, BP is a gradient based first order optimization method. Many modifications to BP include delta-bar-delta, extended-delta, cumulative-delta etc. The momentum and learning coefficients also favor speedy convergence. BPTT is an extension of BP for dynamic (in time) NNs. Most of the efforts are in the direction of modifying back propagation (BP) algorithm and feasibility studies with the available galaxy of optimization algorithms to train connecting weights from input to hidden (WIH) and hidden to output (WHO) layers. These classical training algorithms are non-self-starting. Therefore, one starts with guess (random numbers between –0.1 to +0.9) W(eight)s. Their optimum magnitudes for a given data set and architecture are obtained by choosing a learning rule (W or parameter change) and optimization (training) algorithm.

Chart 49: Limitations of BP
- Slow - Trapped in local minima - Intractable for large-scale optimization - Cannot transform (rotation etc) of profiles **Remedy:** Complex_ BP

Inter disciplinary research focusses vague/unclear/difficult aspects of grazy borderline/merging point with unforeseen new directions and benefits of pure science. However, sometimes it is associated with the menace of starting at lower end methods in one of the component fields especially in weaker of two disciplines coupled. SLP starting with steepest descent method missed the bus of well nurtured tools of optimizations for over a decade or two. Further, the efforts were mostly to improve back-propagation algorithm reported in hundreds of publications for many real life (tiny compared mega) tasks.

Almost all optimization methods viz. second order gradient procedures, quasi-Newton methods (BFGS, Marquardt, CG), pseudo inverse and global stochastic optimization (SAA) and direct (Brent, bisection) methods, non-gradient/global procedures viz. SAA, simplex have been implemented during the last two decades in refining even a large number of Ws. Kalman filter (KF), Extended KF, Dynamic-EKF and their extensions are in routine use in training dynamic (in space or time) NNs. During the last ten years, the impact of nature inspired algorithms (E-man) is new phase of MLP research. The application scientists carry the torch of well-established techniques and thus again a gap of quality of tools between those practiced and available is also a natural trend. With the necessity of multiple-object functions and complex spacio-temporal systems, nature mimicking algorithms like GA, GP, EA, EP, ACA, PSO etc. produced astounding results. A chronological survey of typical improvements in basic BP and remedial measures for the limitations (chart 49) are in appendix-A2b. RBF_NN trained with BP loses discriminating information during the initial learning phase. But, it results in compact representation. A panoramic view of evolution of training algorithm in MLP_NN is briefly discussed (vide infra).

Eqns. 1: Object function and layer wise output in MLP_NN

$$objFn = \min(ESS)$$

$$ESS = \frac{1}{2*NP} * trace\left[(ynn-y)^T * (ynn-y)\right]$$

$$Y^{L+1} = TF\left(Y^L * W^L\right)$$

$$yNN = \left(Y^{OL} * W^{OL}\right)$$

y:	Observed response
yNN:	NN output or (Calculated y)
OL:	Last (i.e. output) layer

Object function (objFn)

The minimization of sum of squares of errors or residuals (ESS) is the object function in training MLP_NN for fixed architecture. The training in NNs is generally performed pattern wise like in on-line processing. All patterns are propagated through NN in epoch. The output of Lth layer is multiplied with the weights between layers L and L + 1 followed by operation with nonlinear activation function.

Sub set of patterns: A subset of patterns in a training set is selected based on retaining the patterns, which change the Ws significantly [16]. In other words the data points, which do not change weights, are not used or deleted in generating the training subset. This method reduces the computational time and is employed in layer wise training. Layer wise training has higher complexity in terms of operations per iteration per pattern.

Classical training algorithms

Weight decay algorithm: Leung [21, 95] modified the weight decay algorithm of the recursive least squares (RecurLS) procedure. In the first modification, weight decay remains constant throughout training i.e. irrespective of epochs. It is more stable with high generalizability. The input perturbation RecurLS leads to robustness in prediction. These on line algorithms are tested for FF_NN.

Back-propagation with Selective training (BP-ST): BP-ST is faster than normal BP and de-emphasizes the over trained patterns. Thus, it solved the shortcomings viz. slow convergence towards the end of training, instability to learn the last few patterns and prevents over training. However, contradictory or overlapping pattern pose a problem. Optimal scaling method alternates between linear and non-linear optimization procedures.

Chart 50: Advantages of complex-BP-training of MLP_NN

- Higher speed of convergence compared to real-valued BP
- Generalization unchanged
- Number of weights and thresholds required for complex_BP are 50% less than those for real-valued BP
- Transform geometric figures, e.g. rotation, similarity transformation and parallel displacement of straight lines, circles, etc

Removal of unimportant W from trained NNs: The Hessian matrix identifies unimportant weights. In an on-line leaning, Hessian matrix is not available since the training patterns are stored after training. In this context, a joint learning-pruning algorithm is proposed for FFNNs. The basis is error covariance matrix of recursive least squares approach. It does not require the training set and hence suitable for on-line training.

Complex BP: The positive features of complex-valued version of BP are described in chart 50. It is used to train MLP_NN where input and output signals, weights and threshold values are all complex numbers. The form of refinement approach is that probability for a "standstill in learning" is very much reduced.

Hybrid BP algorithms

B P + recursive orthogonal least-squares: A hybrid training procedure for type-2 fuzzy logic systems was proposed. BP fine tunes antecedent and recursive orthogonal least-squares refines consequents. It is applied to interval singleton, interval type-1 non-singleton, and interval type-2 non-singleton cases. MLP_NN with geometric mean as accumulation function in neuron and resilent propagation training algorithm performs better than BP / simple RPROP in accuracy/ CPU time for real life data sets.

BP + GA in Fuzzy_NN: The hybridization of GA with BP in Fuzzy_NN for seismic reservoir task was employed. It was applied to extract rules of optimal drill position in oil field exploration. The mfs of antecedents and consequents are optimized making use of multi-encoding of GA. The first order predicate logic based rules are pulled out from trained Fuzzy_NN. A linear combination of cross-entropy cost function with Humpert error function significantly improves BP learning. A few typical reports in hybridizing BP with PSO, differential evolution, GA etc. are summarized in table 21.

Table 21: Hybridization of BP with nature inspired algorithms (E-man)

BP+$$$		Application	Author
Diff.Evol	Phase I: search for global initial connection weights & thresholds of BPNN with adaptive differential evolution (Adapt.Diff.Evol) Phase II: BPNN thoroughly searches for the optimal weights and thresholds. Adapt.Diff.Evol >> [BPNN, ARIMA]	Computer-assisted colonoscopic detection of malignant regions	L Wang & G D Magoulas
GA	GA Initializes network connection weights and thresholds of BP PSO Iterative refinement	Geological hazard risk	M Liu
PSO	+ More accurate than hyperbolic and image models + local and global search	Soil–structure interaction involving a complicated mechanism of load transfer from pile to supporting geologic medium	A. Ismail
PSO	SLP_NN (BP) + ARIMA Input parameter Selection	Gansu of China from 2001 to 2006 Daily average wind speed data of Jiuquan and 6-hourly wind speed data of Yumen	C Ren
PSO	Preprocessing Trend removal BP Weights (WIH & WHO) refinement PSO #hidden layer neurons		T Kuremoto

	⇨ Learning rates		
Random fuzzy		+ Accurate learning + Increases probability of escaping from the local minima	Y Chen
SA	**GA**	☞ Tongue inspection color distortion	

Table 21b: Output of om_ref_JAVATYP.m **Advances in back Propagation**	
A. Ismail, D.S. Jeng, L.L. Zhang ▶ An optimised product-unit neural network with a novel PSO–BP hybrid training algorithm: Applications to load–deformation analysis of axially loaded piles	Engineering Applications of Artificial Intelligence, 26, 10, (2013) 2305-2314
A. Sedki, D. Ouazar, E. El Mazoudi ▶ Evolving neural network using real coded genetic algorithm for daily rainfall–runoff forecasting	Expert Systems with Applications, 36, 3, (2009) 4523-4527
Benedikt K. Humpert ▶ Improving back propagation with a new error function	Neural Networks, 7, 8, 1994, 1191-1192
C. Zhang, W. Wu, X.H. Chen, Y. Xiong ▶ Convergence of BP algorithm for product unit neural networks with exponential weights	Neurocomputing, 72, 1–3 (2008) 513-520
C.C. Chuang, S.F. Su, C.C. Hsiao ▶ The annealing robust back propagation (BP) learning algorithm	IEEE Trans. Neural Networks 11 (5) (2000) 1067–1077
Chao Ren, Ning An, Jianzhou Wang, Lian Li, Bin Hu, Duo Shang ▶ Optimal parameters selection for BP neural network based on particle swarm optimization: A case study of wind speed forecasting	Knowledge-Based Systems, 56 (2014) 226-239
D.S. Chen, R.C. Jain ▶ A robust back-propagation learning algorithm for function approximation	IEEE Trans. Neural Networks 5(3) (1994) 467–479
El-Sayed A. El-Dahshan, Heba M. Mohsen, Kenneth Revett, Abdel-Badeeh M. Salem ▶ Computer-aided diagnosis of human brain tumor through MRI: A survey and a new algorithm	Expert Systems with Applications, 41, 11 (2014) 5526-5545
George D Magoulas, Vassilis P Plagianakos, Michael N Vrahatis ▶ Neural network-based colonoscopic diagnosis using on-line learning and differential evolution	Applied Soft Computing, 4, 4, (2004) 369-379
Gerardo M. Méndez, M. de los Angeles Hernandez ▶ Hybrid learning for interval type-2 fuzzy logic systems based on orthogonal least-squares and back-propagation methods	Information Sciences, 179, 13 (2009) 2146-2157
Li Zhuo, Jing Zhang, Pei Dong, Yingdi Zhao, Bo Peng ▶ An SA–GA–BP neural network-based color correction algorithm for TCM tongue images	Neurocomputing, 13 (4) (2014) 111-116
Lin Wang, Yi Zeng, Tao Chen ▶ Back propagation neural network with adaptive differential evolution algorithm for time series forecasting	Expert Systems with Applications, (In Press)

Lin Wang, Yi Zeng, Tao Chen ▶ Back propagation neural network with adaptive differential evolution algorithm for time series forecasting	Expert Systems with Applications (In Press)
Md. Shiblee, B. Chandra, P.K. Kalra ▶ Learning of geometric mean neuron model using resilient propagation algorithm	Expert Systems with Applications, 37, 12, (2010) 7449-7455
Ming Liu, Yude He, Jiaxin Wang, Heow Pueh Lee, Yanchun Liang ▶ Hybrid intelligent algorithm and its application in geological hazard risk assessment	Neurocomputing, (In Press)
Muhammad R. Widyanto, Hajime Nobuhara, Kazuhiko Kawamoto, Kaoru Hirota, Benyamin Kusumoputro ▶ Improving recognition and generalization capability of back-propagation NN using a self-organized network inspired by immune algorithm (SONIA)	Applied Soft Computing, 6, 1, (2005) Pages 72-84
Neil Vaughan, Venketesh N. Dubey, Michael Y.K. Wee, Richard Isaacs ▶ Parametric model of human body shape and ligaments for patient-specific epidural simulation	Artificial Intelligence in Medicine, (In Press)
Shane D. Murnion ▶ Comparison of back propagation and binary diamond neural networks in the classification of a Landsat TM image	Computers & Geosciences, 22, 9, (1996) 995- 1001
Sherif Khattab, Rami Melhem, Daniel Mossé, Taieb Znati ▶ Honeypot back-propagation for mitigating spoofing distributed Denial-of-Service attacks	Journal of Parallel and Distributed Computing, 66, 9 (2006) 1152-1164
Shih-Wei Lin, Tsung-Yuan Tseng, Shuo-Yan Chou, Shih-Chieh Chen ▶ Simulated-annealing-based approach for simultaneous parameter optimization and feature selection of back-propagation networks	Expert Systems with Applications, 34, 2, (2008) 1491-1499
Shiwei Yu, Xiufu Guo, Kejun Zhu, Juan Du ▶ A neuro-fuzzy GA-BP method of seismic reservoir fuzzy rules extraction	Expert Systems with Applications, 37, 3, (2010) 2037-2042
Takashi Kuremoto, Shinsuke Kimura, Kunikazu Kobayashi, Masanao Obayashi ▶ Time series forecasting using a deep belief network with restricted Boltzmann machines	Neurocomputing, 137 (2014) 47-56
Yudong Zhang, Lenan Wu ▶ Stock market prediction of S&P 500 via combination of improved BCO approach and BP neural network	Expert Systems with Applications, 36, 5, (2009) 8849-8854
Yu-Ju Chen, Tsung-Chuan Huang, Rey-Chue Hwang ▶ An effective learning of neural network by using RFBP learning algorithm	Information Sciences, 167, 1–4 (2004) 77-86
Zuriani Mustaffa, Yuhanis Yusof, Siti Sakira Kamaruddin ▶ Enhanced artificial bee colony for training least squares support vector machines in commodity price forecasting	Journal of Computational Science, 5, 2 (2014) 196-205

13. Universal function approximation

Mathematically universal approximation theory was proved for any shape, of course restricted to certain class of basis functions (KB. 4). In NN paradigm, mathematical function approximation is proved with sigmoid and Gaussian TFs [303]. But, recently several other basis functions viz. pseudo Gaussian, raised cosine, ridge, binary cube, multi-wavelet with ortho normal multi scaling, multivariate functions (those with high input variability), smooth functions, Tickohnov regularization and clustering functions are considered**.** The approximation of a continuous function is dense if

$\left| y(x) - g(x) \right| < \varepsilon \quad where \varepsilon > 0 \; and \; x \in [0 \quad 1]^n$. This is called density theorem and is widely used in approximation theory. In addition to normal mathematical space, Sobolov space is also studied. Clustering for function approximation was used to initialize centers of RBF. . Respecting the constraints imposed in universal approximation theory, it is possible to arrive at a RBF or MLP_NN (with number of neurons less than the number of points), to reproduce 1-D to m-D profiles.

KB. 4a: Theorems in universal function approximation

If	Function is Riemann integrable & TF is non polynomial ride on closed interval (a,b)
Then	Σ^3 (a,b) is dense in C(K) with respect to uniform norm for all components K⊂R
If	Function is essentially bounded (instead of Riemann integrable)
Then	Σ^3 (a,b) is dense in L^p (μ) for any compactly supported measure of μ
If	Function is analytic (instead of Riemann integrable)
Then	Σ^3 (a,{b}) is dense in C(K) and in in L^p (μ) {b} : single value
If	Fn and TF are continuous
Then	f(.) , f(. –x) is Rieman integrable & convergence assumed

KB. 4b : Knowledge Base for function approximation

If	TF in HL is RBF	A1	&
	TF is continuous almost every where	A2	&
	Bounded	A3	&
	Integrable on R^n	A4	&
	Integration ≠ 0	A5	
Then	SLP_NN approximates any function in $L^p(R^n)$ wrt L^p with 1 <= p <= ∞	C1	
If	A1 & A2 & A3		
Then	C1		
If	A1 & A2 &A3		&
	Not a polynomial	A6	
Then	C1		

KB. 4c : Effect of input dimension

If	input dimension is less
Then	RBF is better than SLP
If	exponential number nodes are required with ridge TF
Then	RBF is a better choice

Yet, the hurdles are noise, outliers and correlation in data structure to obtain a solution of desired quality. The optimisation method, object function (performance, error, parameter reliability) and ranges of data play a major role in solution, generalizability, reliability, predictability, etc. Further, universal approximation theorem does not explicitly tell the number of neurons, layers, TFs, tools for solution for a specific problem. The number of parameters, their characteristics makes the solution of a problem hard and NL complete. Hence, it is solved with various approximations at different phases. The optimized Ws and scale parameters of wavelet-like functions in NNs are used for function approximation for higher accuracies. When training of NN fails, it is to be attributed to inadequate learning method, incorrect number of neurons in the hidden layer, insufficient training data, poor initialization of Ws.

14. A priori knowledge of data structure and/or profiles

If the functional form of data (y = f(X)) contains linear terms, direct connections between input and output units model the linear trend. Instead even when a NL-TF is used, the results are distorted. Irrespective of routine practice, it is optimum to use direct connections also when prior knowledge is available. If numerical accuracy of data is vague or errors do not follow statistical distribution, fuzzy sets and interval manipulations are desirable. When data is correlated extensively, PCs/ PLSCs are calculated in another

NN and used as input for I/O transformation. In the case of time series, if linear trends are established for similar tasks, the residuals of ARMA output are connected to the input layer of MLP_NN. In cases where the periodicity is known from other studies, FFT is a good choice in pre-processing. The dynamics in parameter values of model and structural change are taken care in Kalman filter and its clones.

15. Emulation of standard statistical/ mathematical techniques by SLP_NNs

The classification of methods based on data structure are given in the form of if-then-else rules in KB. 5. FF-NN for linearly equivalent separable classification task is equivalent to support vector machines (SVM). In the first few epochs, it mimics SVM and then classifies clusters with non-linear separation boundaries. The hardness of the margin in SVM is correlated with the number of epochs of back propagation algorithm. The knowledge in calculating principal components with IO_NN and SLP_NN are documented in KB. 6.

KB. 5: Classification method selection based on data structure

Necessary Condition
Number of clusters known

If Number of classes = 2 &
pdf1, pdf2 are Gaussian &
cov(c1) = cov(c2)
Then Fisher linear discriminant analysis (LDA)

If pdf1, pdf2 are Gaussian &
cov(c1) ≠ cov(c2) &
Then Quadratic Bayesian classifier (QDA)

If Nature of distribution (pdf) is non Gaussian
Then non-parametric (Parzen estimator)

Cov : Covariance
pdf : Probability density function

KB. 6: Output characteristics based on relative number of input and hidden neurons in SLP_NN

If SLP_NN &
I# = O#
Then Non-linear PCs

If SLP_NN &
I# > H#
Then Dimension reduction

If SLP_NN &
H# > >I#
Then Mapping into high dimensional space
[Similar to SVM]

If Response output is constant over a certain region
Then Increase number of sigmoid functions
- CPU time increases with H#

Remedy
Hypersphere FAM
R_RBF_NN

Chart 29b: Output of om_ref_JAVATYP.m

Principal component Analysis (PCA)

Erkki *Oja* ▶ A Simplified neuron model as a principal component analyzer	*J. of Mathematical Biology* *15(3) (1982) 267–273*
Erkki *Oja* ▶ Neural Networks, Principal Components and Subspaces	International J. of Neural Systems 1 (1) (1989) 61–68
N. Japkowicz, S.J. Hanson, M.A. Gluck ▶ Non-linear autoassociation is not equivalent to PCA	Neural computation 12 (2000)531-545

om_ref_JAVATYP.m

object module (om_) reference (ref_)

Journal Author Volume And (JAVATYP) Title Year Pages
matlab function(.m)

Posterior probability

Ito and Srinivasan [7] applied Bayesian decision theory for SLP_NN. A way of obtaining posterior probabilities for classification tasks from the output of SLP_NN are described in the first order logic format in KB.7.

KB. 7a: Output of SLP and probability

If Number_of_classes = 2 &
Number_of _hidden_ neurons of SLP = dimX
Then Output approximates to posterior probability

If Number_of_classes = 2 &
d-dimensional space adheres to binomial, Poisson, multi-nominal state conditional probability distribution
Then d-hidden neurons approximate posterior probability of data set.

If Number_of_classes = 2 &
MLP with small number of hidden neurons &
NN trained with Rucket method &
normal state-conditional probability distribution
Then Output approximates to a posterior probability
Extension : It is applicable to d-dimensional feature space

If Inner potential of the output unit approximates log ratio &
Activation function is logistic
Then Output approximates posterior probability

KB. 7b: Output of SLP and probability

If Log ratio of posterior probabilities linear &
d#-1 architecture

Then log (ratio of posterior distribution) = u0 * x + a0 = u01*x1 + ... + u0d * xd + u0

If log (ratio of posterior distribution) is quadratic &
d-nonlinear hidden layer neurons &
d-linear inputs and direct connections between input-to-output layers
Then NN output cannot estimate state conditional pdfs
Remedy If prior knowledge (or measurement during training) of density p(x) is available
Then probability distribution is obtained as the product

If Log ratio of posterior probabilities is polynomial of low degree &
Sigmoid TF is used
Then SLP approximates posterior probabilities of multiple (two or more) class data

Chart 29b: Output of om_ref_JAVATYP.m

Posteriori probability

B.D. Ripley
► Statistical aspect of neural networks, in: O.E. Bardorff-Nielsen, et al. (Ed.), Networks and Chaos—Statistical and Probabilistic Aspects
Chapman & Hall, London, 1993, pp. 40–123.

B.D. Ripley
► Statistical aspect of neural networks, in: O.E. Bardorff-Nielsen, et al. (Ed.), Networks and Chaos—Statistical and Probabilistic Aspects
Chapman & Hall, London, 1993, pp. 40–123.

M.D. Richard, R.P. Lipmann
► Neural networkclassifiers estimate Bayesian a posteriori probabilities
Neural Comput. 3 (1991) 461–483

M.D. Ruck, S. Rogers, M. Kabrisky, H. Oxley, B. Sutter
► The multilayer perceptron as an approximator to a Bayes optimal discriminant function
IEEE Trans. Neural Networks 1 (1990) 296–298

H. White ▶ Learning in artificial neural networks: a statistical perspective	Neural Comput. 1 (1989) 425–464.

om_ref_JAVATYP.m

object module (om_) reference (ref_)
Journal Author Volume And (JAVATYP) Title Year Pages
matlab function(.m)

16. Distribution of information in NNs [17]

Although there is no theoretical basis or proof yet, the information is distributed in connection weights between neurons of all layers, transfer functions, cumulative operators, scaling factors and so on. It helps to probe into

- ∇ estimate tolerance of NNs for internal perturbations
- ∇ develop criteria to select best solution from a set of different nets
- ∇ relate performance index with components of NNs

In the last decade, DAPRA had mission of adding knowledge bits every year to its common-sense base. Max Planck Institute for Computer Science automated extraction of knowledge from Wikipedia in its YAGO (chart 51). The size is around ten million entries consisting of 120 million facts. It is used in Watson AI system.

Chart 51: YAGO
Yet Another Great Ontology

Source	Categories
Wikipedia	Categories Redirects Infoboxes
Wordnet	Synsets Hyponymy
Geonames	
Linked to	Dbpedia ontology SUMO ontology
Query mode	?SPARQL

17. Current state of MLP_NN in research mode (2014)

The experimental/ simulated/ quantum chemical tensorial data for tasks in chemometrics, enviromentrics and medicinometrics are processed in computer (software/hardware) systems' laboratory. The outcome is consolidated information followed by extraction of process knowledge, sieving for meta knowledge and detecting sparkling intelligent bits for integration and refinement in the infinite cycle of research pursuit.

The core algorithm comprising of equations of model and solution methods and numerical accuracy are of prime concern for every (NN) procedure. From inter disciplinary users' and commercial package point of view, input output (IO) user interface (UI) is the center of attraction. The developers render the software user friendly by adding intelligent input interface (III, I^3) and also novice to expert mode guided intelligent output interface (IOI). The recent add-ons are context/case based (CB) or data driven (DD) UIs with a (virtual) feel of experts' personal touch. But, from mis-usage diminution/ appropriate use and/or inter disciplinary research stand point, necessary/sufficient conditions, data structure, numerical accuracy, failure conditions, remedial measures, alternate (equivalent/better) methods are of real concern for a steadfast activity of data to knowledge processing. No doubt, this monitors breadthwise growth generally. But, for core groups devoted for improvement and bringing up new methods, it becomes a cake walk to find gaps and holes in the process-continuum. Neocognitron is a hierarchical MLP_NN continuously refined by introducing new layers, learning rules for robust recognition of characters/digits/geometric shapes etc.

Chart. 52 incorporates state-of-MLP_NN in research mode with intelligent frames displaying context based popup menus. The learning and training evolution is summarized in Appendix-2.

Chart 52: State-of-art-of- FF_MLP_NN in research mode

Intelligent input interface (III, I^3)

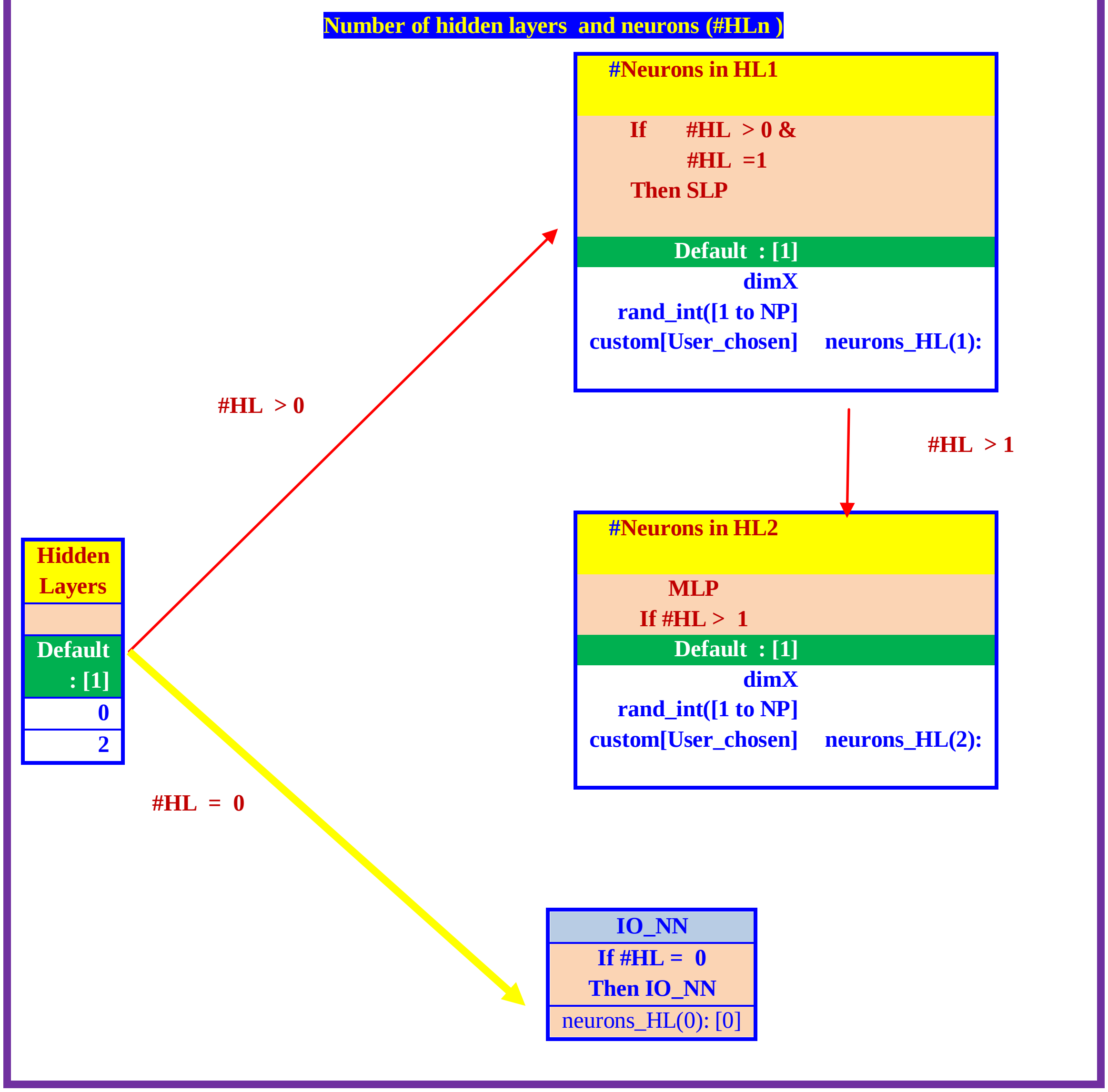

Transfer functions

TFs _Fnbase
Real
Complex
Quaternion

Real .TFs
Continuous
Discrete

Real .continuous. TFs
Sigmoid
Tanh
Elliot
…

Real . Discrete. TFs
Hardlimitor
Rectangular
…

Object functions

ObjFn	
Single	
Multiple	Standard
	Pareto

ObjFn
Unconstrained
Constrained
…..

Goal
Minimization
Maximization
….

Learning /Training methods

Learning /training
Ws
Architecture
Both

Inhibitory. Learning. Ws
Fixed
Variable
No surround
Surround
Excitatory
Fixed
Variable
……..

Winner. learning. Ws
Winner-takes-most
Winner-take-all
Winner-kills-looser
…

Loser. learning. Ws
Winner-kills-looser
Loser-exits
Achieve
…

Winner-Loser Interaction. Learning. Ws	
crossover	
Mutation	
Elite	Retention
	Avoiding
Looser deficiencies	
	Elimination
	Remedial measures
…..	

Learned. Learning. Ws	
Learned	Robustly accepted → Retain
Deformed unlearned	Robustly accepted
Irrelevant	Erroneously accepted →To be rejected

Silent. learning. Ws
Add-if-silent
Ignore-if-silent
Eliminate-if -silent

Training. Ws
Back-propagation
LM
Pseudo inervse
….

18. Future scope

Neuron_2020

The set of neurons proposed over last half a century are not even nearer to biological neurons of brain, although many complex dynamic real life tasks have been predicted with astounding success compared to statistical/mathematical paradigms. FF-NNs with TF-based neurons excelled in performance in function approximation, classification, parameterization, solution of algebraic/differential equations of multivariate-multidimensional complex hyper-surfaces. Support vector machine neuron (SVM_neuron) is a new addition to the list of neurons.

Neuron with glial cell

The small, but neglected influence of glial cells, astrocytes in biological neurons is now a matter concern. The neuron model incorporating complete effect of biological glial cells and astrocytes is awaited. It is interesting to foresee the gross influence of such smaller and analogous effects in artificial neurons. Another approach enhancing machine intelligence is using fuzzy logic through computation of words, sentences and concepts.

Early attempts of flying machines attempted to model the bird. This was done because the bird was the only working model of flight in those days. It was not until Wilbur and Orville Write chose an alternate model of nature. The first aircraft created was that with first fixed wings. Perhaps modeling AI programs after nature analogous to modeling airplanes after birds and a much better model than the neural network exists. One had to wait for a fairy tide in future. Alternatively, leaving aside the idea of mimicking biological neurons with ion channels and complex interactions, a new basic structure with higher accumulated wisdom will open new vistas in intelligent computation or computational intelligence. This will be at the base level as a building block to explore machine intelligence from another direction.

An integrated form and research mode of TF-based neuron is a comprehensive model accepting tensorial input and capable of operating with Clifford geometry. Dynamic neuron incorporating feedback signals with single/multiple delays in distributed/undistributed form paved the way to the state of art modeling of spacio-temporal variations of numerical data, image processing, dynamic scene analysis etc. A single super-neuron/hyper-neuron along with strengthened weight estimation procedures is a step forward to realize multi-objective real time/real life tasks in environment, drug discovery and electronic industry including nano-structures in civilian/defense sectors. The miraculous sparkles of computational thinking of 2020 will enable one to compute nearer if not nearest to the normal healthy human brain.

Acknowledgments: The authors thank editor-in-chief and executive editor for improving the readability of this series of neural network reviews.

I (RSR) bow my head to my first teacher who laid foundation stone of formal learning. I remember vividly majestic gesture of Sri Subba Rao, for taking pains to induce systematic approach of learning (now I understand) in fourth and fifth classes at elementary school, Vijayawada in late nineteen fifties. I place on record my profound gratitude to my teachers Smt.Eligebeth, Smt Padmavati, Sri Kesava Rao and Sri Bhavani who generously infused curiosity and paved way to learn alphabets in general science/mathematics at C V R (Chunduru Venkata Reddi) GMH (Government municipal high) school, Vijayawada in early sixties. I learnt basics of physics, chemistry, mathematics and languages from learned lecturers, K Rama Krishna, Moses, Vijaya Kumar, S S S Somayajulu, Mohan, Prajapathi Rao, N Radha Krishana Murthy, Khasim Peeran, Bhavannarayana, Kedareswara Rao, Raghavachari (Hofined professor), Subrahmanyam, Narasimham and Jamadagni at SRR (Sri Raja Rangayya Appa Rao) & CVR Govt. college, Vijayawada in late sixties. I feel at heart overwhelming happiness to express my gratitude to Sri Lakshminarayana garu for sparing time in 1968 amidst his busy schedule for vocal practice of Rudradhayam in Yajur veda with his reverberating metallic voice.

The wise counseling of Prof. S R Sagi, Prof. L S A Dikshitulu, Prof. Manta Suryanarayana, Prof. N Venkateswara Rao, Prof. L Rama Chandra Rao, Prof. C Bheema Sankara Rao, Prof.A S R Anjaneyulu in lecture halls and laboratories of Andhra University (1969-1971) widened my vocabulary in chemistry. My regards to Prof Gandikota Gopala Rao for showering on me the bliss of hearing to him long hours in his office in physical chemistry during mid-seventies. I thank Gandikota Murali Krishna for sparing many reprints in analysis of redox systems.

I am ever indebted to Dr. Lakshmi Kantam (Director), Dr. Sai Prasad, Dr. Narahari Sastry (Bhatnagar awardee), Dr. Bhanu Prakash, scientists at I I C T for generously permitting online search and downloading of electronic prime journals since 2000.

The print versions of chemical abstracts/journals up to nineteen nineties, CD_ROMs in late nineties, online services of Science Direct, ACS, RSC etc. with keywords searches in this century and cover to cover browsing, downloaded papers/focus articles/ state-of-art-(critical)-reviews from e_journals are instrumental to integrate knowledge both breadth and depth wise. The referees and editors of journals polished the critical perspective of translation of outcome of designed experiments along with consolidation of literature with ethics to a presentable form.

References

Multi-layer perceptron (MLP)_NN

[1] M. A. Costa, A. de Pa du Braga, B. R. de Menezes, *NeuroComput.*, **2007**, 70, 1342-1347.
[2] C. Yu, M.T. Manry, J. Li, P. L. Narasimha, *NeuroComput.*, **2006**, 70, 525-535.
[3] E. R. Hruschka, N. F.F. Ebecken, *NeuroComput.*, **2006**, 70, 384-397.
[4] L. Franco, *NeuroComput.*, **2006**, 70, 351-361.
[5] S. K. Oh, W. rycz, Ho-Sung Park, *NeuroComput.*, **2005**, 64, 397-431.
[6] M. Ghiassi, H. Saidane, *NeuroComput.*, **2005**, 63, 397-413.
[7] Y. Ito, C. Srinivasan, *NeuroComput.*, **2005**, 63, 209-228.
[8] J. Wang, Z. Tang, R. Wang, *NeuroComput.*, **2004**, 57, 485-492.
[9] R. K. Brouwer, *NeuroComput.*, **2004**, 57, 345-360.
[10] E. Romero, L. Marquez, X. Carreras, *NeuroComput.*, **2004**, 57, 313-344.
[11] P. Guo, M. R. Lyu, *NeuroComput.*, **2004**, 56, 101-121.
[12] K. P. Ferentinos, *Neural Netw.*, **2005**, 18, 934-950.
[13] A. Eleuteri, R. Tagliaferri, L. Milano, *Neural Netw.*, **2005**, 18, 1309-1318.
[14] J. Gary Polhill, M. K. Weir, *Neural Netw.*, **2001**, 14, 1035-1048.
[15] M. Lehtokangas, *Neural Netw.*, **2000**, 13, 525-531.
[16] S. D. Hunt, J. R. Deller Jr., *Neural Netw.*, **1995**, 8, 6, 931-944.
[17] Ali A. Miani, R. D.Williams, *Neural Netw.*, **1994**, 7, 5, 783-796.
[18] T. Karkkainen, *Neural comput.*, **2002**, 14, 1451-1480.
[19] L. S. Camargo, T. Yoneyama, *Neural comput.*, **2001**, 13, 2673-2680.
[20] A. W. Savich, M. Moussa, S. Areibi, *IEEE Trans. Neural Netw.*,**2007**, 18, 1,240-252.
[21] Chi-Sing Leung, Ah-Chung Tsoi, Lai Wan Chan, *IEEE Trans. Neural Netw.*,**2001**, 12(6), 1314-1332.
[22] E. J. Bayro-Corrochano, *IEEE Trans. Neural Netw.*,**2001**, 12, 5, 968-986.
[23] J. V. Shah, C. S. Poon, *IEEE Trans. Neural Netw.*,**1999**, 10, 1,10-18.
[24] M. Banerjee, S. Mitra, S. K. Pal, *IEEE Trans. Neural Netw.*,**1998**, 9, 6, 1203.
[25] D. Svozil, V. Kvasnicka, J. Pospichal, *Chemometrics and Intelligent Laboratory Systems*, **1997**, 39, 43-62.

Back propagation

[26] B. Widrow, *Proc. IEEE*, **1990**, 78, 9,1415-1442.
[27] X.G. Wang, Z. Tang, H. Tamura, M. Ishii, *NeuroComput.*, **2004**, 57, 477-484.
[28] X. G. Wang, Z. Tang, H. Tamura, M. Ishii, W.D. Sun, *NeuroComput.*, **2004**, 56, 455- 460.
[29] A. Bhaya, E. Kaszkurewicz, *Neural Netw.*, **2004**, 17, 65-71.
[30] A. Nikov, S. Stoeva, *Neural Netw.*, **2001**, 14, 231-244.
[31] S. Stroeve, *Neural Netw.*, **1998**, 11, 709-721.
[32] D. McLean, Z. Bandar, J. D. O. Shea, *Neural Netw.*, **1998**, 11, 1685-1694.

[33] B. K. Humpert, *Neural Netw.*, **1994**, 7, 8, 1191-1192.
[34] K. Niahiyma, K Suzuki IEEE Trans. Neural Netw., **2001**, 12(6), 1265-1277.
[35] C. C. Chuang, S. F. Su, C. C. Hsiao, *IEEE Trans. Neural Netw.*,**2000**, 11, 5, 1067-1077
[36] J. S. R Jang, *IEEE Trans. Neural Netw.*,**1992**, 3, 5, 714-716.
[37] M. Fukumi, S. Omatu, *IEEE Trans. Neural Netw.*, **1992**, 3, 5, 535-537.
[38] S. ichiHorikawa, T. Furuhashi, Y. Uchikawa, *IEEE Trans. Neural Netw.*, **1992**, 3, 1, 801-806.
[39] R.C.Lacher, S. I. Hruska, D. C.Kuncicky, IEEE trans. Neural netw.,**1992**, 3, 1, 62-72.
[40] L. Holmstorm, P. Koistinen, *IEEE Trans. Neural Netw.*,**1992**, 3, 1, 24-35.

Learning algorithms

[41] H. Yang, J. Li, F. Ding, *NeuroComput.*, **2007**, 70, 625-632.
[42] J. Hirayama, J. Yoshimoto, S. Ishii, *NeuroComput.*, **2006**, 69, 1954-1961.
[43] Y. Nishimori, S. Akaho, *NeuroComput.*, **2005**, 67, 106-135.
[44] Wako Yoshida, Shin Ishiia, *NeuroComput.*, **2005**, 63, 253-269.
[45] B. Ster, *NeuroComput.*, **2004**, 57, 215- 238.
[46] V. G. Red'ko, O. P. Mosalov, D. V. Prokhorov, *Neural Netw.*, **2005**, 18, 738-745.
[47] A. V. Robins, S. J. R. McCallum, *Neural Netw.*, **2004**, 17, 313-326.
[48] H. Miyamoto, J. Morimoto, K. Doya, M. Kawato, *Neural Netw.*, **2004**, 17, 299-305.
[49] K. Hara, M. Okada, *Neural Netw.*, **2004**, 17, 215-223.
[50] B. J. Jain, F. Wysotzk, *Neural Netw.*, **2004**, 17, 143-154.
[51] S. Sakamoto, S. Seki, Y. Kobuchi, *Neural Netw.*, **2004**, 17, 1101-1107.
[52] T. Kimoto, M. Okada, *Neural Netw.*, **2004**, 17, 103-112.
[53] K. Hirasawa, S. ho kim, J. Hu, J. Murata, M. Han, C. jin, *Neural Netw.*, **2001**, 14, 1389-1404.
[54] N. Ampazis, S. J. Perantonis, J. G. Taylor, *Neural Netw.*, **2001**, 14, 1075-1088.
[55] S. Watanabe, *Neural Netw.*, **2001**, 14, 1049-1060.
[56] D. Ormoneit, *Neural Netw.*, **1999**, 12, 1405-1412.
[57] Y. Liu, X. Yao, *Neural Netw.*, **1999**, 12, 1399-1404.
[58] K. Yamauchi, M. Oota, N. Ishii, *Neural Netw.*, **1999**, 12, 1347-1358.
[59] K. Chena, L. Xu, H. Chi, *Neural Netw.*, **1999**, 12, 1229-1252.
[60] J. Zhang, A. J. Morris, *Neural Netw.*, **1998**, 11, 1, 65–80.
[61] Fu. L. chung, T. lee, *Neural Netw.*, **1996**, 7, 3, 539-551.
[62] R. Vitthal, P. Sunthar, Ch. D. Prasad rao, *Neural Netw.*, **1995**, 8, 4, 563-569.
[63] H. Yamakawa, Y. OkAbe, *Neural Netw.*, **1995**, 8, 3, 363-373.
[64] S. J. Perantonis, D. A. Karras, *Neural Netw.*, **1995**, 8, 2, 237-249.
[65] W. Bialek, I. N. N. Tishby, *Neural Netw.*, **1994**, 7, 9, 1351-1378.
[66] K. Ochiai, N. Toda, S. Usui, *Neural Netw.*, **1994**, 7, 5, 797-807.
[67] V. Kasparian, C. Batur, H. Zhang, J. Padovan, *Neural Netw.*, **1994**, 7, 4, 661-670.
[68] E. Castillo, O. F. Romero, B. G. Berdinas, A. A. Betanzos, *Neural comput.*, **2002**, 14, 1429-1449.
[69] M. Ishii, I. Kumazawa, *Neural comput.*, **2001**, 13, 2851-2863.
[70] H. Gu, H. Takahashi, *Neural comput.*, **2000**, 12, 795-809.
[71] H. SchWenk, Y. Bengio, *Neural comput.*, **2000**, 12, 1869-188.
[72] A. N. Vazquez, A. R. F. Vidal, *Neural comput.*, **2000**, 12, 1429-1447.
[73] A. Goltsev, *Neural computati on*, **2004**, 62, 405-426.
[74] Y. Wang, B. Samson, D. Ellison, L. Natanson, *Neural Comput & Applic.*, **2001,** 10, 253-263.
[75] B. Apolloni, A. Esposito, D. Malchiodi, C. Orovas, G. Palmas, J. G. Taylor, *IEEE Trans. Neural Netw.*,**2004**, 15, 6.
[76] J. V. Gorp, R. Pintelon, *IEEE Trans. Neural Netw.*,**2000**, 11, 2, 402-414.
[77] M. L. Wong, K. S. Leung, *IEEE Trans. Evolut. Comput.*, **2004**, 8, 4, 378-404.
[78] G. A. Jamieson, K. j. Vicente, *Comput. Chem. Eng.*, **2001**, 25 1055-1074.
[79] N.R. Sakthivel, V. Sugumaran, Binoy B. Nair Appl. St Comput., **2012,** *12 (1)*, 196-203.

[80] Yoon-Seok Timothy Hong Journal Hydrology, **2012,** *468–469,* 11-21.
[81] Chao Shang, Fan Yang, Dexian Huang, Wenxiang Lyu J. Process Control, **2014,** *24 (3),* 223-233.
[82] J. Martínez, M. López, J.M. Matías, J. Taboada Math. Comput. Model., **2013** *57 (7–8),* 1716-1721.
[83] Sanjeev S. Malalur, Michael T. Manry, Praveen Jesudhas NeuroComput., **2014.**
[84] Michael Georgiopoulos, Cong Li, Taskin Kocak Performance Evaluation,**2011,** *68 (4),* 361-384.

Training methods

[85] J. Xua, D. W.C. Hob, *NeuroComput.*, **2006**, 70, 544-558.
[86] A. D. Anastasiadis, G. D. Magoulas, M. N. Vrahatis, *NeuroComput.*, **2005**, 64, 253-270.
[87] Uro. S. Lotri, *NeuroComput.*, **2004**, 62, 179-196.
[88] P. Chandra, Y. Singh, *NeuroComput.*, **2004**, 61, 429- 437.
[89] O. Giustolisi, *NeuroComput.*, **2004,** 56, 285-304.
[90] T. W. S.Chow, Y. Fang, *NeuroComput.*, **2000**, 30, 333-337.
[91] J. A. Drakopoulos, A. Abdulkader, *Neural Netw.*, **2005**, 18, 595-601.
[92] E. M. Callaway, Neural Netw., **2004**, 17, 625-632.
[93] L. Ma, K. Khorasani, *Neural Netw.*, **2004**, 17, 589-609.
[94] S. Draghici, *Neural Netw.*, **2001**, 14, 527-550.
[95] Chi-Sing leung, Kwok-Wo wong, Pui-Fai Sum, Lai-Wam Chan, *Neural Netw.*, **2001**, 14, 147-174.
[96] K. Hagiwara, T. Hayasaka, N.Toda, S. Usui, K. kuno, *Neural Netw.*, **2001**, 14, 1419-1429.
[97] C. dang, *Neural Netw.*, **2000**, 13, 801-810.
[98] K. M. Adeney, M. J. Korennerg, *Neural Netw.*, **2000**, 13, 787-799.
[99] S. J. Perantonis, V. Virvilis, *Neural Netw.*, **2000**, 13, 351-364.
[100] G. Zhou, J. Si, *Neural Netw.*, **1999**, 12, 79-89.
[101] S.V. Kamarthi, S. Pittner, *Neural Netw.*, **1999**, 12, 1285-1299.
[102] R. Lengelle, T. denceux, *Neural Netw.*, **1996**, 9, 2, 83-87.
[103] M. plutowski, G. Cottrell, H. White, *Neural Netw.*, **1996**, 9, 2, 273-294.
[104] S. Ishii, K. Fukumizu, S. Watanabe, *Neural Netw.*, **1996**, 9, 1, 25-40.
[105] S. D. Hunt, J. R. Deller Jr, *Neural Netw.*, **1995**, 8, 6, 931-944.
[106] J. W. Andgary, G. R. Green, *Neural Netw.*, **1995**, 8, 1, 31-37.
[107] P. Patrick van der Smagt, *Neural Netw.*, **1994**, 7, 1, 1-11.
[108] E. Hartman, *Neural comput.*, *2000*, 12, 811-829.
[109] Y. Bengio, *Neural comput.*, **2000**, 12, 1889-1900.
[110] K. Ahmad, B. L. Vrusias, A. Ledford, *Neural Comput & applic.*, **2001**, 10, 56-66.
[111] P. K. H. Phua, D. Ming, *IEEE Trans. Neural Netw.,***2003**, 14, 6, 1460-1468.
[112] J. A. K. Suykens, J. Vandewalle, *IEEE Trans. Neural Netw.,***1999**, 10, 4.
[113] L. M. Reyneri, *IEEE Trans. Neural Netw.,***1999**, 10, 4.[114] M. H. Choueiki, C. A. M. Campbell, *IEEE Trans. Neural Netw.,***1999**, 10, 1, 56-63.
[115] A. Savich, M. Moussa, S. Areibi, Microprocessors and Microsystems, *36 (2),* **2012,** 138-150.

Applications

[116] V. Nourani, M. S. Fard, *Adv. Eng. Software,***2012,** 47 (1), 127-146.
[117] M. Akhoondzadeh, *Adv. Space Research,* **2013,** 51 (11), 2048-2057.
[118] A. P. Piotrowski, J. J. Napiorkowski, *Adv. Water Resources,***2012,** 49, 97-113.
[119] M. Hayati, B. Akhlaghi, *AEU – Int. J. Electronics Com.*, **2013,** 67 (2), 123-129.
[120] S. Sasikala, S. Appavu alias Balamurugan, S. Geetha, *Appl. Comput. Informatics,***2014 (in press).**
[121] C.Voyant, C. Darras, M. Muselli, C. Paoli, M. L. Nivet, P. Poggi, *Appl. Energy,* **2014,** 114, 218-226.
[122] A. Marvuglia, A. Messineo, *Appl. Energy,* **2012,** 98, 574-583.
[123] A. R. Tahavvor, M. Yaghoubi, *Appl. Math. Model.,* **2012,** 36 (7), 3176-3188.
[124] B. Vahdani, S.H. Iranmanesh, S. M. Mousavi, M. Abdollahzade, *Appl. Math. Model.,* **2012,** 36 (10), 4714-4727.

[125] D. Ren, Mao. Ye, *Appl. Math. Comput.,* **2012,** 218 (9), 5726-5738.
[126] E. Kolay, T. Baser, *Appl. Soft. Comput.,* **2014,** 18, 223-231.
[127] V. M. Janakiraman, X. Nguyen, D.Assanis, *Appl. Soft. Comput.,***2013,** 13 (5), 2375-2389.
[128] S. Rampone, *Appl. Soft. Comput.,* **2013,** 13 (10), 4077-4086.
[129] J. Sanz, R. Perera, C. Huerta, *Appl. Soft Computing,* **2012,** 12 (9), 2867-2878.
[130] A. E. Sherme, *Appl. Soft. Comput.,***2012,** 12 (1), 453-461.
[131] N. N. Charniya, S. V. Dudul, *Appl. Soft. Comput.,***2012,** 12 (1), 543-552.
[132] S. Polak, B. Wiśniowska, M. Ahamadi, A. Mendyk, *Appl. Soft. Comput.,* **2011,** 11 (2), 2611-2617.
[133] A. Wefky, F. Espinosa, A. Prieto, J.J. Garcia, C. Barrios, *Appl. Soft. Comput.,* **2011,**11(4), 3580-3599.
[134] A. Azadeh, Z.S. Faiz, *Appl. Soft. Comput.,* **2011,** 11 (1), 614-620.
[135] M. M. Etghani, M. H. Shojaeefard, A. Khalkhali, M. Akbari, *Appl. Thermal Eng.,***2013,** 59 (1–2), 309-315.
[136] J. Yang, H. Singh, E. L. Hines, F. Schlaghecken, D. D. Iliescu, M. S. Leeson, N. G. Stocks, *Art. Intel. Med.***2012,** 55 (2), 117-126.
[137] A. P. Balsamà, L. De Biase, G. J. Maenhout, V. Pagliari, *Atmospheric Env.,* **2014,**89, 581-592.
[138] J. H. Chen, M. C. Su, C. Yi. Chen, Fu-H. Hsu, C. C. Wu, *Automation in Construction,***2011,** 20 (7), 935-939.
[139] S. Sharma, S. S. Tambe, *Biochem. Eng. J.,***2014,** 85, 89-100.
[140] M. F. Abbod, K. Y. Cheng, X. R. Cui, S. J. Huang, Y. Yi Han, J. S. Shieh, *Biomed. Signal Processing Control,* **2011,** 6 (4), 414-421.
[141] E. T. Borroto, C. G. P. Rivas, J. C. V. Chagoyán, N. Castañedo, F. J. Prado-Prado, X. G. Mera, H. G. Díaz, *Bioorganic & Med. Chem.,***2012,** 20 (20), 6181-6194.
[142] E. V. Suprun, A. A. Saveliev, G. A. Evtugyn, A. V. Lisitsa, T. V. Bulko, V. V. Shumyantseva, A. I. Archakov, *Biosensors Bioelectronics,* **2012,**33(1), 158-164.
[143] G. S. Gill, A. Kumar, R. Agarwal, *Biosys. Eng.,* **2013,** 116 (2), 198-204.
[144] M.A. Vazquez-Cruz, R. Luna-Rubio, L.M. C. Medina, I. Torres-Pacheco, R.G. G. Gonzalez, *Biosys. Eng.,* **2012,** 112 (4), 319-327.
[145] S. S.K. Kwok, R. K.K. Yuen, Eric W.M. Lee, *Build. Env.,* **2011,** 46 (8), 1681-1690.
[146] M. ławryńczuk, *Chem. Eng. Sci.,* **2011,** 66 (21), 5253-5267.
[147] A. Abbasi, R. Eslamloueyan, *Chemomet. Intel. Lab. Syst.,* **2014,** 132, 39-51.
[148] A. Park, S. J. Baek, A. Shen, J. Hu, *Chemomet. Intel. Lab. Syst.,***2013,** 121, 52-56.
[149] A. Ghosh, B. Tudu, P. Tamuly, N. Bhattacharyya, R. Bandyopadhyay, *Chemomet. Intel. Lab. Syst.,***2012,** 116, 57-66.
[150] J.Gajewski, T.Sadowski, *Computational Materials Sci.,* **2014,** 82, 114-117.
[151] Z. Wang, B. Zineddin, J.Liang, N.Zeng, Y.Li, M. Du, J. Cao, X. Liu, *Comput. Methods Programs in Biomed.,***2013,** 111 (1), 189-198.
[152] J. Park, F. Diehl, M.J.F. Gales, M. Tomalin, P.C. Woodland, *Comput. Speech & Language* **2011,** 25 (3), 519-534.
[153] D.Ren, M. Ye, *Comput. Elect. Eng.,* **2011,** 37 (6), 1171-1181.
[154] A. Jahangirian, A. Shahrokhi, *Comput. & Fluids,* **2011,** 46 (1), 270-276.
[155] I. K. Kapageridis, A.G. Triantafyllou, *Comput. & Geosci.,* **2011,** 37 (4), 634-644.
[156] M. Ataş, Y. Yardimci, A. Temizel, *Comput. Electronics in Agriculture,***2012,** 87, 129-141.
[157] A. Tahmasbi, F. Saki, S. B. Shokouhi, *Comput. in Biol. Med.,***2011,** 41 (8), 726-735.
[158] G. Sermpinis, C. Dunis, J. Laws, C. Stasinakis, *Decision Support Systems,***2012,** 54 (1), 316-329.
[159] A. Baeza, J. Miranda, J. Guillén, J.A. Corbacho, R. Pérez, *Detectors Associated Equipment,* **2011,** 652(1), 450-453.
[160] S. M. Mirhassani, H. N. Ting, *Digital Signal Process.,***2014,** 31, 102-114.
[161] A. Özçift, A. Gülten, *Digital Signal Process.,***2013,** 23 (1), 230-237.
[162] H. Joutsijoki, K. Meissner, M. Gabbouj, S. Kiranyaz, J. Raitoharju, J. Ärje, S. Kärkkäinen, V. Tirronen, T. Turpeinen, M. Juhola, *Ecological Informatics,* **2014,** 20, 1-12.

[163] C. Bhuvaneswari, P. Aruna, D. Loganathan, *Egyptian Informatics J.*,**2014,** 15 (2), 69-77.
[164] E.A. Zanaty, *Egyptian Informatics J.*,**2012,** 13 (3), 177-183.
[165] K. Bacha, S. Souahlia, M. Gossa, *Electric Power Systems Res.*,**2012,** 83 (1), 73-79.
[166] A. Keçebaş, İ. Yabanova, *Energy Buildings*,**2012,** 50, 339-346.
[167] Z. Dong, D. Yang, T. Reindl, W. M. Walsh, *Energy Conversion Manag.*,**2014,** 79, 66-73.
[168] H.R. A. Siahoui, A.R. Dehghani, M. Razavi, M.R. Khani, *Energy Conversion Manag.*, **2011,** 52 (1), 505-511.
[169] C. Voyant, M. Muselli, C. Paoli, M. L. Nivet, *Energy*,**2011,** 36 (1), 348-359.
[170] M.M. Rashidi, N. Galanis, F. Nazari, A. Basiri Parsa, L. Shamekhi, *Energy,* **2011,** 36 (9), 5728-5740.
[171] J. Abdi, B. h. Moshiri, B. Abdulhai, A. K. Sedigh, *Eng. Appl. Art. Int.*, **2012,** 25 (5), 1022-1042.
[172] I. Z. M. Darus, Ali A. M. Al-Khafaji, *Eng. Appl. Art. Int.*,**2012,** 25 (1), 94-106.
[173] J. Eynard, S. Grieu, M. Polit, *Eng. Appl. Art. Int.*, **2011,** 24 (3), 501-516.
[174] Z. Gurocak, P. Solanki, S. Alemdag, M. M. Zaman, *Eng. Geol.*, **2012,** 145–146, 1-8.
[175] X. Li, A. C. Zecchin, H. R. Maier, *Env. Model. Softw.*, **2014,** 59, 162-186.
[176] D. F. Millie, G. R. Weckman, W. A. Young II, J. E. Ivey, D. P. Fries, E. Ardjmand, G. L. Fahnenstiel, *Estuarine, Coastal Shelf Sci.*,**2013,** 125, 57-67.
[177] F. P. Prado, X. G. Mera, P. Abeijón, N. Alonso, O. Caamaño, M. Yáñez, T. Gárate, M. Mezo, M. G. Warleta, L. Muiño, F. M. Ubeira, H. G. Díaz, *Eur. J. Med. Chem.*,**2011,** 46 (4), 1074-1094.
[178] F. P. Prado, X. G. Mera, M. Escobar, E. S. Sánchez, M. Yañez, P. R. Fernandez, H. G. Díaz, *Eur. J. Med. Chem.*,**2011,** 46 (12), 5838-5851.
[179] P. J. G. Laencina, J. L. S. Gómez, A. R. F. Vidal, *Expert Syst. Appl.*,**2013,** 40 (4), 1333-1341.
[180] A. P. Piotrowski, P. M. Rowinski, J. J. Napiorkowski, *Expert Syst. Appl.*, **2012,** 39 (1), 1354-1361.
[181] M. R. Homaeinezhad, S.A. Atyabi, E. Tavakkoli, H.N. Toosi, A. Ghaffari, R. Ebrahimpour, *Expert Syst. Appl.*, **2012,** 39 (2), 2047-2058.
[182] O. Castillo, P. Melin, E. Ramírez, J. Soria, *Expert Syst. Appl.*,**2012,** 39 (3), 2947-2955.
[183] N. Kamaruddin, A. Wahab, C. Quek, *Expert Syst. Appl.*,**2012,** 39 (5), 5115-5133.
[184] G. Sermpinis, J. Laws, A. Karathanasopoulos, C. L. Dunis, *Expert Syst. Appl.*, **2012,** 39 (10), 8865-8877.
[185] M. Bahoura, Y. Simard, *Expert Syst. Appl.*,**2012,** 39 (11), 9986-9993.
[186] E. Guresen, G. Kayakutlu, T. U. Daim, *Expert Syst. Appl.*,**2011,** 38 (8), 10389-10397.
[187] F. F. Navarro, C. H. Martínez, C. G. Alonso, M. T. Jimenez, *Expert Syst. Appl.*,**2011,** 38 (10), 12483-12490.
[188] A. F. Abidin, A. Mohamed, H. Shareef, *Expert Syst. Appl.*, **2011,** 38 (12), 14969-14975.
[189] M.H. Nisanci, E.U. Küçüksille, Y. Cengiz, A. Orlandi, A. Duffy, *Expert Syst. Appl.*,**2011,** 38 (3), 1689-1696.
[190] M. Türk, H. Oğraş, *Expert Syst. Appl.*, **2011,** 38 (3), 2557-2565.
[191] A. E. Shrme, *Expert Syst. Appl.*, **2011,** 38 (5), 6000-6006.
[192] C.M. Vong, P.K. Wong, *Expert Syst. Appl.*, **2011,** 38 (7), 8563-8570.
[193] M. M. Mostafa, *Expert Syst. Appl.*, **2011,** 38 (7), 8782-8803.
[194] M. Akın, *Expert Syst. Appl.*, **2011,** 38 (8), 9207-9210.
[195] M. Caner, E. Gedik, A. Keçebaş, *Expert Syst. Appl.*, **2011,** 38 (3), 1668-1674.
[196] D. Bastani, M.E. Hamzehie, F. Davardoost, S. Mazinani, A. Poorbashiri, *Fluid Phase Equilibria,* **2013,** 354 (25), 6-11.
[197] A. Z. Hezave, M. Lashkarbolooki, S. Raeissi, *Fluid Phase Equilibria,* **2012,** 314, 128-133.
[198] M. Lashkarblooki, A. Z. Hezave, A. M. Al-Ajmi, S. Ayatollahi, *Fluid Phase Equilibria,* **2012,** 326, 15-20.
[199] M. Lashkarbolooki, B. Vaferi, M.R. Rahimpour, *Fluid Phase Equilibria*, **2011,** 308 (1–2), 35-43.
[200] F. Mateo, R. Gadea, E. M. Mateo, M. Jiménez, *Food Control*, **2011,** 22 (1), 89-95.
[201] Y. Brandão, J. Teodosio, F. Dias, W. Eustáquio, Moh. Benachour, *Fuel,***2013,** 110, 185-195.
[202] Zhao Bo, *IERI Procedia*, **2012,** 1, 248-253.

[203] J. Luengo, F. Herrera, *Informat. Sci.*,**2012,** 185 (1), 43-65.
[204] P. Sussner, E. L. Esmi, *Informat. Sci.*, **2011,** 181 (10), 1929-1950.
[205] S. Mirjalili, S. M. Mirjalili, A. Lewis, *Informat. Sci.*, **2014,** 269, 188-209.
[206] M. Balcilar, A.S. Dalkilic, A. Suriyawong, T. Yiamsawas, S. Wongwises, *Int. Comm. in Heat Mass Transfer*,**2012,**39(3), 424-431.
[207] M. Balcilar, A.S. Dalkilic, O. Agra, S.O. Atayilmaz, S. Wongwises, *Int. Comm. in Heat Mass Transfer,* **2012,** 39 (7), 937-944.
[208] M. Balcilar, A.S. Dalkilic, S. Wongwises, *Int. Comm. in Heat Mass Transfer*, **2011,** 38 (1), 75-84.
[209] D. Tian, X. jun Zeng, J. Keane, *Int. J. Approximate Reasoning*,**2011,** 52 (6), 863-880.
[210] A. Sharifian, S. Sharifian, *Int. J. Electrical Power & Energy Systems*, **2015,** 64, 71-87.
[211] W. C. Yeh, Y. M. Yeh, Po-C. Chang, Y. C. Ke, V. Chung, *Int. J. of Electrical Power & Energy Systems*,**2014,** 55, 741-748.
[212] S. Souahlia, K. Bacha, A. Chaari, *Int. J. of Electrical Power & Energy Systems*,**2012,** 43(1), 1346-1353.
[213] F. Nakhaei, M.R. Mosavi, A. Sam, Y. Vaghei, *Int. J. of Mineral Process.*, **2012,** 110–111, 140-154.
[214] N. Babanouri, S. K. Nasab, S. Sarafrazi, *Int. J. of Rock Mechanics Mining Sci.*, **2013,** 60, 66-74.
[215] N. Babanouri, S. K. Nasab, S. Sarafrazi, *Int. J. of Rock Mechanics Mining Sci.*,**2013,** 60, 66-74.
[216] V. Gitifar, A. Abbasi, P. Setoodeh, M. Poursadegh, Z. Sahebnazar, A. Alamdari, *Int. J. of Thermal Sci.*,**2014,** 83, 45-55.
[217] P. Bagheripour, *J. Appl. Geophys*.,**2014,** 104, 142-148.
[218] M. Abedi, G. H. Norouzi, *J. Appl. Geophys.*, **2012,** 83, 35-45.
[219] A. K. Singal, P. S. Kamath, *J. Clinical Experimental Hepatology*,**2013,** 3 (1), 50-60.
[220] R. Cerri, R. C. Barros, A. C.P.L.F. de Carvalho, *J. Comput. Syst. Sci.*,**2014,** 80 (1), 39-56.
[221] B. Vaferi, M. Bahmani, P. Keshavarz, D. Mowla, *J. Environ. Chem. Eng.*,**2014,** 2 (3), 1252-1260.
[222] M. Arebey, M.A. Hannan, R.A. Begum, H. Basri, *J. Environ. Manag.*,**2012,** 104, 9-18.
[223] A. Loutfi, S. Coradeschi, G. K. Mani, P. Shankar, J. Bosco B. Rayappan, *J. Food Eng.*, **2015,** 144, 103-111.
[224] V. Nourani, A. H. Baghanam, J. Adamowski, O. Kisi,**2014,** 514, 358-377.
[225] J. He, C. Valeo, A. Chu, N. F. Neumann, *J. Hydrology*, **2011,** 400 (1–2), 10-23.
[226] A. P. Piotrowski, J. J. Napiorkowski, *J. Hydrology*, **2011,** 407 (1–4), 12-27.
[227] M. Cobaner, *J. Hydrology*, **2011** 398 (3–4), 292-302.
[228] M. Ay, O. Kisi, *J. Hydrology*,**2014** 511 (16), 279-289
[229] P. D. Rodríguez, J. C. Cancilla, G. Matute, J. S. Torrecilla, *J. Ind. Eng. Chem.*,**2014.,** (in press)
[230] G. Sermpinis, C. Stasinakis, C. Dunis, *J. Int. Financial Markets, Institutions Money*,**2014**, 30, 21-54.
[231] J. Park, S. Han, J. Kim, *J. Iron Steel Res.*, **2014**, 21 (3), 321-327.
[232] W.L. Tan, N.M. Nor, M.Z. Abu Bakar, Z. Ahmad, S.A. Sata, *J. Loss Prevention in the Process Industries*, **2012**, 25 (1), 138-141.
[233] M. Khayet, C. Cojocaru, M. Essalhi, *J. Membrane Sci.*, **2011**, 368 (1–2), 202-214.
[234] D. Palomba, G. E. Vazquez, M. F. Díaz, *J. Molecular Graphics Modelling*, **2012**, 38, 137-147.
[235] N. Saghatoleslami, G. H. Vatankhah, H. Karimi, S. H. Noie, *J. Natural Gas Sci. Eng.*, **2011**, 3 (1), 319-325.
[236] A. Shahsavand, F. D. Fard, F. Sotoudeh, *J. Natural Gas Sci. Eng.*, **2011**, 3 (3), 518-529.
[237] B. Vaferi, V. Gitifar, P. Darvishi, D. Mowla, *J. Petroleum Sci. Eng.*, **2014**, 119, 69-78.
[238] M.S. Karambeigi, R. Zabihi, Z. Hekmat, *J. Petroleum Sci. Eng.*, **2011**, 78 (2), 208-219.
[239] B. Vaferi, R. Eslamloueyan, S. Ayatollahi, *J. Petroleum Sci. Eng.*, **2011**, 77 (3–4), 254-262.
[240] F. A.A. Souza, R. Araújo, T. Matias, J. Mendes, *J. Process Control*, **2013**, 23 (10), 1371-1378.
[241] A. B. Nassif, D. Ho, L. F. Capretz, *J. Systems Software*, **2013**, 86 (1), 144-160.
[242] S. Dehuri, R. Roy, S. B. Cho, A. Ghosh, *J. Systems Software*, **2012**, 85 (6), 1333-1345.
[243] A. R. Mehrabian, A. Y. Koma, *J. Franklin Institute*, **2011**, 348 (1), 12-23.

[244] H. G. Díaz, F. P. Prado, E. S. Sánchez, M.Haddad, S. M. Chevalley, A. Valentin, J. Q. Leclercq, M. A. Dea-Ayuela, M. T. Gomez-Muños, C. R. Munteanu, J. J. T. Labandeira, X.G. Mera, R. A. Tapia, F. M. Ubeira, *J. Theoretical Biology*, **2011**, 276 (1), 229-249.
[245] G. Wang, J. Ma, L. Huang, K. Xu, *Knowledge-Based Systems*, **2012**, 26, 61-68.
[246] C. F. Tsai, Yu-Hsin Lu, D. C. Yen, *Knowledge-Based Systems,* **2012**, 31, 67-77.
[247] S. A. Kumar, S. G. S. Raman, T.S.N. Sankara Narayanan, R. Gnanamoorthy, *Materials & Design,***2013**, 49, 992-999.
[248] H. PourAsiabi, H. PourAsiabi, Z. AmirZadeh, M. BabaZadeh, *Materials & Design*,**2012**, 35, 782-789.
[249] N. Razmjooy, B. Somayeh Mousavi, F. Soleymani, *Mathematical Comput. Model.*,**2013**, 57 (3–4), 848-856.
[250] A. Azadeh, Z.S. Faiz, S.M. Asadzadeh, R. Tavakkoli-Moghaddam, *Math. Comput. Simul.,* **2011**, 82(4), 666-678.
[251] G.H. Roshani, S.A.H. Feghhi, A. Mahmoudi-Aznaveh, E. Nazemi, A. Adineh-Vand, *Measurement*,**2014**, 51, 34-41.
[252] A. Gharehbaghi, T. Dutoit, P.Ask, L. Sörnmo, *Medical Eng. & Physics*,**2014**, 36 (4), 477-483.
[253] V. Malekian, R. Amirfattahi, S. Sadri, M.Mokhtari, A. Aghaie, M. Rezaeian, *Micron*, **2013**, 45, 59-67.
[254] A. Armato, L. Fanucci, E.P. Scilingo, D. De Rossi, *Microprocessors Microsystems,* **2011**, 35 (6), 557-567.
[255] M. F. Delgado, E. Cernadas, S. Barro, J. Ribeiro, J. Neves, *Neural Networks,***2014**, 50, 60-71.
[256] S. S.T. Bathaie, Z.N. S. Vanini, K. Khorasani, *NeuroComput.*, **2014**, 125, 153-165.
[257] B. Ploj, R. Harb, M. Zorman, *NeuroComput.,* **2014**, 126, 180-187.
[258] Yi. C. Hu, *NeuroComput.,* **2014**, 129, 306-314.
[259] T. Kuremoto, S. Kimura, K. Kobayashi, M.Obayashi, *NeuroComput.,***2014**, 137, 47-56.
[260] S. A. Rahim, A. M. Yusof, T. Bräunl, *NeuroComput.*, **2014**, 133, 84-94.
[261] S. M. Siniscalchi, D. Yu, Li. Deng, C. H. Lee, *NeuroComput.*, **2013**, 106, 148-157.
[262] M. Castellani, *NeuroComput.*, **2013**, 99, 214-229.
[263] L. C. Calvo, S. S. Sanz, J. Luterbacher, *NeuroComput.*, **2013**, 113, 262-268.
[264] S. K. Oh, W. D. Kim, B. J. Park, W. Pedrycz, *NeuroComput.*, **2013**, 119, 292-307.
[265] J. F. R. Villegas, D. F. R. Moreno, *NeuroComput.,* **2012**, 77 (1), 82-100.
[266] X. Wang, X. Gao, Y. Yuan, D. Tao, J. Li, *NeuroComput.*, **2010**, 73 (10-12), 2186-2195.
[267] C. D. Hacker, T. O. Laumann, N. P. Szrama, A. Baldassarre, A. Z. Snyder, E.C. Leuthardt, M. Corbetta, *NeuroImage,* **2013**, 82, 616-633.
[268] W. Kusakunniran, Q. Wu, J. Zhang, H. Li, *Pattern Recognition Let.*, **2012**, 33 (7), 882-889.
[269] A. Majumder, L. Behera, V. K. Subramanian, *Pattern Recognition*, **2014**, 47 (3), 1282-1293.
[270] M. Szaleniec, *Pharmacological Reports,* **2012**, 64 (4), 761-781.
[271] S. Olyaee, S. Hamedi, Z. Dashtban, *Precision Eng.* **2012**, 36 (3), 379–387.
[272] W. K. Shams, A. Wahab, I. Fakhri, *Procedia - Social Behavioral Sci.*, **2013**, 97, 54-62.
[273] K. S. Rahnuma, A. Wahab, H. A Majid, B.Crüts, *Procedia - Social Behavioral Sci.*, **2011**, 27, 299-305.
[274] L. Aggarwal, K. Aggarwal, R. J. Urbanic, *Procedia CIRP*, **2014**, 17, 812-817.
[275] J. Anderson, K. Mokhtari, A. Kulkarni, *Procedia Comput. Sci.*, **2012**, 12, 294-299.
[276] T. Kajiyama, D. D'Alimonte, Jośe C. Cunha, *Procedia Comput. Sci.*, **2011**, 4, 2186-2195.
[277] T. A. Boran Şekeroğlu, *Procedia Technology*, **2012**, 1, 449-452.
[278] M. Bagheri, S.A. Mirbagheri, M. Ehteshami, Z. Bagheri, *Process Safety Environ. Protection,* **2014** (in press)
[279] Y. Chetouani, *Process Safety Environ. Protection,***2014**, 92 (3), 206-214.
[280] B. Su, X. Zeng, J. Zhai, Y. Wang, X. Li, *Quaternary International*, **2014**,(in press).
[281] M. Rumbayan, A. Abudureyimu, K. Nagasaka, *Renewable Sustainable Energy,* **2012**, 16 (3), 1437-1449.

[282] A. Azadeh, R. Babazadeh, S.M. Asadzadeh, *Renewable Sustainable Energy Reviews,* **2013**, 27, 605-612.
[283] A. Paniagua-Tineo, S. Salcedo-Sanz, C. C. Mateo, E.G. O. García, M.A. Cony, E. H.Martín, *Renewable Energy,* **2011**, 36 (11), 3054-3060.
[284] A. Azadeh, M. Sheikhalishahi, S.M. Asadzadeh, *Renewable Energy,* **2011**, 36 (12), 3394-3401.
[285] Z. Csépe, L. Makra, D. Voukantsis, I. Matyasovszky, G. Tusnády, K. Karatzas, M. Thibaudon, *Sci. of The Total Environ,* **2014**, 476–477, 542-552.
[286] D. Voukantsis, K. Karatzas, J. Kukkonen, T. Räsänen, A. Karppinen, M. Kolehmainen, *Sci. of The Total Environ.,* **2011**, 409 (7), 1266-1276.
[287] J. Amani, R. Moeini, *Scientia Iranica,***2012**, 19 (2), 242-248.
[288] A.R. Kazemi, F. Sobhanmanesh, *Scientia Iranica,* **2011**, 18 (6), 1443-1449.
[289] M.R. Homaeinezhad, E. Tavakkoli, S.A. Atyabi, A. Ghaffari, R. Ebrahimpour, *Scientia Iranica,* **2011**, 18 (3), 423-431.
[290] D. Gao, F. Liu, Ji. Wang, *Sensors Actuators B: Chemical*, **2012**, 161 (1), 578-586.
[291] T. Danisman, I. M. Bilasco, J. Martinet, C.Djeraba, *Signal Process.,* **2013**, 93 (6), 1547-1556.
[292] A. A. Kulaksız, R. Akkaya, *Solar Energy*, **2012**, 86 (9), 2366-2375.
[293] S. Ikbal, H. Misra, H. Hermansky, M. M. Doss, *Speech Communication,* 2012 54 (7), 867-880.
[294] M. J. Diamantopoulou, *Sustainable Computing: Informatics Syst.*,**2012**, 2 (4), 190-197.
[295] Mu. C. Su, S. C. Lai, S. C. Lin, L. Fu. You, *Swarm Evolutionary Computation,***2012**, 6, 39-46.
[296] Y. Chetouani, *Systems Eng. Procedia*,**2011**, 1, 473-480.
[297] B. Vaferi, M. Karimi, M. Azizi, H. Esmaeili, *The J. Supercritical Fluids,* **2013**, 77, 44-51.
[298] A. J. Choobbasti, H. Tavakoli, S. S. Kutanaei, *Tunnelling Underground Space Tech.,***2014**, 40, 192-202.
[299] S. Mahdevari, S. R. Torabi, *Tunnelling Underground Space Technology,* **2012**, 28, 218-228.
[300] Md. S. Islam, M.A. Hannan, H. Basri, A. Hussain, M. Arebey, *Waste Manag.*,**2014**, 34 (2), 281-290.
[301] M.A. Hannan, M. Arebey, R.A. Begum, H.Basri, *Waste Manag.*,**2012**, 32 (12), 2229-2238.
[302] D.J.C. MacKay, *Neural Comput.* **1992**, 4, 448–472.

Speciometrics, Kinetometrics, Chemometrics and Piscimetrics

[303] K. RamaKrishna, V. Anantha Ramam, R. Sambasiva Rao, *J. Applicable Chem.*, **2014**, 3, 5, 1807-1893.
[304] K. RamaKrishna, V. Anantha Ramam, R. Sambasiva Rao, *J. Applicable Chem.*, **2014**, 3, 4, 1337-1422.
[305] K. RamaKrishna, V. Anantha Ramam, R. Sambasiva Rao, *J. Applicable Chem.*, **2014**, 3, 3, 919-989.
[306] K. RamaKrishna, V. Anantha Ramam, R. Sambasiva Rao, *J. Applicable Chem.*, **2014**, 3, 2, 834-884.
[307] K. RamaKrishna, R. Sambasiva Rao, *J. Applicable Chem.*, **2014**, 3, 2, 449-492.
[308] K. RamaKrishna, Ch.V. Kameswara Rao, V. Anantha Ramam, R. Sambasiva Rao, *J. Applicable Chem.*, **2014**, 3, 1, 006-029.
[309] K. RamaKrishna, G. Ram kumar, R Sambasiva Rao, *J. Applicable Chem.*, **2013**, 2, 6, 1413-1458.
[310] K. RamaKrishna, Ch.V. Kameswara Rao, R Sambasiva Rao, *J. Applicable Chem.*, **2013**, 2, 5, 1007-1034.
[311] K. RamaKrishna, Ch.V. Kameswara Rao, R. Sambasiva Rao, *J. Applicable Chem.*, **2013**, 2 (4): 698-713.
[312] M.V. Subba Rao, V Ananta Ramam, V. Muralidhara Rao, R. Sambasiva Rao, *Research J. Science and Tech.*, **2013**, 5, 4, 412-420.
[313] K. Viswanath, R. Sambasiva Rao, Ch. V. Kameswara Rao, K Rama Krishna, B Rama Krishna, G. E. G. Santhosh, *Journal Applicable Chemistry*, **2012**, 1, 1, 109-124.
[314] K. RamaKrishna, Ch. V. Kameswara Rao, V. Ananta Ramam, R. Sambasiva Rao, M. V. Subba Rao, *Indian Journal Chemistry*, **2012**, 51A, 571-579.

[315] M. V. Subba Rao, V. Ananta Ramam, V. Muralidhara Rao, R. Sambasiva Rao, *Asian J Chem*., **2010**, 22, 5937-5950.
[316] I. Suryanarayana, A. Braibanti, R. Sambasiva Rao, V. Ananta Ramam, D. Sudarsan, G. Nageswara Rao, *Fisheries Research*, **2008**, 92, 115-139.
[317] I. Suryanarayana, V. Ananta Ramam, K. M. M. Krishna Prasad, R. Sambasiva Rao, *Ind. J. Chem.*, **2008**, 47A, 199-206.
[318] V. Ananta Ramam, V. V. Panakala Rao, K. Rama Krishna, R. Sambasiva Rao, *Ind. J. Chem,* **2006**, 45A, 100-105.
[319] R. Sambasiva Rao, G. Nageswara Rao, *Computer applications in Chemistry*, Himalya Publisher, New Delhi (India), **2005**.
[320] A. Braibanti, R. Sambasiva Rao, G. Nageswara Rao, V. Ananta Ramam, S.V.V. Satyanarayana Rao, *Ann. Chim. Rome,* **2002**, 92, 689-704.
[321] A. Braibanti, G. Nageswara Rao, S. B. Jonnalagadda, D. Sudarsan, R. Sambasiva Rao, Ann. *Chim.(Rome)*, **2001**, 91, 29-39.
[322] L. H Abdel Rehman, K. Sambasiva Rao, G. Nageswara Rao, R. Sambasiva Rao, *J. Ind. Council. Chemists*, **2001**, 17, 33-50.
[323] V. V. Panakala Rao, V. Ananta Raman, G. Nageswara Rao, R. Sambasiva Rao, *Proc National Seminar on Environmental Geology and Waste Management*, **2000**, Andhra University.
[324] A. Braibanti, R. Sambasiva Rao, G Priyabrinda, G. Nageswara Rao, *Ann. Chim.*, **1989**, 89, 193-209.
[325] A. Braibanti, E. Fisicaro, C. Compari, A. Ghiozzi, R. Sambasiva Rao, G. Nageswara Rao, *Reactive and Functional polymers,* **1998**, 36, 3, 245-249.
[326] E. Fisicaro, A. Braibanti, R. Sambasiva Rao, C. Compari, A Ghiozzi, G. Nageswara Rao, *Talanta*, **1998**, 45, 6, 1267-79.
[327] A. Braibanti, R. Sambasiva Rao, G. Nageswara Rao, N. Satyanarayana, *Talanta*, **1998**, 47, 109-120.
[328] G. Nageswara Rao, V. Ananta Ramam, S. Satyanarayana Rao, R. Sambasiva Rao, *J. Ind. Chem. Soc.*, **1998**, 75, 236-47.
[329] K. Sambasiva Rao, R. Sambasiva Rao, *J. Korean Phys. Soc.*, **1998**, 32, S1850-S1851.
[330] G. Priyabrinda, G. Nageswara Rao, R. Sambasiva Rao, *J. T R Chem.*, **1997**, 4, 2, 29-42.
[331] V. Anantha Ramam, G. Nageswara Rao, S. V. Rama Sastri, R. Sambasiva Rao, *Ind. J Chem.,* **1997**, 36A, 964-969.
[332] G. Nageswara Rao, V. Anantha Ramam, R. Sambasiva Rao, *Bull. Soc. Kinet. Ind.,* **1997**, 19, 2, 1-6.
[333] A. Braibanti, R. Sambasiva Rao, G. Nageswara Rao, N. Satyanarayna, *J. Ind. Council. Chem.*, **1997**, 12, 27-40.
[334] A. Braibanti, K Sambasiva Rao, Ch. S. V Prasad, R. Sambasiva Rao, *Samyak J.Chem*., **1997**, 1(1), 17-21.
[335] V. Ananta Ramam, D. Subrahmanyam, S.V.V. Satyanarayna Rao, R. Sambasiva Rao, *J. Teaching and Research in Chem.,* **1997**, 4, 20-28.
[336] S.V.V. Satyanarayana Rao, J. S. V. M. Lingeswara Rao, A. Ravindra Babu, D. Murali Krishna, R. Sambasiva Rao, *J. Ind. Chem. Soc.,* **1996**, 73, 9-19.
[337] G. Nageswara Rao, R. Sambasiva Rao, *J. Teaching & Research in Chem.,* **1995**, 2, 15-28.
[338] A. Ravindra Babu, J.S.V.M Lingeswara Rao, D. Murali Krishna, R. Sambasiva Rao, *Anal. Chim. Acta.,* **1995**, 306, 297-300.
[339] A. Braibanti, R. Sambasiva Rao, A. Ravindra Babu, G. Nageswara Rao, *Ann. Chim. Rome,* **1995**, 85, 17-29.
[340] J. S. V. M. Lingeswara Rao, N. Satyanarayana, D. Muralikrishna, G. Nageswara Rao, R. Sambasiva Rao, *Chem. & Edu.,* **1994**, 26-33.
[341] M.W. Pandit, R. Sambasiva Rao, S.V.V. Satyanarayana, G. Nageswara Rao, D. Murali Krishna, *Bull.Pure & Appl.Sci.,* **1994**, 13G, 41-49.
[342] A. Braibanti, E. Fisicaro, F. Dallavalle, J. D. Lamb, J. L. Oscarson, R. Sambasiva Rao, *J. Phys. Chem.,* **1994**, 98, 626-634.
[343] R. Sambasiva Rao, *J. Chem. Sci.,* **1993**, 14, 23-44.

[344] A. Ravindra Babu, D. Murali Krishna, R. Sambasiva Rao, *Talanta*, **1993**, 40, 1873-1882.
[345] A. Ravindra Babu, D. Murali Krishna, R. Sambasiva Rao, *Ind. J. Chem.*, **1993**, 32A, 1064-1071.
[346] V. Hari babu, A. Ravindrababu, G. NageswaraRao, K. V. Ramana, R. Sambasiva Rao, *Bull.Pure & Appl.Sci.*, **1993**, 12C, 31-43.
[347] G. Nageswara Rao, R. Sambasiva Rao, *Ind. Council Chemists*, **1992**, VIII, 12-28.
[348] A. Ravindra Babu, R. Sambasiva Rao, *J. Chem.& Eng. Data*, **1992**, 37, 526-531.
[349] G. Nageswara Rao, S. V. V. Satyanarayana Rao, A. Ravindra Babu, R. Sambasiva Rao, *Asian J. Chem.*, **1992**, 4, 99.
[350] G. Nageswara Rao, K.V. Ramana, R. Sambasiva Rao, *J. Ind. Chem. Soc***., 1991,** 68, 34.
[351] G. Nageswara Rao, S.V.V. Satyanarayana, R. Sambasiva Rao, *Ind. J. Chem. Sci.*, **1990**, 4, 73-112.
[352] N. Padmaja, M. Sarat Chandra Babu, G. Nageswara Rao, R. Sambasiva Rao, K.V. Ramana, *Polyhedron*, **1990**, 20, 2497.
[353] S. V. V. Satyanarayana Rao, A. Ravindra babu, G. Nageswara Rao, A. Satynarayana, R. Sambasiva Rao, *Acta Cien. Indica*, **1989,** 15, 321.
[354] G. Nageswara Rao, V. M. Ch. Vinaya Kumari, K.V. Ramana, R. Sambasiva Rao, *Ind. J. Chem.*, **1989**, 28A, 709-712.
[355] S. V. V. Satyanarayana Rao, A. Ravindra babu, G. Nageswara Rao, A. Satynarayana, R. Sambasiva Rao, *Ind. J. Chem*, **1989**, 28A, 292-297.
[356] K. V. Bapanaiah, A. Ravindra Babu, G. Nageswara Rao, R. Sambasiva Rao, *J. Ind. Council Chemists*, **1988**, 4, 79-83.
[357] C. Rambabu, R. Sambasiva Rao, P. V. Krishna Rao, *Acta Ciencia Indica*, **1988**, 14, 43-50.
[358] G. Nageswara Rao, S. V. V. Satyanarayna Rao, A. Ravindra Babu,R. Sambasiva Rao, *J. Ind.Council Chemists*, **1988**, 4, 77-92.
[359] S. V. V. Satyanarayana Rao, G. Nageswara Rao, A. Ravindra Babu, R. Sambasiva Rao, *J.Chem.Science.*, **1987**, 13, 1-31.
[360] C.Rambabu, R. Sambasiva Rao A. Satyanarayana, P. V. Krishna Rao, *Proc. Nat.Acad.Sci. India*, **1987**, 57(A) III, 292-298.
[361] C. Rambabu, P. V. Krishna Rao, A. Satyanarayna, R. Sambasiva Rao, *Chem.Anal.(Warsaw)*, **1987**, 32, 51-64.
[362] G. Nageswara Rao, K. V. Ramana, R. Sambasiva Rao, *Ind. J. Chem.*, **1987**, 26A, 849-852.
[363] P. V. Krishna Rao, A. Satyanarayana, R. Sambasiva Rao, *Proc. Nat. Acad.Sci. India*, **1987**, 57(A) III, 293-298.
[364] C. Rambabu, R. Sambasiva Rao, A. Satyanarayana, P. V. Krishna Rao, *Ind. J. Chem.*, **1987**, 26A, 1073-1075.
[365] C. Rambabu, R. Sambasiva Rao, A. Satyanarayana, P. V. Krishna Rao, *Chimica Acta Turcica*, **1986**, 14, 183-197.
[366] C. Rambabu, R. Sambasiva Rao, A. Satyanarayana, P. V. Krishna Rao, *Chimica.Acta Turcica*, **1986**, 14, 75-86.
[367] P. V. Krishna Rao, S. Appa Rao, R. Sambasiva Rao, A. Satyanarayana, *Chem. Anal. (Warsaw)*, **1986**, 31, 21-28.
[368] C. Kamala Sastry, K. M. M. Krishna Prasad, A. Satyanarayana, R. Sambasiva Rao, *Proc. summer. Computer. simul. conf.* **1986**, 348-353.
[369] C. Rambabu, R. Sambasiva Rao, A. Satyanarayana, P. V. Krishna Rao, *Ind. J. Chem*., **1985**, 24A, 1079-1081.
[370] K. M. M. Krishna Prasad, C. Kamala Sastry, A. Satyanarayana, R. Sambasiva Rao, *Bull. Pure and App. Sci.*, **1985**, 4, 13-37.
[371] K. M. M. Krishna Prasad, R. Sambasiva Rao, C. Kamala Sastry, A. Satyanarayana, *Proc. Summer Simulation Conference*, **1985**, 359-364.
[372] R. Sambasiva Rao, A. Satyanarayana, P.V. Krishna Rao, Proc. *Summer Simulation Conference*, **1984**, 563-568.
[373] C. Rambabu, R. Sambasiva Rao, P.V. Krishna Rao, *Curr. Sci.*, **1984**, 53, 527-528.

[374] P.V. Krishna Rao, R. Sambasiva Rao, A. Satyanarayana, *Data for Science and Technology*, **1983,** 237-240.
[375] K. V. Bapanaiah, R. Sambasiva Rao, *Ind. Chem. J.*, **1980**, 7, 22-23.
[376] P.V. Krishna Rao, Ch. Rambabu, R. Sambasiva Rao, *Nat. Acad. Sci. Letters*, **1980**, 3, 150-152.
[377] P.V. Krishna Rao, Ch. Rambabu, A. Satyanarayana, R. Sambasiva Rao, *Chem. anal. (Warsaw)*, **1979**, 24, 755-760.
[378] P.V. Krishna Rao, R. Sambasiva Rao, Ch. Rambabu, *Nat. Acad. Sci. Letters*, **1979**, 2, 55-57.
[379] P.V. Krishna Rao, R. Sambasiva Rao, *Acta Ciencia Indica*, **1979**, 5, 205-208.
[380] P.V. Krishna Rao, R. Sambasiva Rao, Ch. Rambabu, *Ind. Chem. J.*, **1978** April**,**.1-2.
[381] P.V. Krishna Rao, R. Sambasiva Rao, A. Satyanarayana, *Ind. J. Chem.*, **1978**, 16A, 909-910.
[382] C. Rambabu, R. Sambasiva Rao, P.V. Krishna Rao, *Chem. Anal. (Warsaw)*, **1978**, 23, 257-260.
[383] P.V. Krishna Rao, R. Sambasiva Rao, Ch. Rambabu, *Curr. Sci.*, **1978**, 47, 542-543.
[384] P.V. Krishna Rao, R. Sambasiva Rao, Ch. Rambabu, *Acta.Ciencia Indica*, **1978**, 4, 13-15.
[385] P.V. Krishna Rao, R. Sambasiva Rao, *Ind. Chem. J.*, **1977,** September,1-2.
[386] P.V. Krishna Rao, R. Sambasiva Rao, *J. Inorg. Nucl. Chem.*, **1977**, 39, 708.
[387] K.V.Bapanaiah, R. Sambasiva Rao, *Science Reporter*, **1975**, 12, 315.
[388] P.V. Krishna Rao, R. Sambasiva Rao, *Curr. Sci.*, **1975**, 44, 551.
[389] P.V. Krishna Rao, R. Sambasiva Rao, *Mikrochim. Acta (Wien)*, **1975**, 237.
[390] R. Sambasiva Rao, G. Bala Bhaskara Rao, P.V. Krishna Rao, *Chem. Anal. (Warsaw)*, **1974**, 19, 927.
[391] P.V.K. Rao, G.B. Bhaskara Rao and R. Sambasiva Rao, *Z Anal. Chem.*, **1973**, 260, 367.
[392] P.V. Krishna Rao, G. Bala Bhaskara Rao, R. Sambasiva Rao, *Anal. Chim. Acta*, **1973**, 65, 227.
[393] Rupenaguntla Naga Satish Chandra, **2003**, Master's thesis, University of Miami, USA, (b) R.N. Satish, D. Sarkar, *IEEE International Conference on Communications*, **2004**, 7, 4082 – 4086.

Appendix A1. An Ant

Artificial Neuron (An)-

(Accumulation_operator Neuron Transfer_function) (Ant)

An artificial neuron is a processing unit or system transforming a set of inputs into single or tensor of outputs. The input data first undergoes **a**ccumulation/confluence operation in the **n**euron. Then **t**ransfer function operates outputting the result (Fig. A1-1). Now, this is simply referred as neuron in computational intelligence paradigm. Although processing unit is in usage as a synonym, the signature of neuron imparts stimulus to reach the ultimate target of artificial brain. Although, the basic structure of neuron remained same over half a century, the complexity increased depending upon data type, dimension of input tensor, confluence operators and/or TFs. The number of distinct neurons in vogue is around two dozen and classified under different heads for comprehension. The broad categories are static, adaptive and dynamic. The concerted efforts especially during the last quarter century in increasing the potency of artificial neurons in adapting to sure to work operators, functions and data structures are from mathematical sciences. The improvements achieved in noisy, imprecise, indefinite and conflicting data are dealt with fuzzy operators/membership functions, tensor/Clifford (geometric) product, stochastic functions, chaotic equations, dynamic/distributed time delay feedback etc. The result is a large number of neurons, consequently subsets of NNs.

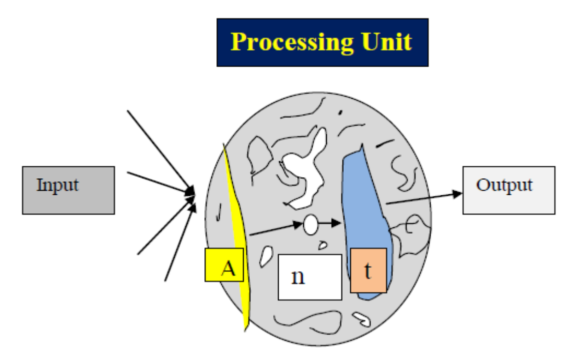

Fig A1- 1: Input → [Accumulation →Neuron →TF] → output
I → Ant → O

Appendix A1a: Transfer Functions

The transfer function is as simple as identity to real/ complex valued algebraic/ trigonometric basis functions. In a neuron, single input (SI) or a set of (multiple) inputs (MI) is transformed into a single output (SO). However, in case of a higher order neuron, a vector of outputs (MO) is generated for each input pattern. They are referred as single-input-multiple-output (SIMO) or multiple-input-multiple-output (MIMO) systems. Chart A1-1 classifies transfer functions based on mathematical terminology.

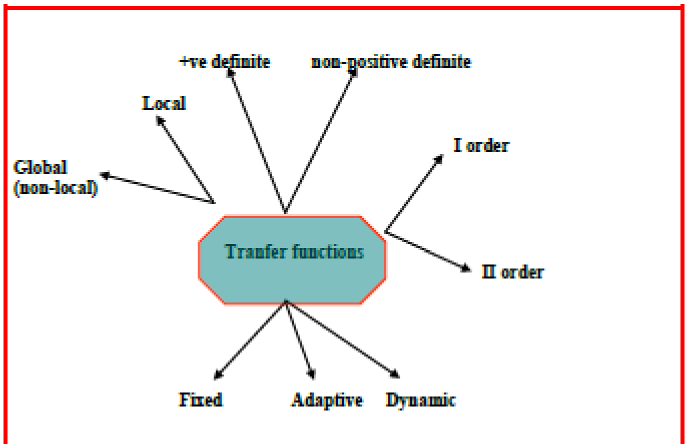

Chart A1-1: Typical classification of TFs based mathematical principles

Real valued TFs

A TF in general consists of variable(s), constant(s) and coefficients/ (empirical/ theoretical) parameters. Product of linear variables, power of a linear variable and exponential/ logarithmic/ transcendental function of a linear variable introduces non-linearity.

Identity function

A generating function of the general type with linear basis function results in a linear $\left[s*x+threshold\right]^{\frac{1}{1-power}}$ and also many non-linear functions of increasing order. A plot of y versus x is linear passing through origin. That is how it is called a linear transfer function. In fact, it is nothing but multiplying it with 1 or identity. With two dimensional spaces, it is identity operating on a column vector of input variables at an ith point (Chart A1-2).

Chart A1-2 Identity TF

$y = LinFun(x) = I(dentity)*x$	$y^T = LinFun(x) = x^T * I(dentity)$
$y = [1]*[x_1] = [x_1]$	$y = [x_1]*[1] = [x_1]$
$y = \begin{bmatrix}1 & 0\\0 & 1\end{bmatrix} * \begin{bmatrix}x_1\\x_2\end{bmatrix} = \begin{bmatrix}x_1\\x_2\end{bmatrix}$	$y = \begin{bmatrix}x_1 & x_2\end{bmatrix} * \begin{bmatrix}1 & 0\\0 & 1\end{bmatrix} = \begin{bmatrix}x_1 & x_2\end{bmatrix}$
$y = \begin{bmatrix}1 & 0 & 0\\0 & 1 & 0\\0 & 0 & 1\end{bmatrix} * \begin{bmatrix}x_1\\x_2\\x_3\end{bmatrix} = \begin{bmatrix}x_1\\x_2\\x_3\end{bmatrix}$	$y = \begin{bmatrix}x_1 & x_2 & x_3\end{bmatrix} * \begin{bmatrix}1 & 0 & 0\\0 & 1 & 0\\0 & 0 & 1\end{bmatrix} = \begin{bmatrix}x_1 & x_2 & x_3\end{bmatrix}$

If	input space is one dimensional	&
	steepness parameter (s) = 1	&
	power = 0	&
	threshold = 0	
Then	$y = LinFun(x) = [1*x+0]^{\frac{1}{1-0}} = 1*x = x$	

Thus, the simplest TF is identity. A few other simple TFs in 1D-input space are '-I', reciprocal, square root, power operator etc.

Stuck function

A function outputting the same value (a constant, zero or one) is called a stuck function and practically serves no purpose expect that it is an obstacle. The erroneous logic in software (Table A1-1) or malfunction in hardware/electronic devices is the reason behind it.

A numerical example with 'and' and 'or' relational operators are used to produce an output of one and zero respectively, irrespective of the input is negative, positive integer/floating point value or even zero. A real number is +ve, -ve or zero only. The antecedent is always satisfied irrespective of the condition and thus, output is stuck at 1. The 'and' clause is never be true and thus the output is always zero. If there is no input to a system, obviously, there is no output. In other words, it is like absolute silence.

Table A1-1 Stuck functions

Stuck at				Ex Input	output
1	Unconditional assignment		y=1	-111	1

	Antecedent never saatisfied for a numeric value	and	function [y] = om_stuck1and(x)
			if x ==0 & x < 0 & x >0
			y=0;
			else
			y = 1;
			end
				0	1

		or	function [y] = om_stuck1(x)
			if x ==0 | x < 0 | x >0
			y = 1;
			else
			y = 0;
			end
				99	1

0	Unconditional assignment		function [y] = om_stuck0(x) y=0;	-111	0

	Antesedent is saatisfied always for a numeric value	or	function [y] = om_stuckor0(x)
			if x ==0 | x < 0 | x >0
			y = 0
			else
			y = 1;
			end
				0	0

	Antesedent is saatisfied always for a numeric value	or	function [y] = om_stuckor1(x)
			if x ==0 | x < 0 | x >0
			y = 1;
			else
			y = 0;
			end
				99	0

Threshold/bias/offset function

It uses algebraic relational operator ('<', '>=') to output two integer (binary/bipolar) values, multiple discrete/continuous values. The two valued function is referred as Hardlimitor

Symmetric Hardlimitor: The mathematical form of hardlimitor is depicted in Table A1-2. A matlab program (m file) implementing the expression as it is using a ' For' loop and if-then-else rule is given. A concise form in tensor notation is also presented.

Hardlimitor: The response is zero or one. It is used in electronics, classification to decipher whether it belongs to a category or not.

Table A1-2: TF.Hardlimitor

Hardlimitor	$If \quad x<0,\ y=0$ $else \quad y=1$	x bi bip --------------- -3 0 -1
Bipolar	$If \quad x<0,\ y=-1$ $else \quad y=1$	-2 0 -1 -1 0 -1 0 1 1 1 1 1 2 1 1 3 1 1

```
%
% om_hardlimitor_binary.m  (R S Rao 6/11/09, 5/4/99)
%
function [y_hardlimitor_binary, y_hardlimitor_bipolar,
df,Name] = om_hardlimitor(x,fig)

if nargin == 0
   clean
  x = xgrid(-3,4,1);fig = 1;
end

y_hardlimitor_binary  = (x >= 0) ;
y_hardlimitor_bipolar = 2*(x >= 0)-1 ;
```

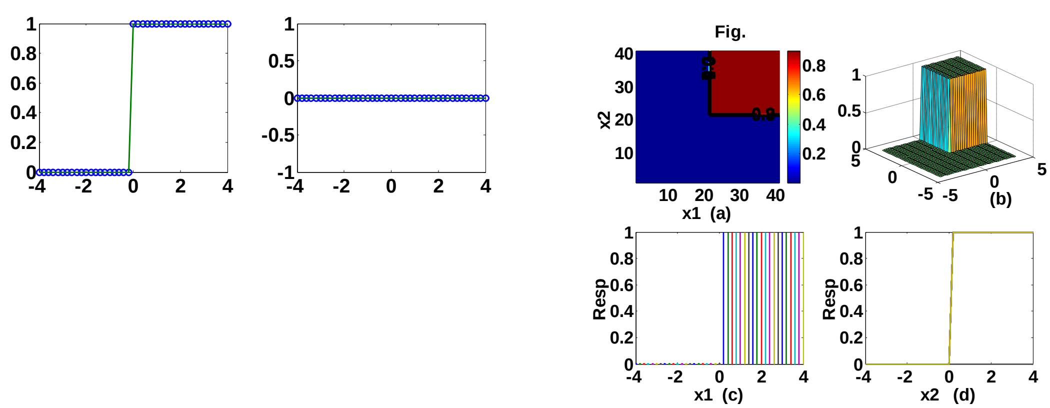

Step function: The step- and multiple step functions which are used as TFs in NNs are summarized in table A1-3.

Table A1-3: TF.Step function

$$TF = \begin{cases} -1 & if\ x \le -1 \\ x-1 & if\ 0 < x < +1 \\ +1 & if\ x \ge +1 \end{cases}$$

```
for i = 1:length(x)
    if  x(i,1)<= (-1)
        y(i,1) = -1;
    end
    if  x(i,1)>= (1)
        y(i,1) = 1;
    end
    if  (0 < x(i,1)) && (x(i,1)< 1)
        y(i,1) = x(i,1)-1;
    end
end
```

-2.0000 0.3000 -4.0000 -5.0000 3.0000
5.0000
-1.0000 -0.7000 -1.0000 -1.0000 1.0000
1.0000

-9.0000 0.6300 0.9000
-1.0000 -0.3700 -0.1000

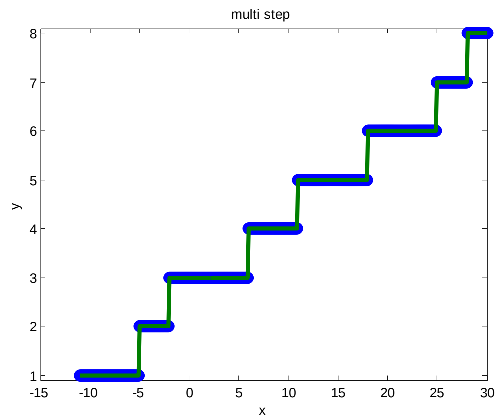

If x <limit1 y = 0
Limit1<x<limit2 y =2
Limit2<x<limit3 y =3
Limit10<x<limit11 y =11

```
%
% om_multiint.m   (R S Rao 24/7/06)
%
function [x,y]= om_multiint(x,ranges,fig)
if nargin <1
   clean, fig = 1;
   [x,one] = xgrid(-11,30,.1);
   ranges = [-5,-2,6,11,18,25, 28]'
end

%%
for ii = 1:size(ranges)-1
    for j = 1:length(x)
        if (x(j,1) <ranges(1,1))
            y(j,1) = 1;
        end
        if (x(j,1) >= ranges(ii,1))&& (x(j,1) <= ranges(ii+1,1))
            y(j,1) = ii+1;
        end
        if (x(j,1) > ranges(length(ranges),1))
            y(j,1) = length(ranges)+1;
        end
    end
end
```

Signum/heavy side function: The graphical profile of response of signum function (Table. A1-4) is similar to hardlimitor function, especially tanh.

Table A1-4: TF.Signum function	

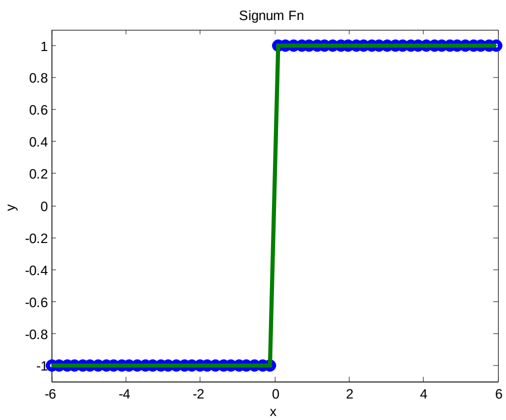

$$\begin{aligned} &If \quad x > 0 \\ &then \quad sign(x) = +1 \\ &elseif \;\; x = 0 \\ &\qquad sign(x) = 0 \\ &\qquad else \quad sign(x) = -1 \\ &endif \end{aligned}$$

```
y = sign(x);
```

Rectangular basis function**:** The output is a binary value depending upon whether the input is within or outside a real interval (a to b) (Table A1-5).

Table A1-5: TF. Rectangular basisfunction

$$rec\tan ular(x) = \begin{cases} 1 \; if \; a \le x \le b \\ 0 \; else \end{cases}$$

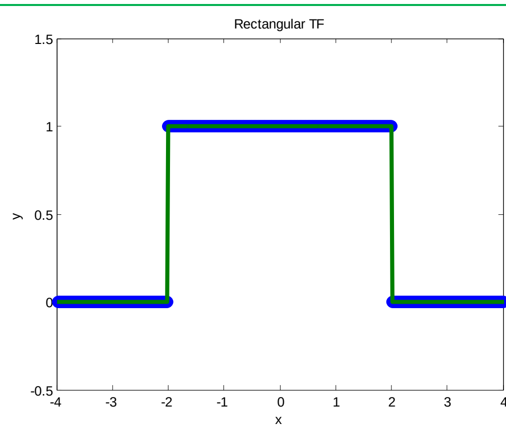


```
 %
% om_rectangular.m    (R S Rao 24/7/06)
%
function [rectangular]= om_rectangular(x,a,b,fig)

 for i = 1:length(x)
     if (le(a,x(i,1)) && x(i,1)<=b)
         rectangular(i,1) = 1;
     else
         rectangular(i,1) = 0;
     end
 end
```

Linear generating function

Typical Linear functions include pure linear, linear_saturated, linear_saturated _symmetric ones. The profiles are straight lines and planes in 2D- input spaces (Table A1-6, Fig. A1-2). The input neurons of a layered NN always have an identity TF, but popularly referred as linear one. In fact, in SLP_NN, MLP_NN, ART_NN, the input layer simply transmits the values as they are. In other words, the output of the input neuron is same as the input signal. In the case of function approximation problems, the output neuron also has the same role. For classification tasks, the hard limiter TF is used to produce a binary discrete classification label.

Table A1-6: TF.Linear functions			
Linear $$$	**Formula**	**Intelligent expression#**	**MATLAB code**
Pure	$\text{TF} = \begin{cases} -1 & if \quad x \le 0 \\ x-1 & if\ 0 \le x \le +1 \\ +1 & if \quad x > +1 \end{cases}$	**max(0,min(1,x))**	`linpure = x;`
Positive	$\text{TF} = \begin{cases} x & if\ x \ge 0 \\ 0 & if\ x < 0 \end{cases}$	**max(0,x)**	`linpos = max(0,x);`
Saturating			`Linsat = max(0,min(1,x));`
Saturating symmetric	$\text{TF} = \begin{cases} -1 & if \quad x \le 1 \\ x & if\ -1 \le x \le +1 \\ +1 & if \quad x > +1 \end{cases}$	**max(-1,min(1,x))**	`Linsatsym = max(-1,min(1,x));`
#:NMATLAB manual			

Fig. A1-2: x-y plots, 3D-surfaces and 2D-contours for linear TF functions

linpure

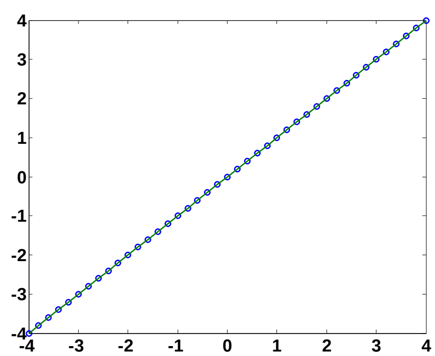

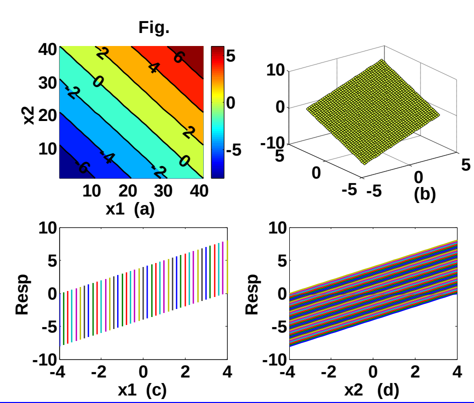

Linpos

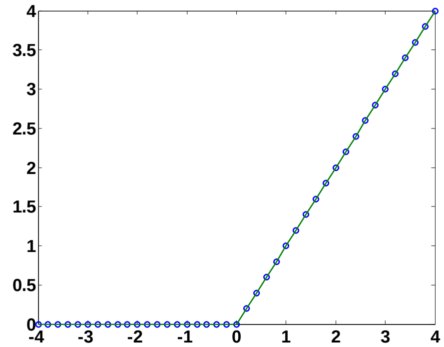	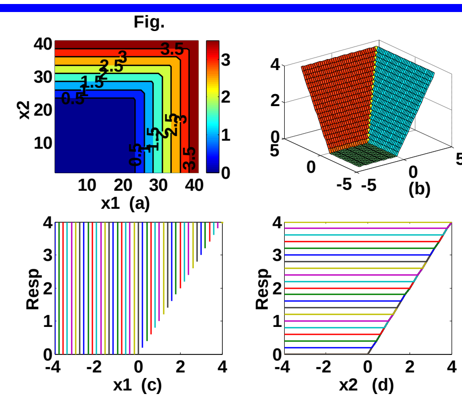
linsat	
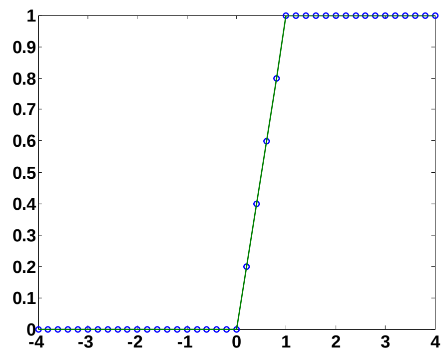	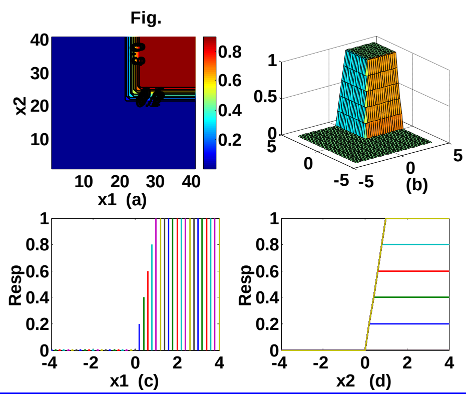
linsatsym	
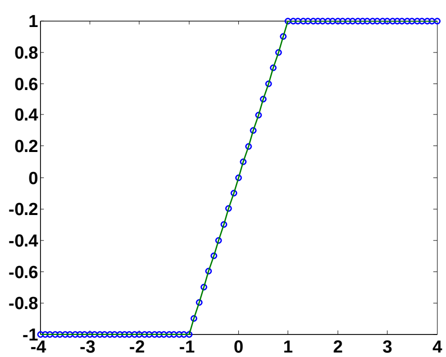	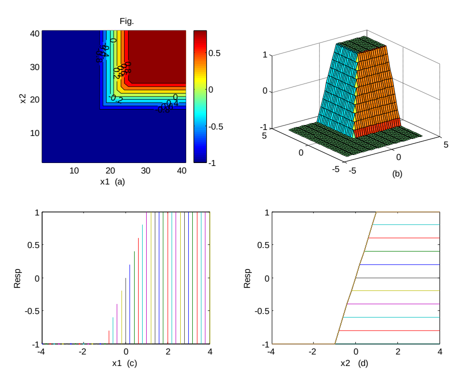

```
% om_lin2x.m   (R S Rao)
%
function [linpure,linsat,linsatsym]=
om_lin2x(x,y,fig)
if nargin <3,fig = 1;
   [x,y]= meshgrid(-2:1:2,-2:1:2);
end

linpure    = x+y;
linpos     = max(0,max(max(1,x),y));
linsat     = max(0,min(min(1,x),y));
linsatsym  = max(-1,min(min(1,x),y));
```

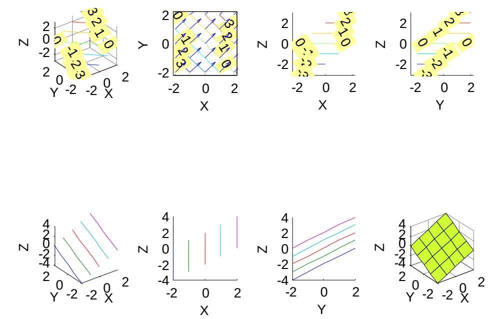

Non-linear functions

The product of two linear (first order) algebraic variables/functions is non-linear. The square (second order), higher integer power (polynomial in one variable) or fractional power (square root) is a source of non-linearity. Sine and cosine (Transcendal functions) are also non-linear but periodic. Of course, these can be expressed as a (in)finite series of exponential functions. The simplest square function in 2D- and 3D- variable space is a circle and sphere. They collapse into ellipse (ellipsoid), plane, line and a dot with variation of the coefficients.

Elliot function

The profile of Elliot function is similar to sigmoid profile (Table A1-7). It is ratio of polynomials of first order with an additional constraint that the modulus of term in the denominator is used. A normalized form is also proposed.

Table A1-7 : Elliot function

$$yElliot(x) = \frac{k*x}{1+abs(k*x)}$$

$$yElliot\_normalised(x) = \frac{yElliot(x)}{\sum abs(x)} = \frac{\left\{\frac{k*x}{1+abs(k*x)}\right\}}{\sum abs(x)}$$

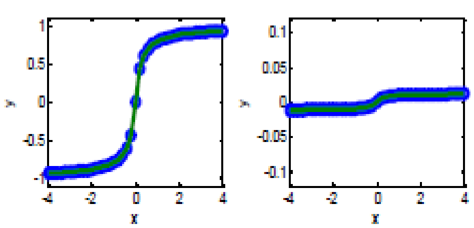

```
%
% om_elliot.m  (R S Rao  17/8/06)
%
function [y_elliot,ynorm_elliot]=om_elliot(x,one,k,fig)

y_elliot     =   k*x./(one+ abs(k*x));
ynorm_elliot =   y_elliot./sum(abs(x));
```

Polynomial function

Polynomial functions in 1D-input space account for non-linearity with single or multiple cliffs. On the other hand, with multi-input cases, the output of a polynomial forms higher order TFs, which include second- and higher-order terms. The second order terms contain squares and binary cross products. The third order set has cubes, ternary cross products and binary products of first order and square terms. These higher order functions and Clifford geometric entities are the prospecting TFs of this decade. There are still only scanty reports in many application fields.

Exponential function

Softmax is normallized exponential function. The combination of simplest exponential functions viz. exp(x) and exp(-x) generate sinh, cosh, and the sought after tanh. The range of tanh is -1 to +1, producing a symmetric profile around zero. The popular RBF is also an exponential function with ($-x^2$) as an argument. The range of output is 0 to 1 as x moves from $-\infty to \infty$ (Table A1-9a). The bipolar output is readily transformable into bipolar sigmoid.

Table A1-8 : Softmax function

$$ysoft\max = \frac{\exp(x)}{\sum \exp(x)}$$

```
%
% om_softmax.m  (R S Rao 5/4/99)
%
function [ysoftmax,Name]= om_softmax(x,one)
expn = exp(x);
ysoftmax = expn./ sum(expn,1);
Name = 'TF_SoftMax';
```

Softmax function (table A1-8)

The range of softmax is 0 to 1.

Sigmoid function

It is a non-decreasing or monotonously increasing smooth function bounded between real values of 0 and 1. Analytical derivatives (gradient and Hessian) exist (chart A1-3). The universal function approximation theorem was proved for MLP_NN with sigmoid TF, the consequence being any non-linear function can be approximated for any desired accuracy. The formulae and object module (om) of matlab functions are given in **table A1-9**. Sigmoid TF produces linearly independent internal representation [23].

Sigmoid on hardware

Armato et al. [254] proposed calculation of low-error approximation of sigmoid and subsequently hyperbolic tangent (tanh) function using piece wise linear procedure. The minimum number of precision bits for convergence for MLP_NN is arrived. This approach resulted in smaller absolute as well as mean relative errors compared to state-of-art-methods. The digital implementation of sigmoid function has favorable score in terms of lower complexity and error. Sigmoid and tanh are used in TFs in artificial neurons. Thus, it plays a crucial role in hardware implementation of **ma**thematical **n**eurons (man). VHDL approximation of Taylor series of sigmoid is with an error of 0.005 in the entire range (Chart A1-4). Another method using CORDIC algorithm calculates hyperbolic sine and cosine functions. Tanh calculated as the ratio of sinh to cosh is used to obtain sigmoid. Two segments (0 to 2 and 2 to 4) are used. When an accurate result is desired more CORDIC rotations are used. The error in this method also remains around 0.005.

Chart A1-4: Hardware computation of sigmoid function

x	SG(x) →	Tanh(x)→	g(TF) →		
				SG	Tanh
If $x \to -\infty$	0	-1		0	0
If $x \to +\infty$	1	1		0	0
If $x = 0$	0	0		--	---

TF_SG

- Shape restriction of profile
  - Remedy : Higher order TF
    - m-SG
    - Generalized RBF

Expert opinions –
(use with caution)

If TF is bipolar sigmoid function (tanh) [-1 to +1]
Then convergence speed increases

	If K,D, L paramters are also refined along with W in BP Then NN approximates a nonlin function more closely	

Chart A1-3 : Sigmoid function and its first (gradient) and second (Hessian) derivatives

TF =	$g(\mathrm{TF}) = \dfrac{d(TF)}{dx} =$	$H(\mathrm{TF}) = \dfrac{d(\mathrm{g}(TF))}{dx} = \dfrac{d^2(TF)}{dx^2} =$
$SG(x) = \dfrac{1}{1+\exp(x*s+b4)}$	s*SG * (1-SG)	s^2 *SG * (1-SG) *(2-SG)
$\tanh(x) = \dfrac{1-\exp(-x)}{1+\exp(-x)}$	$\dfrac{(1+\tanh)*(1-\tanh)}{2}$	$-\dfrac{\tanh}{2}*(1+\tanh)*(1-\tanh)$
par_SG : [s,threshold] ; ySG = SG(x;par_SG) = SG(x)		

Table A1-9a: sigmoid TF	

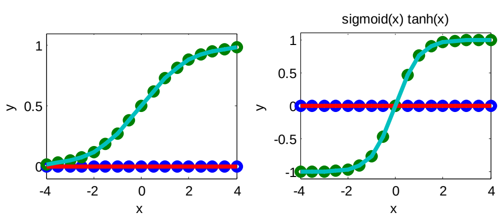	`%`
	`% om_sg.m (R S Rao 5/4/99)`
	`%`
	`function [sg,dsg,d2sg,name] = om_sg(x,s,threshold,one)`
	`sg = one./(one + exp(-x*s + threshold *one));`
	`dsg = sg.* (one-sg);`
	`d2sg = sg.* (one-sg).* (one - 2*sg);`
	`name = 'Sigmoid';`

	`%`
	`% om_tanh.m (R S Rao 8/8/10, 5/4/99)`
	`%`
	`function [tanhx,dtanhx] = om_tanh(x,one,t)`
	`tanhx = (exp(x/t) - exp(-x/t))./(exp(x/t)+ exp(-x/t));`
	`dtanhx = (one+tanhx).*(one-tanhx)/2;`

The multiplication two vectors by the rules of extended matrix notation (i.e. element wise multiplication) is used (table A1-9b).

Table A1-9b: Sigmoid function in two dimensions

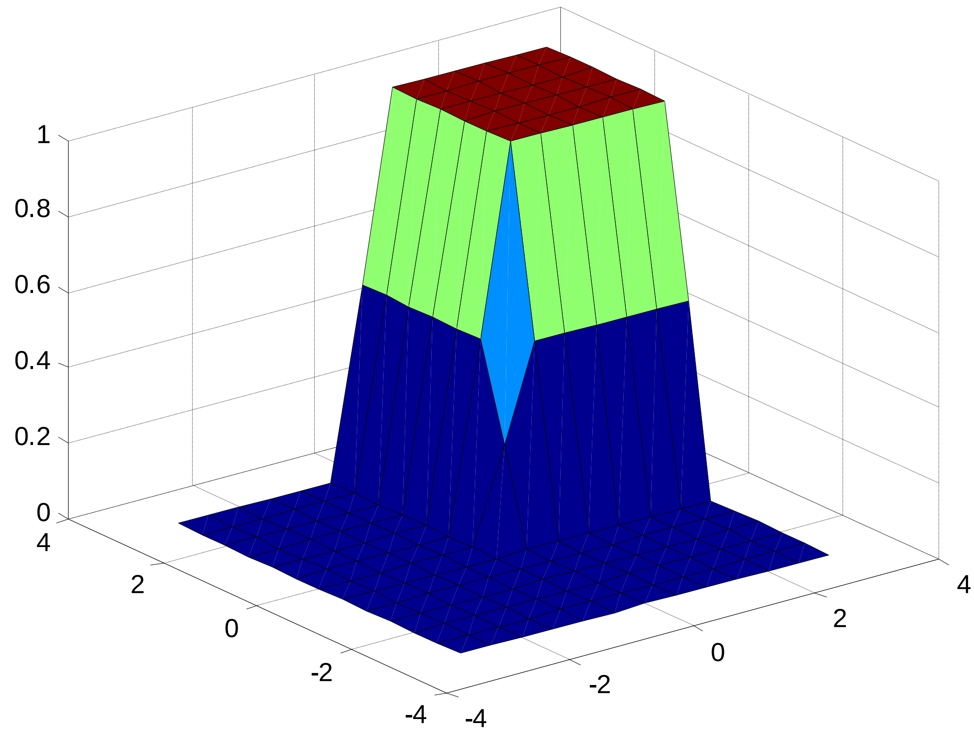


```
%
%  dem_sg2x.m   18/10/03 (12:00 hrs)
%
function [sg2sum] = om_sg2xT(xx,yy,steep,threshold,fig)
if nargin<4, clean,fig = 1;
 [xx,yy]= meshgrid(-3:0.5:3,-3:0.5:3);
 threshold = 0;steep = 1e4,A = 1;
end

 [r,c]= size(xx); one = ones(r,c);
 [sg1,dsg,d2sg,name] = om_sg(xx,steep,threshold,one);   % Table A1-9a (om_sg.m)
 [sg2,dsg,d2sg,name] = om_sg(yy,steep,threshold,one);
  surf(xx,yy, sg1.*sg2)
```

By changing the threshold and steepness parameters, sigmoid emulates hard limiter, linear functions etc. (table A1-10).

Table A1-10: sigmoid function emulating hardlimitor, straight line

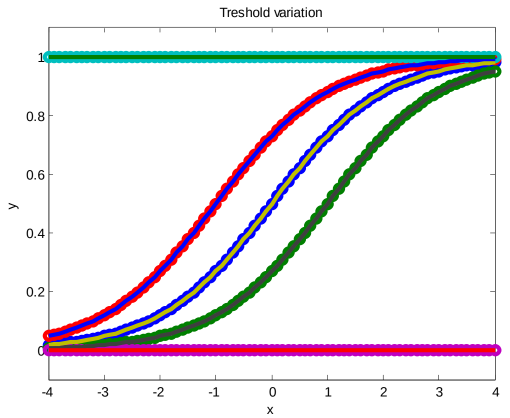	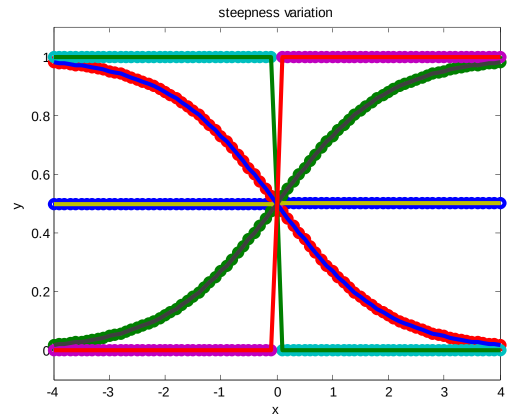
Threshold: [1e-4 1 -1 -100 100]' Slope = 1	Steepness : [1e-4 1 -1 -1e2 1e2] Threshold = 0

```
%
%  dem_sgk.m   (R S Rao 12/05/05 ; R Naga Satish 30/07/2001)
%
 clean
 [x] = [-4:.1:4]';
 [r,c]=size(x); one = ones(r,c);
 format short g
%
%    Threshold
%
 k = 1;
 thz = [ 1e-4   1 -1 -1e2 1e2   ]';
 [rth,cth]=size(thz);
 for i = 1:rth
     th = thz(i,1);
     [t2] = om_sg(x,k,th,one);
      T3(:,i)= t2;
 end
plot2d(x,T3)
plot2d(x,T3(:,1),T3(:,2),T3(:,3),T3(:,4),T3(:,5))
%
%    steepness
%
kz = [  1e-4   1 -1 -1e2 1e2     ]';
  [rk,ck]=size(kz);
 for i = 1:rk
     k = kz(i,1);
     [t2] = om_sg(x,k,0,one);
      T4(:,i)= t2;
 end
 plot2d(x,T4)
 plot2d(x,T4(:,1),T4(:,2),T4(:,3),T4(:,4),T4(:,5))
```

Table A1-11 shows the effect of variation of power in extended-sigmoid function profiles.

Table A1-11: Effect of power parameter on sigmoid function profiles

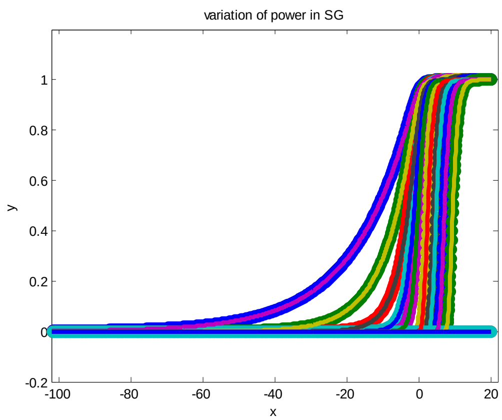

X scale : -100 to 20

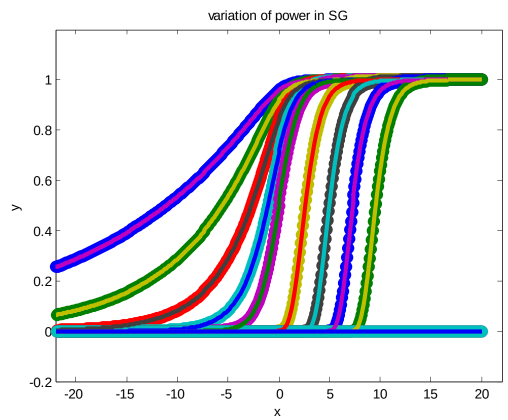

X scale : -20 to 20

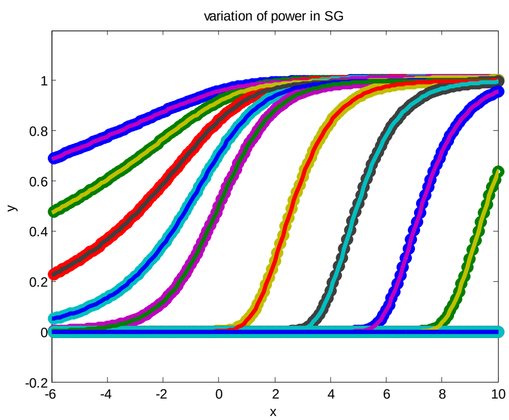

X scale : -6 to 10

Variation of m in sigmoid function

$$SGm(x) = \left[\frac{1}{1+\exp\left(x * s + b4\right)}\right]^m$$

```
%
% dem_sgpower.m   12/05/05
%
 clean
[x] = [-103:.1:20]';
mz = [1/16,1/8,1/4,1/2,1,10,100,1000,1e4,1e10,1e20]'

[r,c]=size(x); one = ones(r,c);
format short g
[sg,dsg,d2sg,name] = om_sg(x,1,0,one);
for i = 1:11
   m = mz(i,1);
   sgm = sg.^m;  T3(:,i)= sgm;
end
 axisz=[-102,22,-0.2,1.2];
figure,om_fig2d(x,T3,'variation of power in SG',axisz);
figure,om_fig2d(x,T3,'variation of power in SG',[-22,22,-0.2,1.2]);
axisz=[-6,10,-0.2,1.2];figu re, om_fig2d(x,T3,'variation of power in SG',axisz);
[x,T3]
```

Tanh function

The range of output of tanh is -1 to +1. It is also a monotonous increasing function like sigmoid. The two functions, sigmoid and tanh are related (table A1-12). The numerical values of tanh from sinh, cosh and expoential functions for a few typical values are incorporated (Table A1-12) and visual appreciation of algebraic equations is evident from the figures and numerical values. This toy approach is a stepping stone to probe into the complex operations in large sized NNs.

Table A1-12: Tanh and sigmoid functions

$$Sinh(x)=\frac{\exp(x)-\exp(-x)}{2} \qquad \cos h(x)=\frac{\exp(x)+\exp(-x)}{2}$$

$$\tanh(x)=\frac{\exp(x)-\exp(-x)}{\exp(x)+\exp(-x)}=\frac{\sinh(x)}{\cosh(x)}$$

$$Sigmoid(x)=\frac{\tanh(x)+1}{2} \qquad \tanh(x)=[2*Sigmoid(x)-1]$$

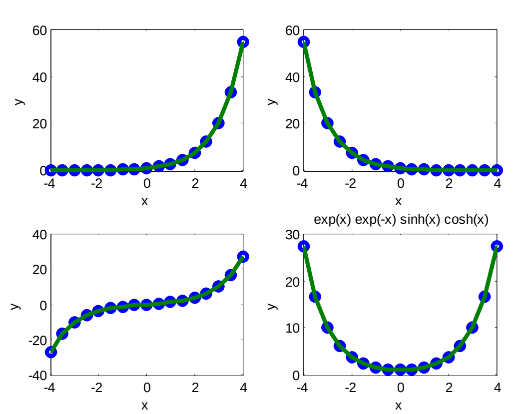

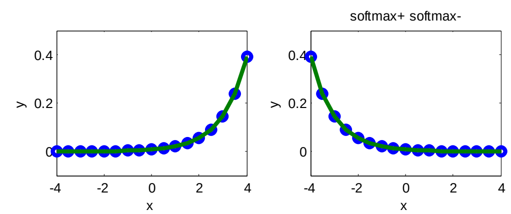


```
%
%  dem_sgdetail.m   12/05/05
%
 clean
 format short g
 [x,one] = xgrid(-4,4,1);t = 1;
%
St01 =' exp(x) exp(-x) sinh(x) cosh(x)';
exppx = exp(x/t); expnx = exp(-x/t);
sinhz = [exp(x/t) - exp(-x/t)]/2;
coshz = [exp(x/t) + exp(-x/t)]/2;
tanhz01 = sinhz./coshz;
[x,sinhz,sinhz-sinh(x),coshz,coshz-cosh(x)]
plot2d(x,exppx,expnx,sinhz,coshz)
title(St01)

ysoftmax = exppx./ sum(exppx,1);
ysoftmax2 = expnx./ sum(expnx,1);
plot2d(x,ysoftmax,ysoftmax2)
title('softmax+ softmax-')
%
% tanh from sigmoid
sg = one./(one + expnx);
tanh01 =  2*sg-one;
x0 = zeros(length(x),1);
% Equivalent formulae
%
```

```
tanhz = (exp(x/t) - exp(-x/t))./(exp(x/t)+ exp(-x/t));
tanh02 =  tanh(x/t);% [x,tanh02,tanhz-tanh02,tanh01-tanh02]
[x tanhz01,tanhz,tanh02]
plot2d(x,[x0,sg],[x0,tanhz])
title('sigmoid(x) tanh(x)')
```

Numerical equivalence of hyperbolic functions

[x,	sinhz,	sinhz-sinh(x),	coshz,	coshz-cosh(x)]
-4	-27.29	0	27.308	0
-3	-10.018	0	10.068	0
-2	-3.6269	0	3.7622	0
-1	-1.1752	-2.2204e-16	1.5431	0
0	0	0	1	0
1	1.1752	2.2204e-16	1.5431	0
2	3.6269	0	3.7622	0
3	10.018	0	10.068	0
4	27.29	0	27.308	0

x	tanhz01,	tanhz,	tanh02
-4	-0.99933	-0.99933	-0.99933
-3	-0.99505	-0.99505	-0.99505
-2	-0.96403	-0.96403	-0.96403
-1	-0.76159	-0.76159	-0.76159
0	0	0	0
1	0.76159	0.76159	0.76159
2	0.96403	0.96403	0.96403
3	0.99505	0.99505	0.99505
4	0.99933	0.99933	0.99933

General form of Exponential function: Considering the general non-linear function NL1 with exponential terms, hyperbolic, tanh, logit and sigmoid functions are simpler forms (Table A1-13).

Table A1-13: Simplified functions of general Expfun

$$Expfun(x) = \frac{\exp(x*s1+b1)-\exp(x*s2+b2)}{\exp(x*s3+b3)+\exp(x*s4+b4)}$$

s: Steepness of function
b: Threshold

Name		Function	Constraint
$Hyp2(x)$	=	$\frac{\exp(x*s)-\exp(x*s)}{\exp(x*s)+\exp(x*s)}$	s1=s2=s3=s4=s b1=b2=b3=b4=0
$\tanh(x)$	=	$\frac{1-\exp(x*s2+b2)}{1+\exp(x*s4+b2)}$	s1 = 0 s3 = 0 b1=b2=0
$\text{logit}(x)$	=	$\frac{\exp(x*s2)}{1+\exp(x*s4)}$	s3=0, b2=b4=0
$SG(x)$	=	$\frac{1}{1+\exp(x*s+b4)}$	
SG2(x)	=	$\frac{1}{1+\exp(-x)}$	s = -1; b4 = 0

Logit function

It is another non-linear function with ratio of exponential functions (Table A1-14).

Adaptive functions

Most of the functions (vide supra) have parameters which influence the output range and profile. The practitioners and software packages fix parameters at definite numerical values depending upon the task. In NN model, simultaneous refinement of Ws and parameters of TFs widens the scope of functioning to cover the shape in a broad sense. Marquardt algorithm is a popular adaptive gradient algorithm mimicking steepest descent, Gauss-Newton and Newton-Raphson methods depending upon the parameter λ in $\left(J^T * J + \lambda * I\right)$, where J is Jacobian. Engelbrecht *et al.* (Table A1-15) reported the effect of changing 'R' and steepness parameter of sigmoid TF. A NN was trained by simultaneous learning of steepness and sigmoid function and Ws.

Table A1-14: Logit function

$$\text{logit}(x) = \frac{\frac{1}{b} * \exp\left(-\frac{x-a}{b}\right)}{\left\{1+\exp\left(-\frac{x-a}{b}\right)\right\}^2}$$

Table A1-15: Engelbrecht.TF

$$SG\_Engelbretcht(x) = \frac{R}{1+\exp\left(x * steepness + thresold\right)}$$

- It is not necessary to scale the data in the range 0 to 1.
- NN performance improves by allowing activation functions to change dynamically with data
- The shape changes with adaptive slope

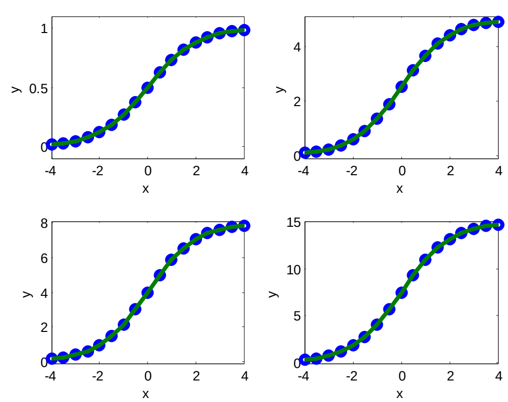

Scale on y is [0 to 1]; [0 to 4]
[0 to 8]; [0 to 15]

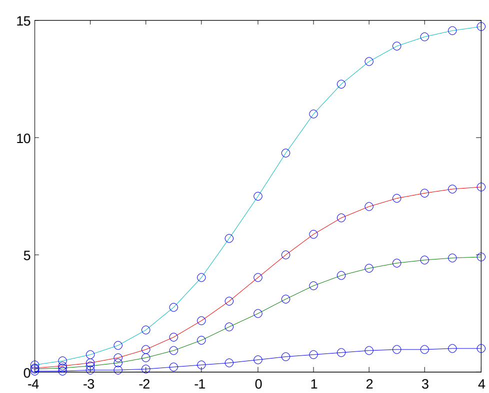

```
%
% om_sg_Engel.m     (R S Rao   8/9/10)
%
function [sg_Engel] = om_sg(x,s,threshold,A)
if nargin <4
   clean
   x  = [-4:0.5:4]';
   s= 1;threshold=0;
end
one = ones(length(x),1);
Az = [1,5,8,15]';
```

```
for i = 1:length(Az)
    A = Az(i,1);
    sg_Engel(:,i) = (A*one)./(one + exp(-x*s + threshold *one));
 end
[x,sg_Engel]
   plot2d(x,sg_Engel(:,1), sg_Engel(:,2), sg_Engel(:,3), sg_Engel(:,4))
figure, plot (x,sg_Engel,x,sg_Engel,'bo')
```

Wavelet function

Wavelet functions played a typical role as TFs to model filtering tasks, which are not easily modeled by local exponential and polynomial functions. Table A1-16 describes x-y plot and 3D-surface for a two variable triangular functions.

Table A1-16: Triangular.TF

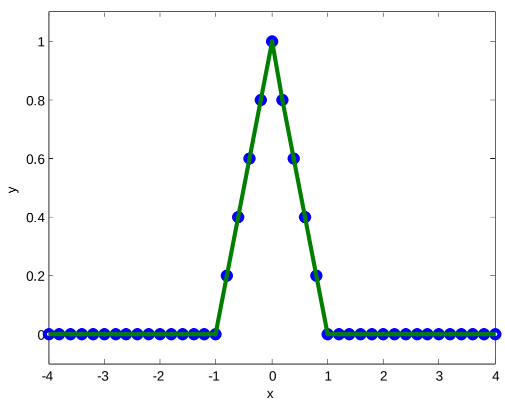

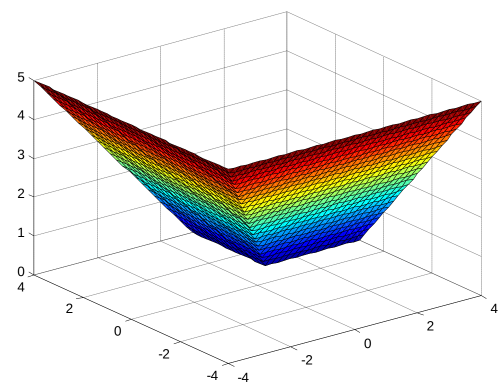

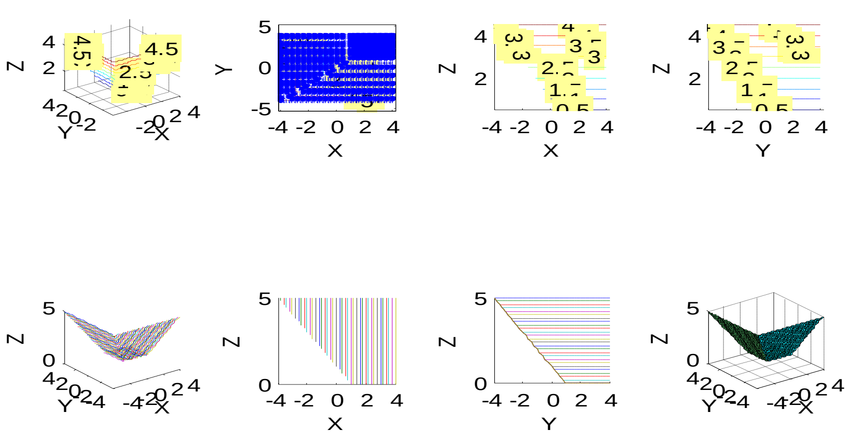

```
%
% om_triangular.m   (R S Rao   7/7/06, 5/4/99)
%
function [f] = om_trianular(x,y,fig)
%
if nargin <1
```

```
    clean,fig= 1;
    [x1,one] = xgrid(-4,4,0.2);
    [x,y,one] = xygrid(-4,4,0.2);
end
%
f =   max(0,1-abs(x1));
% 2D-
[r,c] = size(x);
for i = 1: r
    for j = 1:r
        z(i,j) = max([0 1-x(i,j),1-y(i,j)]');
    end
end
%
if fig
    plot2d(x1,f )
    figure,surf(x,y,z)% ,figure, contour(x,y,z)
    plot3d(x,y,z)
end
```

Advances in TFs

Future computational paradigm

Discrete and continuous numerical values are routine for input as well as output of a TF. Hither to polynomial, exponential, transcendental and mathematical functions are employed as activation functions in (artificial) mathematical neurons (A man!). Recently, fuzzy, probability and complex domains had influenced TFs employed in NNs. A function matrix representation with diagonal elements corresponding to TFs has the advantage, so that, it becomes trivial to define a matrix vector product. The algorithms for optimization, supporting tools are to be available in a chip in a portable and white-box language. Incorporating basis functions, learning rules and heuristics etc. will be in the next phase. External intelligent and self-adaptive tools operating on the modules in chip will evolve and will become an external layer for core processing functions. Their translation into parallel code, I/O transactions in networks and cloud computing and knowledge shared prime sites will take computing a step ahead to meet the real life mega tasks.

Appendix A1b: Neuron

ॐ McCulloch-Pitts neuron

McCulloch and Pitts in 1949 developed an artificial neuron (An). It is a simplified model of the biological neuron, a basic constituent of (human) brain. It is now called MP neuron. The inspiration is from biological science that a neuron fires an impulse only if its' value exceeds a threshold. These neurons were only handcrafted on a paper with a pencil. There was no realization of learning like in humans or animals. MP-neuron computes scalar product of the input vector and its weight (in analogy with synaptic strength) vector and compared with a fixed threshold. The brain consists of large number (10^{11}) of neurons and flexible/adaptive nervous system. These authors are the first to use

Neuron_McCulloch-Pitts				
Binary input	Confluence	TF	out	
	$\sum\prod(inp,w)$	Threshold	Scalar (Binary)	Output

the phrase 'Neural network'. Using these neurons, McCulloch and Pitts neural network explained Boolean gates ('AND', 'OR', 'NOT'). Table A1.17 details copying operation with this NN. But, MP-NN is too simple a model to explain miraculous and sparkling endeavors of human brain in wakeup, sleep and dream states, leave alone at mind and conscious levels.

Table A1-17 Copying operation with a neuron

Artificial neuron	Operation of TF	Result	Example	
			Input	Output
Input output	I(dentity)	Copying	1	1
			-1	1
	-I	Inversion	1	-1
			-1	1

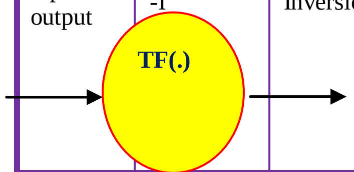

Formulae: one = unit column vector; inp = input vector to neuron;
OI: output of input
x = inp^T*one;
OI = TF(x);

Ex 1: copying: inp = 1; TF = eye(1); one = [1];
x = inp^T*one = [1]*[1] = 1; OI = TF(x) = I(x) = I(1) = 1;

Ex 2:Negation : inp = 1; TF = -I;
x = inp^T*one = [1]*[1] = 1; OI = TF(x) = -I(x) = -I(1) = -1;

$$ynn = TF\left(X^T * W\right)$$

If *TF is linear (Identity)*

$$Then\; TF\left(X^T * W\right) = I\left(X^T * W\right) = \left(X^T * W\right)$$

If *threshold is included*

$$Then\;\; ynn = \left(X^T * W\right) + threshold$$

McCulloch and Pitts neuron

- First mathematical model of a biological neuron
- Emulates binary 'and, or, not' gates

- Fixed threshold
- Fixed weights
- Hard-wired logic devices that were setup manually
- No ability to learn

Remedy : Hebb's learning rule

ॐ Outstar and instar type neurons

Stephen Grossberg used the analogy of inwardly radiating star to describe the connections between neurons or a neuron and networks. If a neuron in the web (net) of other neurons receives a large number of inputs, then it is termed as instar (Fig. A1-3a). Ideally, an instar neuron is not expected to have any connections going out of it. The net input to an instar type neuron is X^T * W. On the other hand, a neuron sending many outputs to other destinations is called an outstar (Fig. A1-3b). A neuron of MISO in input/output or hidden layer (SLP, MLP) is an 'instar' type. On the other hand, SIMO, 2IMO prevalent in higher order neurons (Fig. A1-3e, f) are predominantly outstar. The neurons in the hidden layers, higher order neurons or those in robots are MIMO category. Hecht-Nielson counter propagation (CP) NN behaves both as instar and outstar.

	Neuron_Bias			
a0	**Confl**	**TF**	**out**	**output**
→	$\sum\prod(a0, I)$	I	a0	→

ॐ Bias (Threshold) neuron

The output of a bias neuron is always one.

There is no input to this neuron. It can be deemed as NISO (No input single output) system with the output is stuck at one. It is used to include a constant (intercept) in a linear model. Threshold, so called bias, can be understood as a weight coefficient of the connection formally added neuron j, where xj = 1

Modified neuron

The net signal i.e. weighted input calculated as the dot product (X^T*W) is passed through a transfer (TF) /activation function (AF) whereby capability of neuron in I/O mapping improves substantially. The TF can be as simple as identity, linear or non-linear.

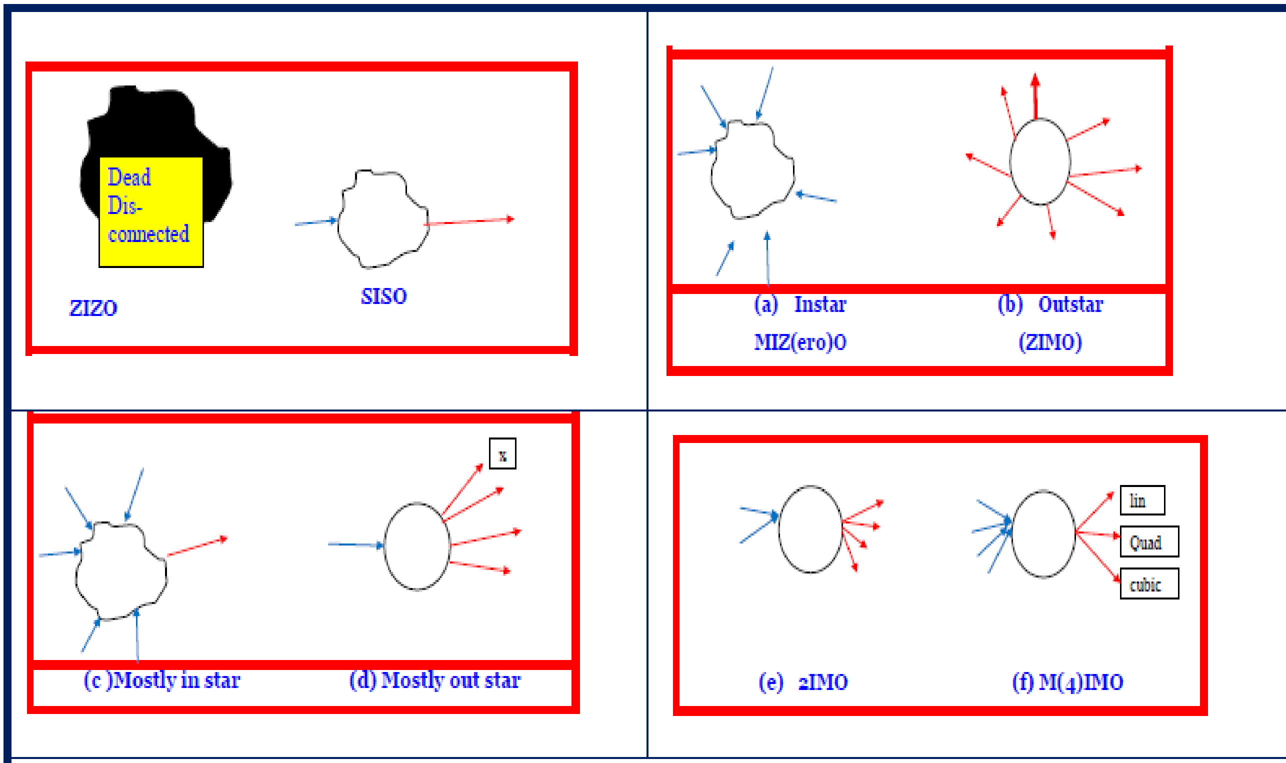

Fig. A1-3: Classification of neuron based number of inputs and outputs

ॐ σ-neuron
The confluence operator in σ-neuron (sigma-neuron) is sum (Chart A1-5). MC-neuron, Rosenblatt neuron, sigmoid neurons are a few examples of it.

ॐ π-neuron
In this neuron, the confluence operator is a product of input element and corresponding weight.

ॐ Power-neuron
In power neuron, the confluence operator is a product of input element raised to the power of corresponding weight.

ॐ Geometric mean neuron
It uses aggregation or accumulation function based on geometric mean of all inputs.

ॐ Rosenblatt perceptron

Frank Rosenblatt invented perceptron at the Cornell Aeronautical Laboratory in 1957. The goal was an attempt to understand human memory, learning, and cognitive processes. In 1960 Rosenblatt demonstrated the Mark I Perceptron. The Mark I was the first machine that could "learn" to identify optical patterns. He proposed a learning neural network model, a significant improvement to McCulloch and Pitts (MP) neuron. Rosenblatt-neuron learns responses by refining weights. It is the start of successful machine learning.

Chart A1-5: Neurons

σ-neuron

$$sum(x'*w)$$

Example

$$\begin{bmatrix} x_1 & x_2 & x_3 \end{bmatrix} * \begin{bmatrix} w_1 \\ w_2 \\ w_3 \end{bmatrix} =$$

$$x_1 * w_1 + x_2 * w_2 + x_3 * w_3$$

π-neuron

$$prod(x.*w)$$

Example

$$\begin{bmatrix} x_1 \\ x_2 \\ x_3 \end{bmatrix} . * \begin{bmatrix} 1 \\ 2 \\ 0.5 \end{bmatrix} = x_1 * 2 * x_2 * 0.5 * x_3$$

power-neuron

$$prod(x.\wedge w)$$

$$\begin{bmatrix} x_1 \\ x_2 \\ x_3 \end{bmatrix} . \wedge \begin{bmatrix} 1 \\ 2 \\ 0.5 \end{bmatrix} =$$

$$x_1 * x_2^2 * \sqrt{x_3}$$

Rosenblatt perceptron

- + Learns linearly separable Boolean gates
  - ('AND', 'OR', 'NOT')
- + Learns patterns (alphabets)
- - Cannot model dynamic tasks
  - Remedy : Dynamic neuron
- - Unable to learn classification tasks
  - with quadratic/non-linear separation boundaries
  - XOR, which is not linearly separable
  - Remedy : Sigmoid neuron

Direct Parallel Perceptron

A Gaussian kernel and a linear classifier (perceptron) are used [255].

Direct Kernel Perceptron (DKP)

Fernández-Delgado et al. [255] proposed direct kernel perceptron (DKP) with inspiration from direct parallel perceptron. DKP is related to SVM and extreme learning machine. The image-coefficients are calculated by analytical closed-form expression directly and thus do not involve any iterative training. It requires only training patterns. Further, this algorithm does not use any tunable regularization parameters. Also, Ws are translatable to image-coefficient employing a variable change.

ॐ Linear neuron

The biological inspiration is from Limulus-eye, cortical micro-circuits and firing rate in nerve cells. The saturating behavior is due to absolute refractory period. The presence of a unique stationary point is the sufficient condition and the output is confined to positive real axis.

$$TF\_linearThreshold = \max\left[\left(x'*w - threshold\right), 0\right]$$

Bernard Widrow (from electrical engineering at Stanford University) with his doctoral student Ted Hoff proposed adaptive linear neuron in the year 1959. The activation/transfer function is a non-saturating one and unbounded.

ॐ Sigmoid neuron

In 1986, Rumelhard used real valued sigmoid function as TF in the neuron. It accepts multiple numerical inputs and generates a single scalar output. The NN with these sigmoid neurons and back-propagation learning successfully modeled XOR task, which remained unsolved for over three decades with linear NN paradigm. Later, different forms of sigmoid type exponential functions viz. tanh, logarithm of sigmoid have become popular as TFs.

Neuron_Lin				
input	**Confl**	**TF**	**out**	**output**
→	$\sum\prod(inp, w)$	sigmoid	scalar	→

Advances in (artificial) neuron or processing unit

RBF-, self organizing-, ART- and recurrent neurons are detailed in our earlier reviews [303-308].

ॐ Wavelet-neuron

It is a neuron with (radial mother) wavelet as TF and also referred as wavelon. The dilation (T_j) and translation (E) operators are used in the Gaussian kernel.

$$y = F\left(\sqrt{\sum_i \frac{(x_i - e_{ji})}{t}}\right)$$

Neuron_Wavelet (wavelon)				
input	**Confl**	**TF**	**out**	**output**
→	$\sum\prod(inp, w)$	wavelet		→

Neuron_Rectang				
input	**Confl**	**TF**	**out**	**output**
→	$\sum\prod(inp, w)$	Rectangular function		→

ॐ Rectangular wave neuron

A rectangular wave neuron has a transfer function of a certain real number with infinite intervals.

ॐ Neuron with more than one TF

Two transfer functions instead of only one are used over the last half a century. A linear combination of the outputs of the two TFs imparts more non-linearity.

Fuzzy Domain

ॐ Fuzzy neuron

In 1970, a fuzzy neuron (table A1-18) was introduced by merging theory of fuzzy sets and McCulloch_Pitt's _model_neuron. Either inputs, weights, aggregation/ activation functions, or all of them are fuzzy data type. Here, excitatory connections are implemented by MAX operation and inhibitory connections by fuzzy logic complements followed by MIN operation. The MAX operator is like winner-takes–all philosophy and extracts most significant value. It is similar to a linear neuron performing a logical sum. On the other hand, min operator performs complimentary operation. But, a threshold level is not assigned. The fuzzy neuron has been successfully used for handwritten character recognition. A defuzzification neuron transforms a fuzzy datum into a crisp value.

Table A1-18: Fuzzy neuron

+ Nearer to human thinking

- No learning of Ws as the membership functions attached to the synaptic connections do not change

Neuron_fuzzy				
input	Confl	TF1	out	output
	Min Max	[Min, max t-norm, s-norm triangular mf]	scalar	

Input	Fuz	Confluence	TF	Defuz	Output
Crisp	No	fuzzy	Crisp	No	Crisp
Crisp	yes	Fuzzy	Fuzzy	yes	Crisp
Fuzzy	No	fuzzy	Fuzzy	No	Fuzzy

Fuz(zification) ; **Defuz**(zification)

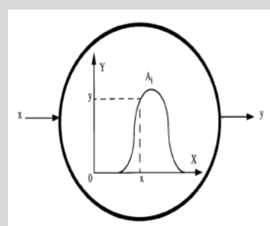

Fuzzification of neuron

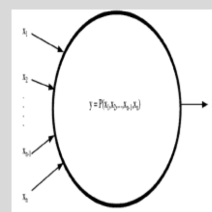

Pessimistic fuzzy neuron

ॐ Neo-fuzzy neuron

In neo-fuzzy neuron (Fig. A1-4), both inputs and weights are fuzzy. In case of crisp inputs, they are transformed into fuzzy values. Triangular member ship function with uniform distribution over the range is used. Neo-fuzzy neurons find place in predictions of classification domain. An input activates only two successive membership functions simultaneously. The sum of the degrees to which an input value belongs to any two neighboring membership functions is always equal to 1. It realizes inference over a fuzzy rule. The weights are trained by incremental updating method.

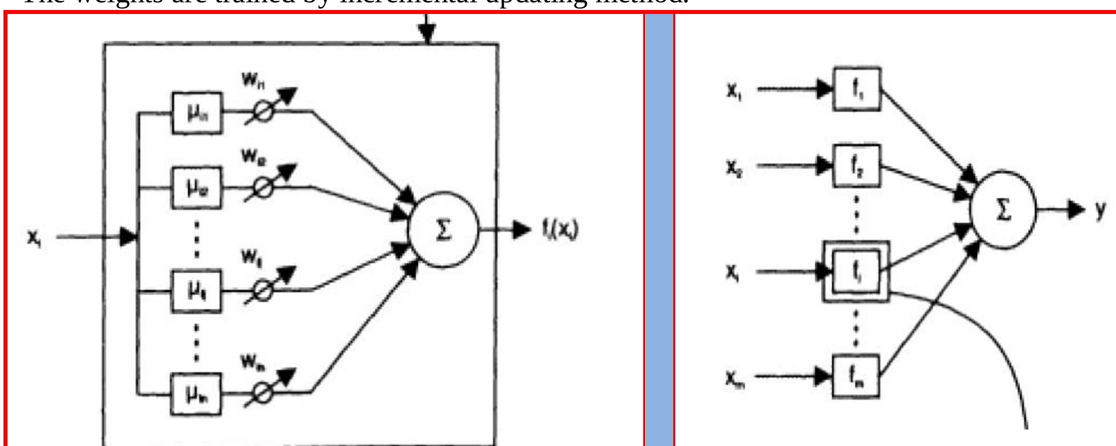

(a)

(b)

$$\Delta w(i,j) = -lr*\left(ynn(k) - y(k)\right)*mf_{ij}(x(i,k))$$

- Guarantees global minimum of trained weight in the error-weight space
- 10^5 faster compared to SLP with back-propagation

Fig. A1-4: Neo-fuzzy neuron (a) one crisp input (b) Multiple crisp inputs

Tolerance fuzzy neuron

It has the origin in fuzzy logic and has advantage that it models smooth boundaries between classes. Tolerance neuron employs fuzzy intervals and results in a general version of intervals in set theory.

Neuron_Tolerence

input	Confl	TF	out	output
	t-norm s-norm	TF_tolerence	scalar	

$$TF = \begin{bmatrix} 0 & if\ x \in [-\infty, 0] \\ x & if\ x \in [\ \ 0, 1] \\ 1 & if\ x \in [\ \ 1, \infty] \end{bmatrix} ; \quad y = TF\left[\ \underset{j \in N}{Sup}\ (w_i, w_i)\right]$$

Pessimistic fuzzy neuron

$$y\_pess.Fuzzy.$$
$$neuron(x_1, x_2, ..., x_n) =$$
$$\min(x_1, x_2, ..., x_n)$$
$$or \prod_{i=1}^{n} x_i$$
$$or \frac{\min(x_1, x_2, ..., x_n) + \max(x_1, x_2, ..., x_n)}{10}$$

$$y\_compensatory.$$
$$Fuzzy.neuron(x_1, x_2) =$$
$$(x_1)^{1-r}_{pessimistic} * (x_2)^{r}_{optimistic}$$

Compensatory degree (r)	
0	Pessimistic
1	optimistic

Optimistic fuzzy neuron

$$y\_optimistic.Fuzzy.$$
$$neuron(x_1, x_2, ..., x_n) =$$
$$\max(x_1, x_2, ..., x_n)$$
$$or \frac{\min(x_1, x_2, ..., x_n) + \max(x_1, x_2, ..., x_n)}{2}$$

Compositional neuron

These compositional neurons are used in emotional recognition based on facial expression.

Compensatory fuzzy neuron

The mapping of pessimistic (x1) and optimistic(x2) inputs to a compensatory fuzzy output is a compromised decision dealing with both the worst and best cases.

Pessimistic neuro

The fuzzy neurons with t-norm are called pessimistic neurons. They make a conservative decision for a pessimistic situation or even for a worst case.

Optimistic fuzzy neuron

This neuron uses an equivalent to t-conorm.

Morphological neuron

An elementary operation of mathematical morphology is performed in the neuron. Then activation (transfer) function operates on it [204]. Many of information granules viz. fuzzy sets, intervals and rough sets are ordered in lattice frame and lattice theory provided underlying framework for mathematical morphology. Thus, morphological-NNs, and fuzzy lattice neurocomputing are the order of day.

Stochastic Frame

ॐ Stochastic Neuron

In biological networks, probabilistic firing of neuron is also prevalent in addition to deterministic constraint. The use of stochastic TF in the PE results in a stochastic neuron. Boltzmann machine uses stochastic neurons and also introduces stochastic element in W. The transfer function of a stochastic neuron is an output probability against the input probability. The probabilities refer to a value of 1 on any given clock cycle. It is used in pulsed RBF-NN.

Stochastic neuron	
$TF\_stochastic = \dfrac{1}{1+\exp(\pm 2 * slope\_pdf * x)}$	**Neuron_stochastic** **input** | **Confl** | **TF** | **out** | **output** $\rightarrow$ | $\sum\prod(inp, w)$ | TF-stochastic | scalar | $\longrightarrow$
✚ Accurate approximation of Gaussian function	

Chaotic realm

ॐ Chaotic Neuron

A chaotic neuron introduced in 1990s (table A1-19) exhibits a wide range of behavior similar to biological neurons. The output is in graded mode and refractoriness decays exponentially. NNs with chaotic neurons have wide and flexible dynamics and arrive at global optima. It is used in Kohonen SOM and clustering ability is increased through controlled randomness. By replacing conventional neurons of Kohonen SOM grid by chaotic neurons, a controlled randomness is developed in the self-organizing process. It improved the ability of clustering task.

Table A1-19: Chaotic neurons	
Aihara	**Dingle**
$y(t+1) = TF\begin{pmatrix} u(t) - scal\_par * \sum\limits_{delay=0}^{t} (decay^4) * \\ refractFun(y(t-delay)) - threshold \end{pmatrix}$	$y(t+1) = 1 - 4 * \begin{pmatrix} 1 - \sum\limits_{i=1}^{NP} (x_i * w_i) * \\ y(t) * (1 - y(t)) \end{pmatrix}$
y(t) range : [0 to 1] ; u(t) : external input(stimulus) at time t	If X'*W < 0.11 then output is chaotic If X'*W range is [0.11 to 0.25] then output is periodic If X'*W > 0.25 then output is a single value which increases with X'*W If X'*W > 0.75 then output is 1

Boolean Frame

ॐ AND neuron

It receives output of tolerance neurons followed by AND operation
out.AND = H(x;w) = tol(x1,w1) .t. tol(x2,w2) ……. .t. tol(xn,wn)
where, w represents collectively the parameters of tolerance neuron and mf is the membership function to a hyper box.

ॐ Higher order neuron

The neuron consists of second (Table A1-20) and/or higher order terms, for example, trigonometric (sine, cosine) and polynomial functions in addition to linear, exponential (SG, RBF) parts. They generate non-linear multi-dimensional hyper surfaces. For a set of input vectors, the binary/ternary terms are weighted and then summed. The terms in summation thus, consists of linear, quadratic or polynomials. In financial modelling, polynomials and trigonometric functions are generally employed.

Table A1-20: Component terms of higher order neuron

	(a) Second order terms (two variables		
2	$inp=[x_1 \quad x_2]$	$Second\_Order\_terms:$ $[lin \quad bcp \quad square]$	Weight
		$lin=[x_1 \quad x_2]$	wlin
		$bcp=[x_1 * x_2]$	wbcp
		$quadratic=[x_1^2 \quad x_2^2]$	wquadratic

(a) Polynomial of third order				
dimx		**HO terms**	**W**	$\sum\prod(HOx,W) = HOx^T * W$
1	$inp=[x]$	$HOx^T = [x^1 \quad x^2 \quad x^3]$	WP	$w1*x + w2*x^2 + w3*x^3$

(c) Higher (>2) order terms			
d>2	$inp=[x_1 \quad x_2 \quad ... \quad x_d]$	$bcp=[x_j * x_k]$	$j=1 \quad to\ d-1$ $k=j+1\ to\ d$
		$quadratic=[x_j.\wedge 2]$	$j=1\ to\ d$
		$cubic=[x_j.\wedge 3]$	$j=1\ to\ d$
		$tcp=[x_j * x_k * x_m]$	$j=1 \quad to\ d-2$ $k=j+1\ to\ d-1$ $m=k+1 to\ d$
lin : Linear ;			

quadratic: square ;
bcp: binary cross product;
Second order : [square, bcp] ;

tcp: ternary cross product
Cubic: cube;

ॐ Lipson-Higher order neuron

Lipson proposed tensors as another type of higher-order-neurons. Their order pertains to internal tensorial order, but not the degree of output (table A1-21). This higher order neuron considers the covariance matrix unlike a classical neuron. It simulates shapes with holes and detached areas. It captures higher order information within a single neuron.

Table A1-21: Higher order neuron

(a) Second order components

Fourth order tensor	$=\langle x_H \quad x_H \quad x_H \quad x_H \rangle = \langle R_H \quad R_H \rangle$
	$=\begin{bmatrix} x1^2 & x1*x2 \\ x1*x2 & x2^2 \end{bmatrix} \otimes \begin{bmatrix} x1^2 & x1*x2 \\ x1*x2 & x2^2 \end{bmatrix}$
	$=\begin{bmatrix} x1^2 * \begin{bmatrix} x1^2 & x1*x2 \\ x1*x2 & x2^2 \end{bmatrix} & x1*x2*\begin{bmatrix} x1^2 & x1*x2 \\ x1*x2 & x2^2 \end{bmatrix} \\ ------------- & ------------- \\ x1*x2*\begin{bmatrix} x1^2 & x1*x2 \\ x1*x2 & x2^2 \end{bmatrix} & x1^2 * \begin{bmatrix} x1^2 & x1*x2 \\ x1*x2 & x2^2 \end{bmatrix} \end{bmatrix}$
	$=\begin{bmatrix} \begin{bmatrix} x1^4 & x1^3*x2 \\ x1^3*x2 & x1^2*x2^2 \end{bmatrix} & \begin{bmatrix} x1^4 & x1^3*x2 \\ x1^3*x2 & x1^2*x2^2 \end{bmatrix} \\ ----------- & ----------- \\ \begin{bmatrix} x1^4 & x1^3*x2 \\ x1^3*x2 & x1^2*x2^2 \end{bmatrix} & \begin{bmatrix} x1^4 & x1^3*x2 \\ x1^3*x2 & x1^2*x2^2 \end{bmatrix} \end{bmatrix}$ *correct it*

(b) First and second order components

Fourth order tensor $=\begin{bmatrix} x1^2 & x1*x2 & x1 \\ x1*x2 & x2^2 & x2 \\ x1 & x2 & 1 \end{bmatrix} \otimes \begin{bmatrix} x1^2 & x1*x2 & x1 \\ x1*x2 & x2^2 & x2 \\ x1 & x2 & 1 \end{bmatrix}$

Lipson-Higher-order -NNs

- Good stability
- Excellent training performance even with Hebbian learning rule

Complex space

ॐ Complex value neuron

Complex numbers were discovered by Sir William Rowan Hamilton. They are used in signal processing, computer graphics and robotics. A complex TF is used in a complex value neuron.

Quaternion frame

ॐ Quaternion Neuron

Quaternion, octonion and seonion belong to hyper-complex systems. Quaternion is four dimensional extension of imaginary values $a+i*b$, where a and b are real. It belongs to hyper complex number systems with a rank of four. This quaternion algebra can also be derived as a special case of Clifford (geometric) algebra. The quaternion consists of one real number and three imaginary (i,j,k) parts and is represented as a vector of real numbers in 4D-space. Chart A1-6 shows the identities satisfied by quaternions and it is clear that multiplication does not follow commutative rule. The states of neurons of Hopfield –Rec-NN are directly coded into quaternions.

The three operations viz. translation, dilation and spaced rotation in 3D-space can be affected by operators of quaternions. The quaternion component of the neuron state takes a bipolar (-1 or +1) value.

Geometric Algebra

ॐ Geometric neuron

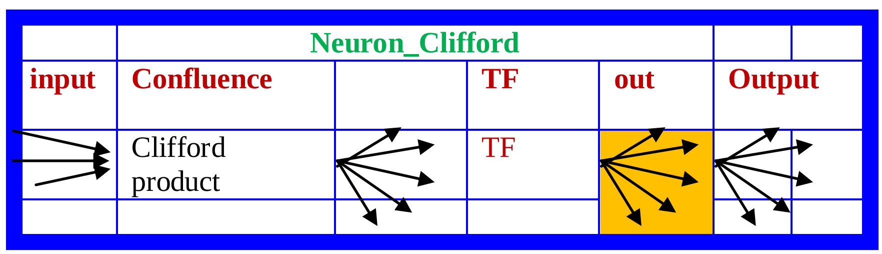

It accepts real, complex, quaternion, double (hyperbolic) and dual inputs. The confluence operator of geometric neuron is Clifford or geometric product (chart A1-6). Spinor Clifford neuron and Isomorphic Clifford neurons are also reported. The TFs for 2D-Clifford algebras are discussed (chart A1-6). It is instructive to compare McCulloch–Pitts with geometric neurons (fig. A1-5) to probe into a smooth transition. The reduction of geometric neuron outputs into FF-NNs is depicted in the fig. A1-5 along with a relevant knowledge base in the first order predicate logic format (chart A1-7).

Chart A1-6: Confluence and TF operators in Clifford geometric neuron

$$dotproduct(x,w) = x^T * w = \sum_j x_i * w_{i,j}$$

$$\begin{aligned}
Clifford_product(x,w) &= x^T * w + (x \wedge w) \\
&= dot\,\mathrm{Pr}\,oduct(x,w) + \\
& s1*\sigma1 + s2*\sigma2 + s3*\sigma3 + \quad \%\,Points\ or\ lines\,(vectors) \\
& s4*\sigma1*\sigma2 + s5*\sigma2*\sigma3 + s6*\sigma3*\sigma1 + \quad \%\,Planes\,(bivectors) \\
& s7*\sigma1*\sigma2*\sigma3 \quad \%\,Volumes\,(trivectors)
\end{aligned}$$

$$
\begin{aligned}
TF\left(Clifford\_product(x,w)\right) &= TF\left(x^{T} * w\right) + TF\left(x \wedge w\right) \\
&= TF\left(x^{T} * w\right) + \\
&\quad TF(s1)*\sigma 1 + TF(s2)*\sigma 2 + TF(s3)*\sigma 3 + \\
&\quad TF(s4)*\sigma 1*\sigma 2 + TF(s5)*\sigma 2*\sigma 3 + TF(s6)*\sigma 3*\sigma 1 + \\
&\quad TF(s7)*\sigma 1*\sigma 2*\sigma 3
\end{aligned}
$$

Geometric (Clifford) neuron

- The outer product gives scalar cross products between individual components of vector. They are multivector components of points, lines (vectors), planes (bivectors), and volumes (trivectors)
- It behaves like a higher order neuron
- But it has additional components i.e. geometric cross correlation.
- The output signal contains more geometric information

Chart A1 Subtle differences between Clifford algebra, tensor calculus and matrix

Clifford algebra

- Co-ordinate free system
- Includes spinors

Tensor calculus

- Covarient i.e. it requires transformation laws for co-ordinate independent relationships
- Does not have spinors
  - **Remedy :** Clifford algebra

Matrix analysis

- Does not have bivector representation of linear operators in null cone
  - **Remedy :** Clifford algebra

Fig. A1-5: McCulloch–Pitts neuron to geometric neurons

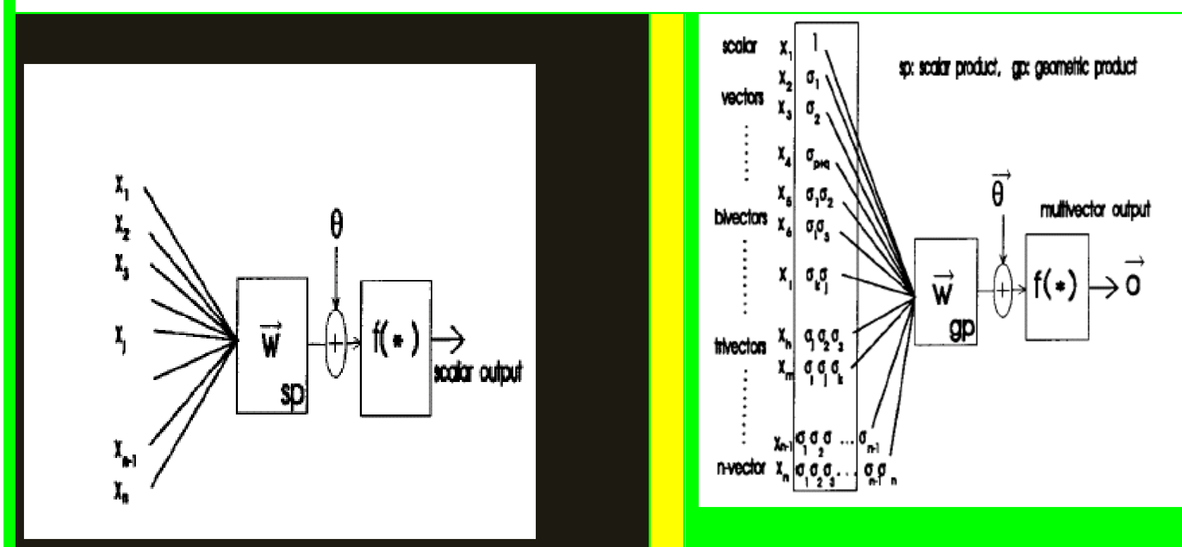

McCulloch–Pitts neuron **Geometric neuron**

Chart A1-7: Quaternion neuron, NN and FF_NN

$$x\_quaternion = x1 + i * x2 + j * x3 + k * x4$$
$$x\_quaternion : (x1,\ x2,\ x3, x4)$$
$$: \left(x1,\ \{x2,\ x3, x4\}\right)$$

x1,x2,x3 and x4	:	real numerical values
$\sigma_1, \sigma_2, \sigma_3$	:	**Orthonormal basis vectors**

$$i = \sigma_2 * \sigma_3$$
$$j = \sigma_3 * \sigma_1$$
$$k = \sigma_1 * \sigma_2$$

$$i^2 = j^2 = k^2 = -1 = i * j * k$$
$$i * j = -j * i;$$
$$j * k = -k * j;$$
$$k * i = -i * k;$$

Equivalence of Geometric NNs with FF-NNs

If	G(0,2,0)
Then	quaternion-valued NN
If	G(1,1,0)
Then	hyperbolic MLP
If	G(0,3,0)
Then	hyperbolic (double) quaternion-valued RBF
If	G(3,0,0)
Then	works in the entire Euclidean 3-D geometric algebra
If	G(4,1,0)
Then	works in the horosphere
If	$G^+(3,3,0)$
Then	bivector null cone

KB for input of a geometric neuron

If	$I^2 = -1$
Then	complex numbers
If	$I^2 = 1$
Then	double or hyperbolic numbers
If	$I^2 = 0$
Then	dual numbers (a degenerated geometric algebra)

Artificial neurons (An ant) not very far away from biological neurons

Bifurcating neuron

Biological inspiration of bifurcating neural activity is from olfactory systems. The state of olfactory bulb wanders in a high dimensional chaotic attractor space in the absence of any detectable odor. When an odor is found, the input through nose shifts to one of the low dimensional attractors. It corresponds to a wing of recognized specific odour. The coherent activities in brain measured in gamma-band centered around 40 Hz are of recent interest in olfactory systems of cat and rat. The primary visual cortex in the cat, monkey and EEGs of human brain above association and motor areas belong to this category.

Chart A1-8: Bifurcating neuron

- It functions as an amplitude-phase converter
- Inherent capacity is a coincidence detector
- Exhibits associative memory of multiple analogue patterns, volume holographic memory
- Switches to different phases of its memory space with change in frequency of the coherent modulation i.e. context sensitive memory

A bifurcating neuron using a third order iterate of quadratic logistic map. The external input is used to govern the dynamics. A certain input shifts the dynamics of a neuron from chaos to one of stable fixed point, while the rest are mapped to chaotic or periodic output. Bifurcating neuron is a model of a neuron augmented by coherent modulation from its environment (chart A1-8).

Hodgkin-Huxley neuron

Alan Lloyd Hodgkin and Andrew Huxley in 1952 proposed the first scientific neuron model to mimic biological neuron closely. It describes how action potentials are developed and propagated. The exchange of neurotransmitters, chemical moieties in the synaptic gap promote communication of signals. The membrane of the cell consists of voltage dependent channels. The conductance of sodium and potassium ions through these channels results in the membrane current of a neuron. The other ionic currents are described by ohmic leakage contribution. It models membrane potential with detailed spike generation based on development of response with changes in several ion channels. The accuracy of the model increases by incorporating the geometry of compartments of the neuron. A few novel advanced processes are incorporated in FitzHugh-Nagumo (1961-1962) and Hindmarsh-Rose (1984) models.

Hodgkin-Huxley neuron

- Computationally intense even from standpoint of today's hard/software
- Mechanistic-physical model of biological neuron is complex

Spiking neuron

A spiking neuron with excitatory and inhibitory signals of a train of stimulated signals with and without noise was proposed. The NN using these neurons performed well in modeling somato sensory system (Table A1-22) and grouping of objects of interest in diabetic retinopathy images. The input (spikes) signals enter the neuron through synaptic connection. It increases the conductance of synapse with changes in post synaptic potential. The weighted sum of all excitatory and inhibitory synaptic conductances results in a stimulus of a train of spikes. Absolute refractory period is a short interval immediately after generation of spike. During this period, the neuron is incapable of responding to any further stimulation (of input). Then, it follows relative refractory period. Here, only very strong stimulations are responded. Post synaptic potential of the neuron is a result of increased synaptic conductance. They used MacGregor's integrate-and-fire model which takes into account threshold membrane potential and potassium channel response. This is simpler compared to Hodgkin-Huxley model in generation of spike. The excitation and inhibition reflect (model) individual channel.

Table A1-22: Architecture of Spiking-NN used for classification of retinopathy images

Layer	Model of	architecture
Sensory	Tactile receptors on the skin	9 x 9
Sub cortical layer-1	Spinal card and brain stem	9 x 9
Sub cortical layer-2	Thalamus	21 x 21 Exc 9 x 9 Inh
Cortical layer	Cortex	21 x 21 Exc 9 x 9 Inh

Exc: excitatory neurons; Inh: inhibitory neurons

If	Stimulus is strong i.e. exceeds the threshold
Then	The neuron fires

Oscillatory Neuron

Inoue and Nagayoshi proposed an oscillatory neuron. It is made up of excitatory as well as inhibitory coupled oscillators. This neuron deals with noisy and chaotic information. Its oscillatory function is described by frequency, phase and amplitude. Oscillatory neurons are not widely used in artificial NNs. This is partially as a result of the feel that many numerical tasks are sufficiently dealt by hither to known artificial neurons. Further, the binary logic hardware structure is not comfortable to implement oscillatory model.

Leaky integrator neuron

The input to output transformation of leaky integrator neuron and knowledge base are given in chart A1-9.

Appendix A1c: Accumulation (confluence) operator

The confluence operators in use are summation, product, power for crisp values, and minimum/maximum in fuzzy domain and so on.

Appendix A1d: Boolean gates

XOR: From the figure (Fig. A1-6), it is clear that it is not a linearly separable problem and thus direct I/O nets (MC-NN) cannot solve the task. This simplest non-linear problem was solved with the introduction of a layer of neurons with non-linear (sigmoid) transfer function in between the input and output layers. This net is popularly known as SLP_NN, or in other words MLP_NN with only one hidden layer. Figure A1-6 incorporates multi-dimensional XOR data.

Case 1: SLP with one hidden neuron and direct I/O connections gracefully solves XOR. To be brief, a non-linear neuron generates non-linear discriminating function.

Case 2 : Two hidden neurons in the hidden layer of SLP (without direct IO connections) is also adequate.

Chart A1-9: Leaky integrated neuron

At time t, x(t) is input, out.y(t) = TF(x'*w)

At time t+1, input is x(t+1),
net input = x(t+1) + feedback
= x(t+1) +TF(x'*w)

output at t+1= y(t+1) =
TF([x(t+1) +TF(x'*w)])

If	there is no external input at the time instance t+1, (i.e. x(t+1) = 0),
Then	y(t+1) = TF([TF(x'*w)]) = function(y(t))
If	feedback is an exponential decay function & x = 1
Then	output repeats it (y = 1)
If	input signal is not present
Then	output value decreases over time

+ It remembers event x at least for some time i.e. last input signal is kept and decays exponentially

- Forgets remembered event in far distant future time

Fig. A1-6: Boolean gates

Input		Output of Boolean gates															
		1	2	3	4	5	6	7	8	9	10	11	12	13	14	15	16
1	1	0	1	0	0	0	1	0	0	1	1	0	0	1	1	1	1
0	0	0	0	1	0	0	1	1	0	0	0	1	1	0	1	1	1
1	0	0	0	0	1	0	0	1	1	1	0	0	1	1	0	1	1
0	1	0	0	0	0	1	0	0	1	0	1	1	1	1	1	0	1
			nor			and		xnor			xor		or			nand	

Input		Output			
x1	x2	OR	NOR (not OR)	XOR	XNOR (not XOR)
		yOR	yNOR	yXOR	yXNOR
0	0	0	1	1	0
1	0	1	0	0	1
0	1	1	0	0	1
1	1	1	0	1	0

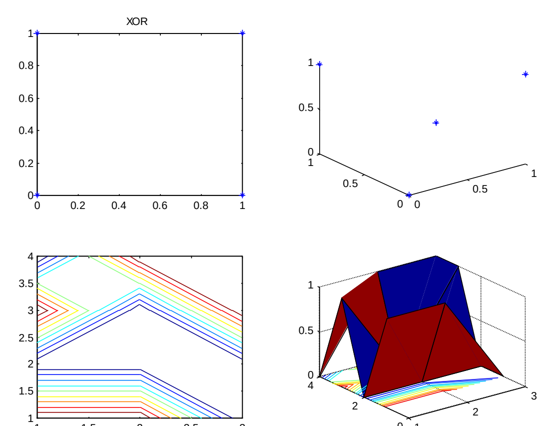

Appendix 2: Salt
State-of-the-art-of (SA) learning/Training

In Mullock Pitts-NN (1943), the weights are fixed and thus there was no process of learning at all. Yet, this network could solve 'AND/OR' Boolean tasks. Hebb's learning (1949) rule is the start of increase or decrease values of W based on activities of neurons. Rossenbault in 1953 conceived linear perceptron updating the formula based on the difference between the observed output and that generated by NN.

Appendix 2a : Salt-learning

The basics of natural learning by humans and machine learning technology are briefed in the appendix of our earlier publication on ARTMAP_NNs [305]. The different learning mechanisms in wide applicability in the context of recurrent NNs, SOM_NNs were described [303,304]. A survey of developments of Hebbian, Oja and competitive learning algorithms is briefed here.

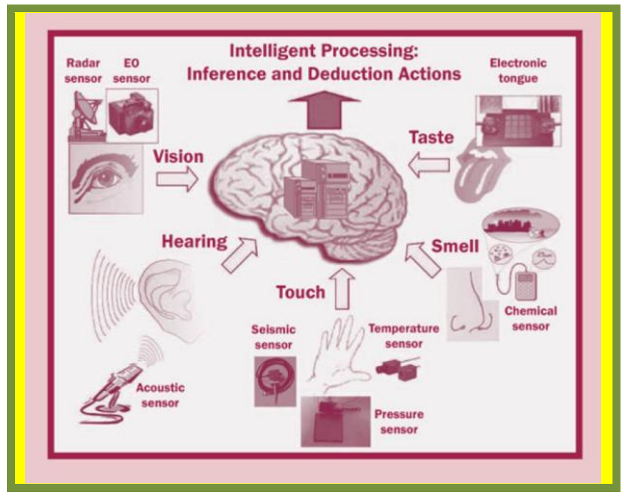

Hebb rule

Hebb, a neuro physiologist inspired by the functioning of brain proposed a model, which is now popularly known as Hebb rule or assembly theory. It states that if a neuronal cell 'A' consistently assists the firing of another cell 'B', then a synaptic knob is developed on the first cell. On the other hand, if the knobs are already present, they are enlarged in contact with the soma of second cell. This striking idea 'cells that fire together, wire together' is emotional. But, it is far away in depicting realistic picture at the biological cell level. But, the learned auto-associated pattern is called an 'engrem' at holistic level which are popular as neuronal/neural networks.

Hebb's rule (chart A2-1, A2-2) is found prevalent at the synapses in marine gastropod. It is an unsupervised learning approach and thus does not require a teacher or observed response. This is a local approach involving two neurons and a synapse. Translating it to ANNs results in training (altering/refining/learning) the weights between (model/artificial) neurons. If two neurons fire (activate) simultaneously then, the weight between them increases. On the other hand, if they are activated separately, the weight is reduced.

Chart A2-1: Hebbian rule

dw = lr * a * p' - dr * w *p'

- Unstable whenever the signal is dominant → fails for many networks
  Remedy: Generalised Hebbian rule, BCM theory, or Oja's rule
  - Lrn_rate is positive → W valued are unbounded → tends to infinity
    ☎ **Remedy :** Hebbian rule with forgetting factor

Hebbian rule with forgetting factor: A forgetting factor is introduced in to Hebbian learning equation and thus prevents w values becoming unbounded.

Generalized Hebbian rule : Combining Gram schmidt orthogonalization process and Oja's rule generalized Hebb rule is proposed for unsupervised linear FF-NN.

Differential Hebbian learning : In this procedure, the product of two previous charges in output are used to calculate Wij.

Oja learning rule or modified Hebbian learning

The synaptic strengths between the neurons in the brain change over time. This inspired Oja to propose a computational form in 1982. Thus, it is a modified Hebbian rule though multiplicative normalization.

Chart A2-2: Output of om_ref_JAVATYP.m

Hebb learning

B. Lu, A. Dibazar, T. W. Berger ▶ Noise-robust acoustic signature recognition using nonlinear Hebbian learning	Neural networks 23(10)(2010)1252-1263
D.O. Hebb, W. Penfield ▶ Human behaviour after extensive bilateral removal from the frontal lobes	Archives of Neurology and Psychiatry 44(1940)421–436
D.O. Hebb ▶ Distinctive features of learning in the higher animal ▶ J. F. Delafresnaye (Ed.): Brain Mechanisms and Learning .	Oxford University Press, (1961) London.
D.O. Hebb ▶ The organization of behavior	New York, Wiley (1949)

om_ref_JAVATYP.m

object module (om_) reference (ref_)
Journal Author Volume And (JAVATYP) Title Year Pages
matlab function(.m)

The stability of Oja's learning rule is derived for Lyapunov function. Here, the change in pre-synaptic w of a single neuron is calculated. The weights are normalized between zero and one. A value of zero corresponds to no weight or (no connection), while one represents that only the corresponding input neuron has all the weight. Oja considered a case resulting in a quadratic form. Of course, linear and any other non-linear form also has the same theoretical rigor and generality. The output activation function can be non-linear and non-static, but it should be continuously differentiable with respect to x and w. Although there is not yet experimental evidence of this rule in biological NNs, it is applied with great success in many image and speech recognition/synthesis and binocular vision systems.

PCs from Oja's rule

Applying Oja's rule to a single neuron, the first PC is obtained. Multi-Oja-NN with generalized Hebbian rule and more number of neurons extracts all PCs and Eigen values.

Widrow-Hoff learning rule

The least mean squares filter (LMS) of Widrow is used to train ADALINE (ADAptive LInear Neuron) and MADALINE (Multiple ADALINE) NNs.

Adaptive learning algorithm: Hara analyzed a learning algorithm employing a margin Kappa a la Gardner in NNs (KB. A2-1)

Add-if-silent rule

Fukushima introduced add-if-silent learning rule for neocognitron model of robust pattern recognition (chart A2-3).

Winner-kills-loser (WKL)
It is a competitive learning rules introduced in the context of training neocognitron neural network. Now, WKL with three thresholds outperforms winner-takes all (WTA) learning in recognition of distorted/blurred/tilted digits/alphabets.

KB. A2-1: Effect of kappa on type of learning

If kappa = 0
Then perceptron learning

If $kappa \to \infty$
Then Hebbian learning

If $kappa \to 1.51 * l$
Then superior generalization compared to Hebbian learning

Chart A2-3: Add- if-silent rule

+ Stable
+ Simple
+ High recognition rate
+ Independent of scale of network

Chart A2-4: Test data sets for border Pairs learning algorithm

Classification	XOR	Iris
Pattern recognition	triangles image	Digits Handwritten Pen-Based
	noisy patterns	

Chart A2-5: Deep_NNs and deep_learning

Deep_NNs
- Complex MLP structures
  - Contains richer information
  - Improved representation ability compared with traditional data-driven models

Deep learning
- Semi-supervised
  - All available process data can be utilized
- Efficient with massive data in practice

Iteriative-EKF learning rule

Iterative extended Kalman filter learning rule is a continuous learning rule derivable from Bayesian framework. The object function is the minimization of sum of MSE and regularization. It is applicable when the non-linear relationship gradually changes over time. The algorithm is found to be superior to on-line BP-EKF while comparable with Black-Scholes benchmark model for German stock exchange index data.

Border Pairs learning algorithm
Ploj et al. **[257]** used border pairs learning algorithm for MLP_NN for a large number of classification and pattern recognition tasks. The learning is affected separately layer as well as neuron wise. This method finds a near-minimal architecture, a desirable feature in NN activity (chart A2-4).

Deep_NN Learning algorithm
The random neural network was introduced in 1989. The learning algorithms are reviewed along with application for classification. The future prospective research ventures identifying the gaps and holes in the field are emphasized. Sussner and Esmi [204] reported competitive learning with winner-take-all mechanism for morphological perceptrons. The results of this method are compared with MLP, fuzzy lattice neurocomputing , kNN and decision trees. The deep_NNs are trained with deep learning strategy (chart A2-5) and applied to calculate heavy diesel 95% cut point of a crude distillation unit (CDU).

Deep_NNs are not simple MLPs and also latent variable models. Thus, they handle highly correlated process variables.

Wake and sleep algorithm

The two phases –wake and sleep—are local learning processes. They are repeated alternatively to reconstruct the input patterns at the output layer of a 3-layer auto-coder. Katayama used Hinton's wake – sleep algorithm to explain response properties of medial superior temporal MST neurons for binary Q = 2 and multiple $(Q \geq 3)$ states. The recognition model represents the architecture from medial temporal MT area to MST area.

Correlation learning

The correlational learning is useful for NNs with discrete input and output values. From the degree of overlap of input patterns a separability factor is defined. The binary values zero and one in a subset of input cells are represented by a uni-directional graph. This is a generalized topological mapping preserving the input pattern relation.

Negative correlation learning

In unbiased individual NNs the errors between them are uncorrelated. A negative correlation learning to design and train an ensemble of NNs simultaneously and interactively was proposed. Introduction of correlation penalty terms in the object error function is the basis of negative correlation learning. Training with this algorithm results in negatively correlated NNs with increased generalization

Learning in NNs from statistical framework perspective

In statistical or mathematical modeling, data is fit into the user chosen model. If it is not adequate, another model is tried. This process is continued till an adequate (not even ambitious) model is arrived at. On the other hand, NNs learn from data set and at the end of this phase, a (blackbox/implicit) model is developed. Learning in NNs also is an estimation of an unknown probability distribution { $p(y/x,W)$ } from statistical point of view.

Arriving at W matrix with a chosen optimization function is called training in NN terminology. The assumption is the existence of a functional relationship between X and y, although not known to the user. The weights of NN are estimated from a set of NP training patterns satisfying the chosen optimization function. The solution procedure adapted depends upon difficulty of data structure, ease of operation of a method in a package and most important mind set etc. A statistical model is realizable if and only if the parameters are uniquely determined from its behavior or mapping from W to $p(y/x,W)$ be one to one. In the conventional statistical theory, Bayesian posterior pdf converges to Gaussian distribution and generalized error is proportional to the number of parameters. Watanabe pointed out that conventional statistical asymptotic theory couldn't be applied to MLP_NN and RBF_NN or Gaussian mixture NNs. It is due to the fact that Fisher information matrices are not positive definite and Ws are non-identifiable. And, going deep into statistical distribution of static/dynamic parameters/ noise in data, non-parametric models and distribution free data processing are beyond the scope here. Thus, from broad perspective, the iterative refinement of parameter models in mathematical optimization/statistical regressions, learning of connection weights in historical NNs and training of Ws in MLP_NN, RBF_NN and Rec_NNs are similar but for terminology.

Appendix A2b: Salt-Training

Back propagation

The typical developments in back propagation algorithm are briefed in Chart A2-6, table A2-1, Alg. 2-1 and Alg. A2-2.

Chart A2-6: Typical BP algorithms

Backpropagation (BP)
Std "Vanilla"
ThroughTime
WeightDecay
Batch
Batch ThroughTime
Batch TimeDelay
Chunk
weight & bias
weight & bias & one vector at a time

Cum-delta
Delta Bar Delta
Delta rule
Directed random search
Ext.DBD
Max Prop
Momentum
Norm-cum-delta
Quick Propogation
Quickprop
Quickprop throughTime
Rprop in CC

Alg. A2-1 : Pseudo inverse training in MLP [11]

```
        Number of hidden neurons = nlayer
        Yapp = X
For layer = 0 to nlayer
        Cal. inv_Yapp = pinv(Yapp)
        ESS = [Norm(Y_layer – inv(Y_layer) – I)]^2
        While ESS > Error_tol
             W_layer = inv(Y_layer)
          % Feed forward the result to the next layer
             Y(layer+1) = TF * (Y_layer * W_layer)
             Inv_Y(layer+1) = pinv(Y(layer+1))
        End while
End layer
YNN = TF [TF[TF(Yap*Wap)] * W1] …..* Wnlayer]
```

Alg. A2-2: BP for RBF

```
Initialization of network
For epoch : 1 to max_epoch
   Repeat for input : 1 to all input vectors
         compute the network output by proceeding forward
         layer by layer
      calculate (error) residual gradient vs parameters layer
      by layer starting from output
      update parameter_w
   end % input
end % epoch
```

Expert Opinion (EO_KB)

- Momentum term has a little effect in training RBF
- Sigmoid as TF_OL improves training
- CV for better generalization

Table A2-1: Chronological developments in learning algorithms (BP) for Ws of NNs

Year	Limitations/ improvement/ modification of BP	Comment	Ref.
1994	- Back propagation error surface is like ravine	**Remedy:** difference of gradients is used as acceleration algorithm to escape from ravine	66
1994	ॐ Davidson's LS	+ One step ahead prediction	67
1995	- Adaptive agent contains not worker but a critic.	**Remedy:** Neural critic adopts a new learning alg	63
1995	ॐ Acceleration of momentum by constrained optimization	+ Optimizes alignment of weights successively. FF MLP	64
2000	**If** input has errors **Then** new cost function based on errors	**Remedy:** Stochastic frame work Marquardt B P for errors in x and y	76

2000	- Block training reduced sensitivity		72
2001	ॐ Linear constraints are introduced into error function		69
2001	ॐ First and higher derivatives included based on regularization	+ Improvement of generalization	53
2001	ॐ Maximum inter quartile range used	+ Active learning reduces amount of data selection	74
2001	ॐ Blowing up technology used in hierarchical learning.	+ Bayesian GE of HLM is smaller than that in regular statistical module	74